









# NAVAL POSTGRADUATE SCHOOL

## Monterey, California



# THESIS

G135

FIXED INTERVAL SMOOTHING ALGORITHM FOR  
AN EXTENDED KALMAN  
FILTER FOR OVER-THE-HORIZON SHIP TRACK-  
ING

by

William J. Galinis

March 1989

Thesis Advisor

Harold A. Titus

Approved for public release; distribution is unlimited.

T241925





# REPORT DOCUMENTATION PAGE

1a Report Security Classification <b>Unclassified</b>			1b Restrictive Markings		
2a Security Classification Authority			3 Distribution Availability of Report		
2b Declassification Downgrading Schedule			Approved for public release; distribution is unlimited.		
4 Performing Organization Report Number(s)			5 Monitoring Organization Report Number(s)		
6a Name of Performing Organization Naval Postgraduate School		6b Office Symbol (if applicable) 62	7a Name of Monitoring Organization Naval Postgraduate School		
6c Address (city, state, and ZIP code) Monterey, CA 93943-5000			7b Address (city, state, and ZIP code) Monterey, CA 93943-5000		
8a Name of Funding Sponsoring Organization		8b Office Symbol (if applicable)	9 Procurement Instrument Identification Number		
8c Address (city, state, and ZIP code)			10 Source of Funding Numbers		
			Program Element No	Project No	Task No
			Work Unit Accession No		
11 Title (include security classification) <b>FIXED INTERVAL SMOOTHING ALGORITHM FOR AN EXTENDED KALMAN FILTER FOR OVER-THE-HORIZON SHIP TRACKING</b>					
12 Personal Author(s) <b>William J. Galinis</b>					
13a Type of Report Master's Thesis		13b Time Covered From To		14 Date of Report (year, month, day) March 1989	15 Page Count 101
16 Supplementary Notation The views expressed in this thesis are those of the author and do not reflect the official policy or position of the Department of Defense or the U.S. Government.					
17 Cosati Codes			18 Subject Terms (continue on reverse if necessary and identify by block number)		
Field	Group	Subgroup	Kalman filter, Smoothing, HFDF, Storm Tracking.		
19 Abstract (continue on reverse if necessary and identify by block number) The performance of an extended Kalman filter used to track a maneuvering surface target using HFDF lines-of-bearing is substantially improved by implementing a fixed interval smoothing algorithm and a maneuver detection method that uses a noise variance estimator process. This tracking routine is designed and implemented in a computer program developed for this thesis. The Hall noise model is used to accurately evaluate the performance of the tracking algorithm in a noisy environment. Several tracking scenarios are simulated and analyzed. The application of the Kalman tracker to a tropical storm tracking problem is investigated. Actual storm tracks obtained from the Joint Typhoon Warning Center in Guam, Mariana Islands are used for this research.					
20 Distribution Availability of Abstract <input checked="" type="checkbox"/> unclassified unlimited <input type="checkbox"/> same as report <input type="checkbox"/> DTIC users			21 Abstract Security Classification Unclassified		
22a Name of Responsible Individual Harold A. Titus			22b Telephone (include Area code) (408) 646-2560	22c Office Symbol 62TS	

Approved for public release; distribution is unlimited.

Fixed Interval Smoothing Algorithm for an Extended Kalman  
Filter for Over-the-Horizon Ship Tracking

by

William J. Galinis  
Lieutenant, United States Navy  
B.S.E.E., United States Naval Academy, 1983

Submitted in partial fulfillment of the  
requirements for the degree of

MASTER OF SCIENCE IN ELECTRICAL ENGINEERING

from the

NAVAL POSTGRADUATE SCHOOL  
March 1989

---



## ABSTRACT

The performance of an extended Kalman filter used to track a maneuvering surface target using HFDF lines-of-bearing is substantially improved by implementing a fixed interval smoothing algorithm and a maneuver detection method that uses a noise variance estimator process. This tracking routine is designed and implemented in a computer program developed for this thesis. The Hall noise model is used to accurately evaluate the performance of the tracking algorithm in a noisy environment. Several tracking scenarios are simulated and analyzed. The application of the Kalman tracker to a tropical storm tracking problem is investigated. Actual storm tracks obtained from the Joint Typhoon Warning Center in Guam, Mariana Islands are used for this research.

G 159  
C.1

## THESIS DISCLAIMER

The reader is cautioned that computer programs developed in this research may not have been exercised for all cases of interest. While every effort has been made, within the time available, to ensure that the programs are free of computational and logic errors, they cannot be considered validated. Any application of these programs without additional verification is at the risk of the user.

## TABLE OF CONTENTS

I. INTRODUCTION .....	1
II. PROBLEM STATEMENT .....	3
A. GENERAL .....	3
B. SYSTEM MODEL .....	4
C. MEASUREMENT MODEL .....	5
III. KALMAN FILTER THEORY .....	8
A. GENERAL .....	8
B. EXTENDED KALMAN FILTER .....	8
C. NOISE PROCESSES .....	10
D. INITIALIZATION AND OPERATION .....	12
E. MANEUVER AND DIVERGENCE DETECTION .....	15
F. SMOOTHING ALGORITHM .....	18
IV. COMPUTER SIMULATIONS .....	20
A. GENERAL .....	20
B. SCENARIO #1 .....	22
C. SCENARIO #2 .....	26
D. SCENARIO #3 .....	30
E. SCENARIO #4 .....	34
F. SCENARIO #5 .....	38
G. SCENARIO #6 .....	42
H. SCENARIO #7 .....	46
I. SCENARIO #8 .....	50
J. SCENARIO #9 .....	54
V. STORM TRACKING .....	58
A. GENERAL .....	58
B. SYSTEM AND MEASUREMENT MODELS .....	58
C. STORM TRACKS .....	59

VI. CONCLUSIONS .....	64
APPENDIX A. SHIPSM.FOR .....	66
APPENDIX B. TRACK.FOR .....	84
LIST OF REFERENCES .....	88
INITIAL DISTRIBUTION LIST .....	90

## LIST OF FIGURES

Figure 1.	Surface Tracking Geometry	3
Figure 2.	White Noise Model	7
Figure 3.	Hall Noise Model	7
Figure 4.	Initialization Process	13
Figure 5.	Processed Data vs Observed Results	23
Figure 6.	Position Error	24
Figure 7.	Variance of Position Error in the X Direction	24
Figure 8.	Scenario #1 Overall Track Results	25
Figure 9.	Processed Data vs Observed Results	27
Figure 10.	Position Error	28
Figure 11.	Variance of Position Error in the X Direction	28
Figure 12.	Scenario #2 Overall Track Results	29
Figure 13.	Processed Data vs Observed Results	31
Figure 14.	Position Error	32
Figure 15.	Variance of Position Error in the X Direction	32
Figure 16.	Scenario #3 Overall Track Results	33
Figure 17.	Processed Data vs Observed Results	35
Figure 18.	Position Error	36
Figure 19.	Variance of Position Error in the X Direction	36
Figure 20.	Scenario #4 Overall Track Results	37
Figure 21.	Processed Data vs Observed Results	39
Figure 22.	Position Error	40
Figure 23.	Variance of Position Error in the X Direction	40
Figure 24.	Scenario #5 Overall Track Results	41
Figure 25.	Processed Data vs Observed Results	43
Figure 26.	Position Error	44
Figure 27.	Variance of Position Error in the X Direction	44
Figure 28.	Scenario #6 Overall Track Results	45
Figure 29.	Processed Data vs Observed Results	47
Figure 30.	Position Error	48
Figure 31.	Variance of Position Error in the X Direction	48



Figure 32.	Scenario #7 Overall Track Results	49
Figure 33.	Processed Data vs Observed Results	51
Figure 34.	Position Error	52
Figure 35.	Variance of Position Error in the X Direction	52
Figure 36.	Scenario #8 Overall Track Results	53
Figure 37.	Processed Data vs Observed Results	55
Figure 38.	Position Error	56
Figure 39.	Variance of Position Error in the X Direction	56
Figure 40.	Scenario #9 Overall Track Results	57
Figure 41.	Storm Track of Typhoon Pat	60
Figure 42.	Filtered and Smoothed Track of Typhoon Pat	61
Figure 43.	Storm Track of Typhoon Tess	62
Figure 44.	Filtered and Smoothed Track of Typhoon Tess	63

## ACKNOWLEDGEMENTS

I would like to express my appreciation to Prof. Hal Titus for his instructive guidance and recommendations that kept resetting the author's learning "process" when this "process" began to diverge excessively from its intended track. I also want to thank my #1 fan, my wife Diana, whose love and support made this thesis "doable" and my son Jared who kept me laughing the whole way.



## I. INTRODUCTION

In 1986, then Deputy Chief of Naval Operations for Surface Warfare (OP-03), Vice Admiral Joseph Metcalf III challenged the leadership of the U.S. Navy's Surface Warfare community to reexamine the traditional concepts of surface warfare-concepts that perhaps are preventing the Navy from taking full advantage of present and future technologies. Thus began Surface Warfare's Revolution at Sea. A vital concept to the "Revolution at Sea" is the constantly expanding oceanic battle space ("up, out, and down"). [Ref. 1]

With the advent of the modern long range cruise missile, U.S. surface forces have the capability to attack enemy surface targets at 250 nautical miles. In order to make full use of this capability however, an accurate and reliable method of over-the-horizon tracking and targeting is necessary. The current methods used to target an enemy surface force at these ranges include the use of satellites, aircraft, and intelligence sources. A major drawback to using these assets is the requirement that they transmit vital targeting information to the attacking ship. A shipboard surveillance system that provides this information locally would allow the attacking forces to operate independently without relying on other sources for targeting data, data that may or may not be available when needed for a number of reasons. In addition, the ability to operate covertly, and to track and target enemy forces without divulging any targeting information, greatly enhances the probability of success of a mission. This requires a passive acquisition system. Surveillance of the high frequency spectrum using passive radio-direction finding (RDF) sensors is one method of passive long range tracking. A shipboard high frequency-direction finding system based on an extended Kalman filter with a fixed interval smoothing algorithm can be used to accurately track and target a maneuvering surface ship.

The major thrust of this thesis deals with the problem of tracking a surface ship at long ranges using lines-of-bearing obtained from radio direction-finding sensors located on two tracking ships. It is not the purpose of this research to address the multitude of problems associated with the hardware aspects of a high frequency radio direction-finding system. The basic assumption used here is that a shipboard direction-finding system is in place that provides a line-of-bearing contaminated by an additive noise process. The extended Kalman filter and the fixed interval smoothing algorithm will be

used to refine the observed lines-of-bearing and improve the accuracy of the target track. The noise added to the observed line-of-bearing is an integral part of the measurement model and should reflect the noise process that would be encountered in the HF environment as accurately as possible. For the simulations conducted, this measurement noise was modeled using first a white noise model and then with a Hall noise model.

This thesis will be an extension of a previous thesis done by Lieutenant Thomas K. Bennett. The major points of that thesis are:

- The development of an extended Kalman filter shiptracking program.
- The observations used in the shiptracking program were RDF lines-of bearing.
- The position errors achieved by this program were 10-15 nautical miles.

This thesis will attempt to improve on the previous research by implementing a fixed interval smoothing algorithm and a maneuver divergence detection scheme that uses a noise variance estimator process. The smoothing algorithm is an off-line calculation that uses all measurements taken during a time interval  $0 \leq k \leq M$  to improve the estimate. By having a more accurate assessment of what the target has done in the past, we will be better able to predict ahead and estimate a target's future course, speed, and position. The computational aspects of the smoothing algorithm will be investigated as well as the types of estimation problems where the improvement due to the smoothed calculations is significant and worth the extra computational effort. The two noise models used in the simulations will be compared as to their accuracy and their advantages or disadvantages of one or the other based on the computer simulations.

The tracking of a tropical storm is a problem similar to the ship tracking problem and is discussed in Chapter 5. The major difference between the filtering applications is that the measurement data in the storm tracker are actual position coordinates given by latitude and longitude values. This leads to a linear measurement process and therefore, the linearization required in the ship tracking problem is unnecessary in the storm tracking scenario.



## II. PROBLEM STATEMENT

### A. GENERAL

The tracking scenario used in this thesis involves two tracking ships moving in the general direction toward a target ship. The positions of the vessels are given in  $x,y$  coordinates. The target-tracker scenario is shown in Figure 1.

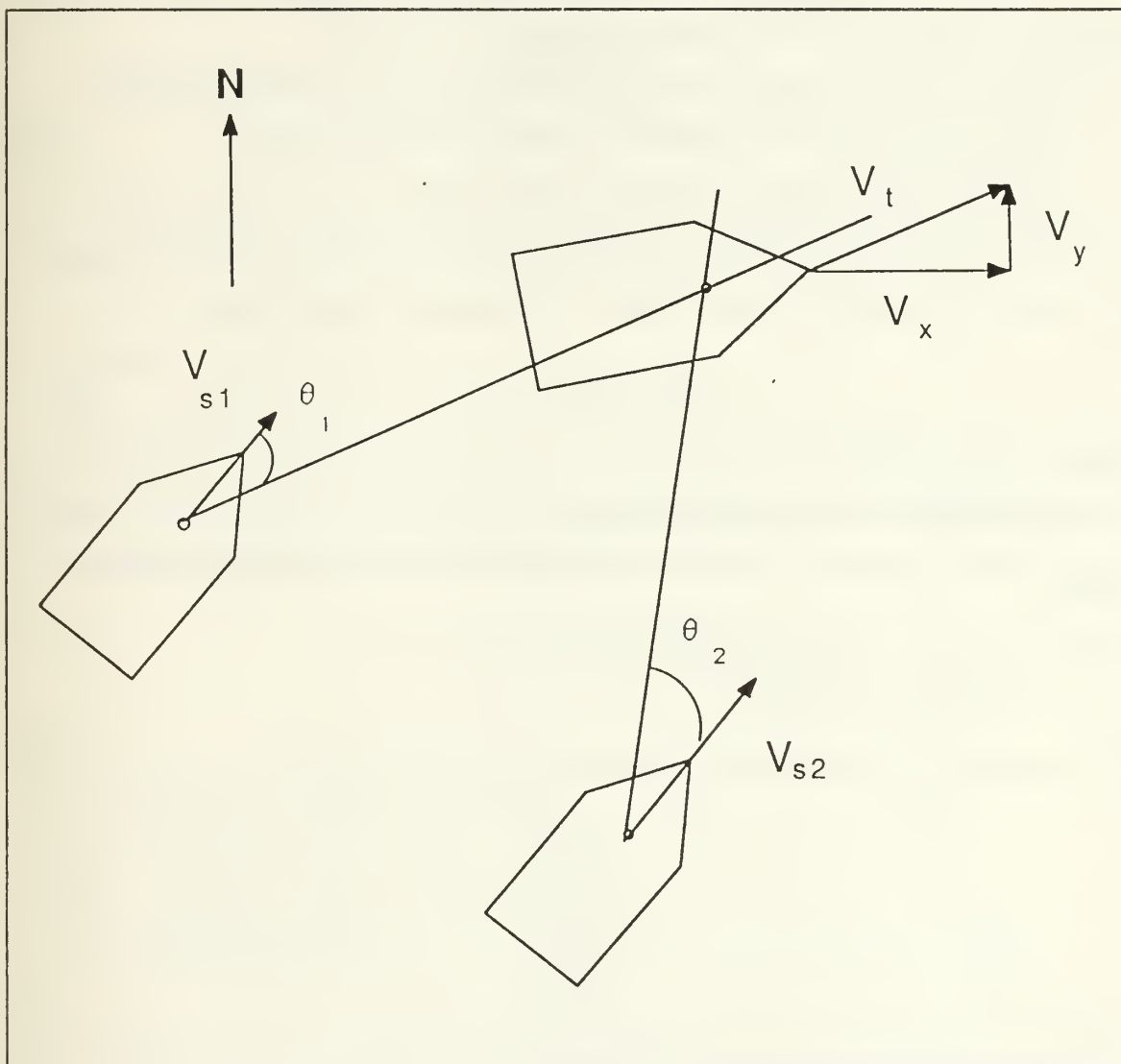


Figure 1. Surface Tracking Geometry

This problem will be developed using state space methods. Given the lines-of-bearing (the measurements) received by a radio direction-finding system, we are interested in estimating the location, course, and speed of the target (the states of the plant). The state variables for this plant are  $x_t$ ,  $\dot{x}_t$ ,  $y_t$ , and  $\dot{y}_t$ .

## B. SYSTEM MODEL

The system to be modeled in this problem is that of a surface ship at sea. In the development of this model, the following assumptions were made.

- The effect of wind, current, and hydrodynamic forces on the ship are neglected.
- The curvature of the earth is neglected; ocean surface area is flat.
- Course and speed inputs are constant (i.e., step inputs).

This is a linear, time-distance system that can be described with the equations of motion for constant acceleration in two dimensions. The state space equation is

$$\underline{x}_{k+1} = \phi_k \underline{x}_k + \Gamma_k a_k \quad (2.1)$$

where

$\underline{x}_k$  = parameter to be estimated (state vector).

$\phi_k$  = state transition matrix which describes how the states of the dynamic system are related

$\Gamma_k$  = system noise coefficient matrix

$a_k$  = random forcing function.

From Equation (2.1) and the above assumptions, the state vector is

$$\underline{x}_k = \begin{bmatrix} x \\ \dot{x} \\ y \\ \dot{y} \end{bmatrix} \quad (2.2)$$

and the system state equation can be expanded as

$$\begin{bmatrix} x \\ \dot{x} \\ y \\ \dot{y} \end{bmatrix}_{k+1} = \begin{bmatrix} 1 & T & 0 & 0 \\ 0 & 1 & 0 & 0 \\ 0 & 0 & 1 & T \\ 0 & 0 & 0 & 1 \end{bmatrix} \begin{bmatrix} x \\ \dot{x} \\ y \\ \dot{y} \end{bmatrix}_k + \begin{bmatrix} \frac{T^2}{2} & 0 \\ 0 & 0 \\ T & \frac{T^2}{2} \\ 0 & T \end{bmatrix} \begin{bmatrix} a_{xk} \\ a_{yk} \end{bmatrix} \quad (2.3)$$

The system noise process for the ship tracking problem is a function of the noise coefficient matrix,  $\Gamma_k$ , and the random forcing function,  $a_k$ , which is simply the acceleration vector.

### C. MEASUREMENT MODEL

For a linear measurement process, the measurements are linearly related to the state variables and can be modeled using the linear measurement equation

$$z_k = H_k x_k + v_k \quad (2.4)$$

where

$z_k$  = set of measurements.

$H_k$  = observation matrix that gives the noiseless relationship between the measurements and the state vector.

$x_k$  = state vector

$v_k$  = measurement noise.

In this tracking problem, the measurements are the lines-of-bearing received by the radio direction-finding sensors located on two surface ships. For the geometry of the problem shown in Figure 1, the relationship of the measurements to the state variables is not linear and the measurement equation becomes

$$z_{nk} = \tan^{-1} \left[ \frac{(x_{tk} - x_{nk})}{(y_{tk} - y_{nk})} \right] + v_k \quad (2.5)$$

where

$z_{nk}$  = observed lines of bearing at time k

$x_{tk}, y_{tk}$  = position of target at time k

$x_{nk}, y_{nk}$  = position of sensor n at time k

$v_k$  = measurement noise.

This nonlinear equation must be linearized prior to processing the measurement data with the filter and the smoothing algorithm. For this problem, an extended Kalman filter is required and will be discussed in the next chapter.

There are several types of noise that affect the propagation of radio signals, however, this noise can basically be divided into two categories, depending on whether it originates from within the receiving system or external to the receiving antenna. For the frequencies of interest in this problem (2-30 MHz), it is the atmospheric noise external

to the receiving system that is of the greatest concern. [Ref. 2: p. 4] This noise is a function of many variables including the time of day, geographical location, season, and frequency. Although this is generally a non-white, non-gaussian noise process, it can be adequately described as a white noise process over an extended period of time. The white noise model was used for the first set of computer simulations.

A deficiency of white noise as a model for atmospheric noise, is its inability to accurately model the impulsive nature of the atmospheric noise associated with lightning discharges. This impulsive noise characteristic was investigated by Hall [Ref. 3] and led to the development of Hall's generalized "t" model which has the form

$$x(t) = m(t)n(t) \quad (2.6)$$

where  $m(t)$  is a slowly varying stationary random process independent of  $n(t)$  and  $n(t)$  is a zero mean, narrowband Gaussian process. The complete development of this model can be found in Hall [Ref. 3].

In [Ref. 4: pp. 13-35], Spaulding outlines a method of generating random noise samples using the Hall model. The procedure for calculating these random samples starts by generating random samples from a uniform distribution,  $V$ , in the interval from zero to one and then modifying the sample according to the distribution required. For the Hall model, the random noise samples are obtained using the equation

$$X_n = \gamma \left( V^{\frac{-2}{\Theta-1}} - 1 \right)^{\frac{1}{2}} \quad (2.7)$$

where  $\Theta = 4$  and  $\gamma = 0.707$ . These values for  $\Theta$  and  $\gamma$  were chosen using the atmospheric noise curves in [Ref. 3: p. 44]. The positive bias in the Hall model was subtracted out prior to inserting the noise data into the ship tracking algorithm. This was done in order to prevent a biased error covariance in the Kalman filter. The two noise models are shown in Figures 2 and 3. Both noise processes are zero mean and  $\pm 3$  variance.

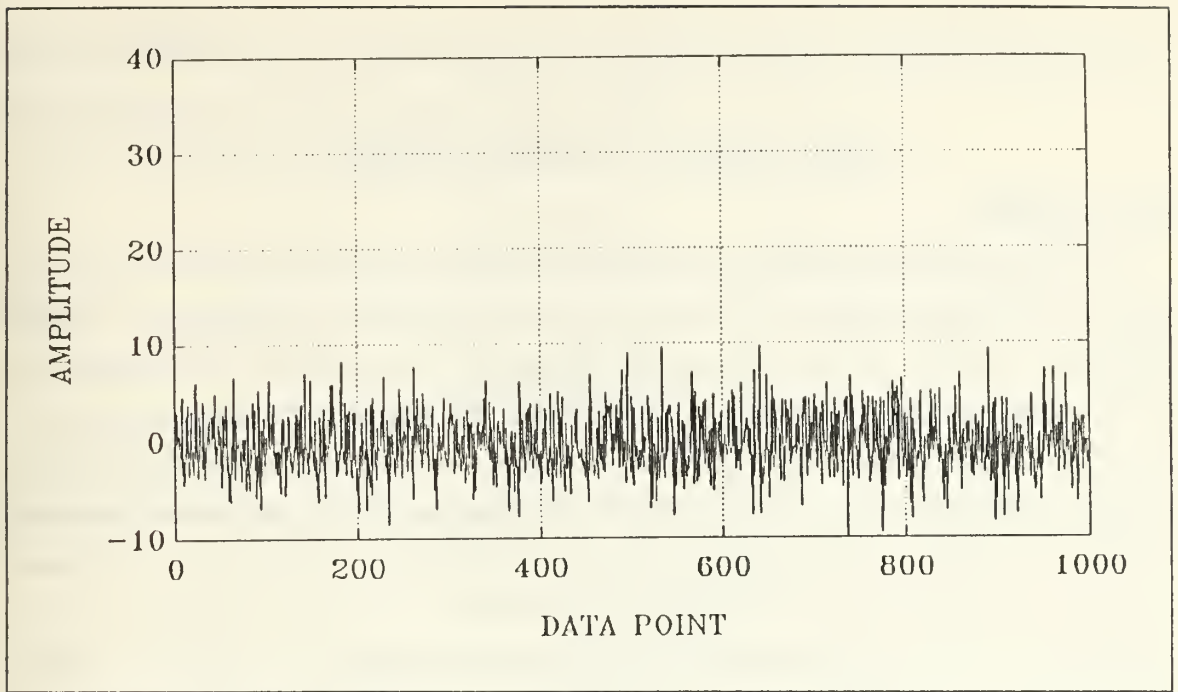


Figure 2. White Noise Model

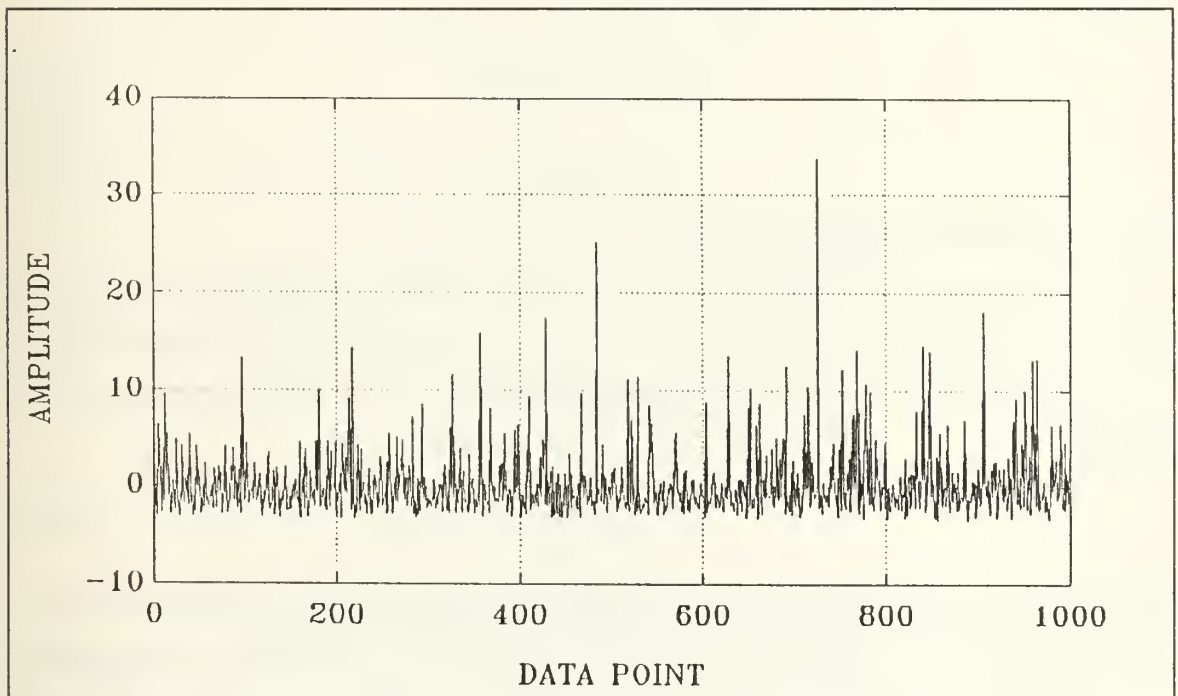


Figure 3. Hall Noise Model



### III. KALMAN FILTER THEORY

#### A. GENERAL

Filtering refers to the process of estimating the state vector at the current time based upon all past measurements. An optimal filter concentrates on optimizing a specific performance measure used to approximate the quality of the estimate. The Kalman filter is the optimal filter in a class of linear filters that minimize the mean square estimation error between the actual and desired output. In other words, the Kalman filter attempts to minimize the elements along the main diagonal of the state error covariance matrix. The filter itself is actually a recursive algorithm for processing discrete measurements or observations in an optimal manner. [Ref. 5: p. 101] It requires a priori knowledge of the state estimate ( $\underline{x}_{k-1}$ ) and its error covariance ( $P_{k-1}$ ), and the current observation ( $\underline{z}_k$ ). The Kalman filter is the proper algorithm to be used when both the system model and the measurement model are linear functions of the state variables and these models can be described by the equations

$$\underline{x}_{k+1} = \phi_k \underline{x}_k + \Gamma_k \underline{u}_k \quad (3.1)$$

$$\underline{z}_k = H_k \underline{x}_k + \underline{v}_k \quad (3.2)$$

#### B. EXTENDED KALMAN FILTER

From equation (2.5), we can see that there is a nonlinear relationship between the observed lines-of-bearing and the state variables. The adaptation of the Kalman filter to a nonlinear application is the extended Kalman filter. The nonlinear measurement equation is

$$\underline{z}_k = h(\underline{x}_k, k) + \underline{v}_k \quad (3.3)$$

where the observation matrix ( $h_k$ ) is a function of the state at each sampling time and the sampling index  $k$ . Linearization of this equation can be accomplished by expanding  $h$  in a Taylor series about an estimated trajectory that is continually updated with the filter's estimates. By keeping only the first term of the series expansion, a first order approximation is obtained. Higher order, more precise filters can be constructed by including more terms of the Taylor series expansion for the nonlinearities, and deriving

recursive relations for the higher moments of the state vector. A detailed discussion of this procedure can be found in Gelb [Ref. 5: p. 100].

This linearization process yields the linear measurement equation

$$z_k = H_k x_k + v_k \quad (3.4)$$

where

$$H_k = \left[ \frac{\delta h(x_k, k)}{\delta x_k} \right] \quad (3.5)$$

Applying this linearization method to equation (2.5), we get

$$H_k = \frac{\delta \left[ \tan^{-1} \left[ \frac{(x_{tk} - x_{nk})}{(y_{tk} - y_{nk})} \right] \right]}{\delta x_k} \quad (3.6)$$

Simplifying equation (3.6)

$$H_k = [h_{11} \quad h_{12} \quad h_{13} \quad h_{14}] \quad (3.7)$$

where

$$h_{11} = \frac{\delta \left[ \tan^{-1} \left[ \frac{(x_{tk} - x_{nk})}{(y_{tk} - y_{nk})} \right] \right]}{\delta x_{tk}} = \frac{(y_{tk} - y_{nk})}{\hat{R}_k^2} \quad (3.8)$$

$$h_{12} = \frac{\delta \left[ \tan^{-1} \left[ \frac{(x_{tk} - x_{nk})}{(y_{tk} - y_{nk})} \right] \right]}{\delta \dot{x}_{tk}} = 0 \quad (3.9)$$

$$h_{13} = \frac{\delta \left[ \tan^{-1} \left[ \frac{(x_{tk} - x_{nk})}{(y_{tk} - y_{nk})} \right] \right]}{\delta y_{tk}} = - \frac{(x_{tk} - x_{nk})}{\hat{R}_k^2} \quad (3.10)$$

$$h_{14} = \frac{\delta \left[ \tan^{-1} \left[ \frac{(x_{tk} - x_{nk})}{(y_{tk} - y_{nk})} \right] \right]}{\delta \dot{y}_{tk}} = 0 \quad (3.11)$$

By replacing  $y_{ik}$  with  $\hat{y}_{i(k|k-1)}$  in equation (3.8) and  $x_{ik}$  with  $\hat{x}_{i(k|k-1)}$  in equation (3.10) the linearized measurement matrix can be written as

$$H_k = \begin{bmatrix} \frac{(\hat{y}_{i(k|k-1)} - y_{nk})}{\hat{R}_k^2} & 0 & -\frac{(\hat{x}_{i(k|k-1)} - x_{nk})}{\hat{R}_k^2} & 0 \end{bmatrix} \quad (3.12)$$

where the range ( $R$ ) is computed as

$$\hat{R}^2 = (\hat{y}_{i(k|k-1)} - y_{nk})^2 + (\hat{x}_{i(k|k-1)} - x_{nk})^2 \quad (3.13)$$

Having linearized the measurement process about  $\hat{\mathbf{x}}_{(k|k-1)}$ , where  $\hat{\mathbf{x}}_{(k|k-1)}$  denotes the state estimate at time  $k$  based on all previous estimates computed at time  $k-1$ , we can now use the normal linear Kalman filter equations.

### C. NOISE PROCESSES

The calculation of the error covariance matrix and the filter gain matrix requires the covariance matrices for the uncorrelated noise process  $\underline{a}_k$  and  $\underline{v}_k$ . For the measurement noise process  $v_k$ , the covariance matrix is

$$E[v_k v_k^T] = R_k \quad (3.14)$$

where  $R_k$  is defined as the state measurement noise covariance matrix. It is based on the sensor accuracy and accounts for unknown disturbances such as steps, white noise, or imperfections in the plant model. The variance of the white noise model and the Hall noise model used in the computer simulations was  $\pm 3$  degrees.

The state excitation matrix,  $Q_k$ , used in the Kalman filter represents the system noise process and is a function of the system noise coefficient matrix,  $\Gamma_k$ , and the random forcing function,  $a_k$ , where

$$Q_k = [\Gamma_k Q'_k \Gamma_k^T] \quad (3.15)$$

where  $Q'_k$  is defined

$$Q'_k = E[a_k a_k^T] = \begin{bmatrix} E[a_{xk}^2] & E[a_{xk} a_{yk}] \\ E[a_{yk} a_{xk}] & E[a_{yk}^2] \end{bmatrix} \quad (3.16)$$

and  $\Gamma_k$  is the same as in equation (2.3). The  $Q_k$  matrix allows for any random target maneuvers as well as inaccuracies in the system model. The magnitude of  $Q_k$  has a direct

bearing on the magnitude of the state error covariance matrix and it prevents the covariance matrix from becoming singular by ensuring some uncertainty in the state estimates.

From Figure 1, the velocity of the target is

$$v_x = v_t \sin \Theta_t \quad (3.17)$$

$$v_y = v_t \cos \Theta_t \quad (3.18)$$

Differentiating equations (3.17) and (3.18) to get the target's acceleration

$$a_x = \dot{v}_t \left[ \frac{v_x}{v_t} \right] + v_t \dot{\Theta}_t \left[ \frac{v_y}{v_t} \right] \quad (3.19)$$

$$a_y = \dot{v}_t \left[ \frac{v_y}{v_t} \right] - v_t \dot{\Theta}_t \left[ \frac{v_x}{v_t} \right] \quad (3.20)$$

where

$$\left[ \frac{v_x}{v_t} \right] = \sin \Theta_t$$

$$\left[ \frac{v_y}{v_t} \right] = \cos \Theta_t$$

Here  $\dot{v}_t$  and  $\dot{\Theta}_t$  are equal to the acceleration along the target's course and the angular velocity or turn rate, respectively. Assuming that

$$E[\dot{\Theta}_t] = E[\dot{v}_t] = 0$$

the variances become

$$E[\dot{\Theta}_t^2] = \sigma_{\Theta_t}^2 \quad (3.21)$$

$$E[\dot{v}_t^2] = \sigma_{v_t}^2 \quad (3.22)$$

Approximate values [Ref. 6: p. 39] for the standard deviations of the accelerations and the angular velocity are

$$\sigma_{\Theta_t} = 0.1 \frac{\text{degrees}}{\text{sec}} \quad (3.23)$$

$$\sigma_{v_t} = 0.01 \frac{\text{knots}}{\text{sec}} \quad (3.24)$$

and the variance values are

$$\sigma_{\Theta_t}^2 = 0.01096 \left( \frac{\text{radians}}{\text{min}} \right)^2 \quad (3.25)$$

$$\sigma_{v_t}^2 = 0.0001 \left( \frac{\text{nm}}{\text{min}^2} \right)^2 \quad (3.26)$$

Taking the expectation of equations (3.19) and (3.20) and substituting in equations (3.21) and (3.22) the elements of the  $Q'$  matrix are

$$E[a_{xk}^2] = \sigma_{v_t}^2 \left[ \frac{v_x}{v_t} \right]^2 + \sigma_{\Theta_t}^2 v_y^2 \quad (3.27)$$

$$E[a_{yk}^2] = \sigma_{v_t}^2 \left[ \frac{v_y}{v_t} \right]^2 + \sigma_{\Theta_t}^2 v_x^2 \quad (3.28)$$

$$E[a_{xk}a_{yk}] = E[a_{yk}a_{xk}] = v_x v_y \left[ \left( \frac{\sigma_{v_t}^2}{v_t} \right)^2 - \sigma_{\Theta_t}^2 \right] \quad (3.29)$$

#### D. INITIALIZATION AND OPERATION

In the ship tracking scenario, the extended Kalman filter and the fixed interval smoothing algorithm are used to minimize the tracking errors. Prior to processing the measurement data, the filter must be initialized with an initial state estimate and an initial error covariance matrix. This initialization process is a very important step in the filter operation and gross inaccuracies in this step may cause the filter to diverge. Divergence occurs when the calculated covariance errors become much smaller than the actual covariance errors. This causes the actual values of the states to pull away from the estimated values. The concept of divergence will be discussed in greater detail in section E of this chapter. The initialization process is shown in Figure 4.



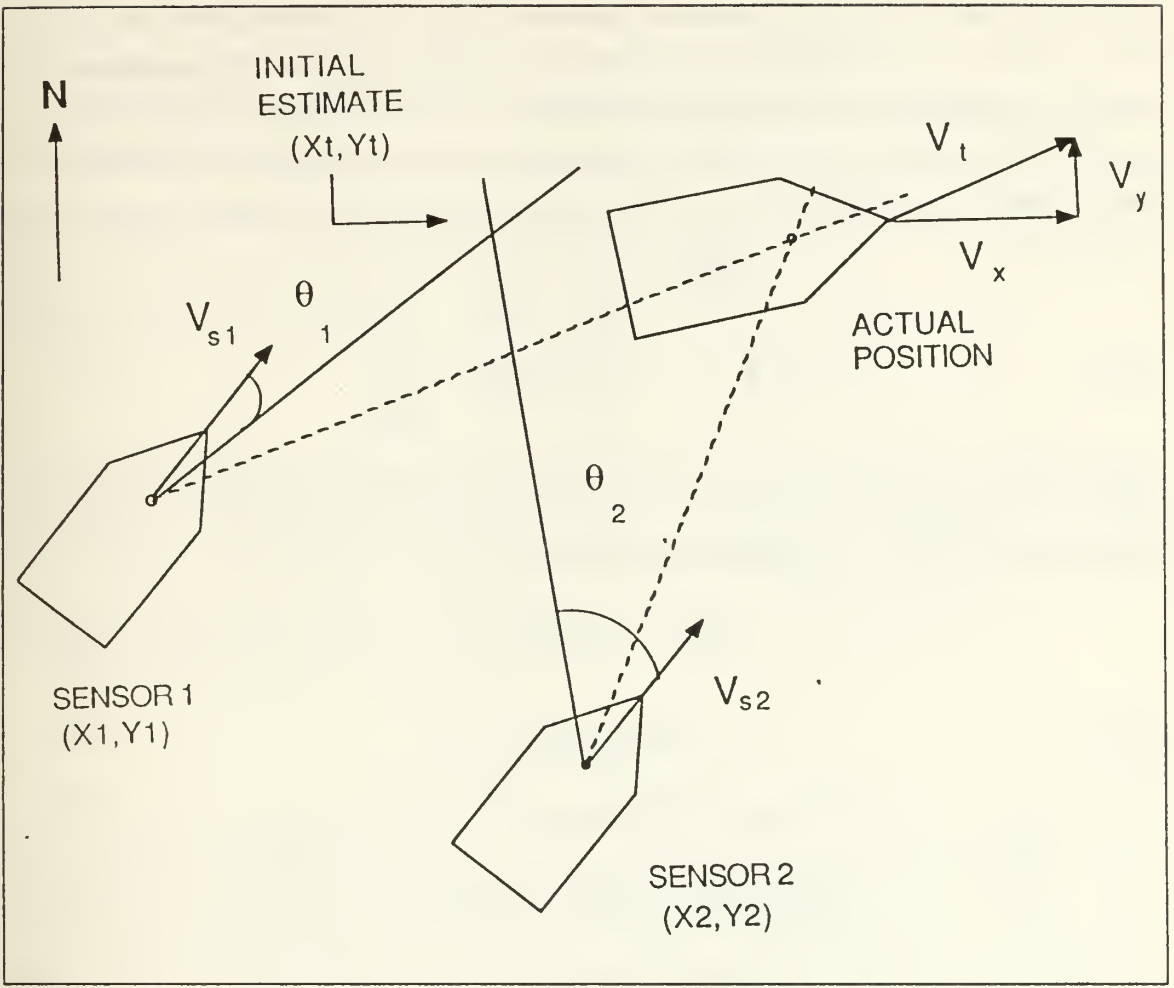


Figure 4. Initialization Process

The state estimates are the target's  $x$  and  $y$  position and the  $x$  and  $y$  components of the velocity. The initial position estimate [Ref. 7: p. 11] is the intersection of the first two lines-of-bearing received by the filter and can be calculated as

$$x_t = \left[ -\frac{y_2 \tan(\theta_2) + y_1 \tan(\theta_1) + x_2 - x_1}{\tan(\theta_1) - \tan(\theta_2)} - y_1 \right] \times \tan(\theta_1) + x_1 \quad (3.30)$$

$$y_t = -\frac{y_2 \tan(\theta_2) + y_1 \tan(\theta_1) + x_2 - x_1}{\tan(\theta_1) - \tan(\theta_2)} \quad (3.31)$$

The initial velocity estimate is taken to be zero since there is no velocity information available to start the problem. The initial state estimates carry with them some error

and it is this error or rather an estimate of this error that is used to construct the initial error covariance matrix. The initial position error is estimated to be 100 nautical miles in the  $x$  and  $y$  position and the initial velocity estimate is taken to be 0.5 nautical miles per minute or 30 knots. The errors are assumed to be zero mean and uncorrelated. Given these error approximations, the initial error covariance matrix can be written as

$$P_{(0|-1)} = \begin{bmatrix} 10000 & 0 & 0 & 0 \\ 0 & 0.25 & 0 & 0 \\ 0 & 0 & 10000 & 0 \\ 0 & 0 & 0 & 0.25 \end{bmatrix} \quad (3.32)$$

The basic operation of the filter is a relatively straightforward recursive process. The equations used in the extended Kalman filter are

$$\hat{\underline{x}}_{(k|k-1)} = \phi_k \hat{\underline{x}}_{(k|k)} \quad (3.33)$$

$$P_{(k|k-1)} = \phi_k P_{(k|k)} \phi_k^T + Q_k \quad (3.34)$$

$$G_k = P_{(k|k-1)} H_k^T (H_k P_{(k|k-1)} H_k^T + R_k)^{-1} \quad (3.35)$$

$$\hat{\underline{x}}_{(k|k)} = \hat{\underline{x}}_{(k|k-1)} + G_k (z_k - H_k \hat{\underline{x}}_{(k|k-1)}) \quad (3.36)$$

$$P_{(k|k)} = (I - G_k H_k) P_{(k|k-1)} \quad (3.37)$$

where

$\hat{\underline{x}}_{(k|k-1)}$  = projected ahead state estimate

$\phi_k$  = state transition matrix given by eq. (2.3)

$P_{(k|k-1)}$  = projected ahead state error covariance matrix

$Q_k$  = state excitation covariance matrix given by eq. (3.15)

$G_k$  = Kalman gain matrix

$R_k$  = state measurement noise covariance matrix given by eq. (3.14)

$H_k$  = linearized measurement matrix given by eq. (3.12).

Once the filter is initialized, we are ready to begin the data processing operation. The a priori state estimate and the state error covariance matrix are calculated using the  $\phi$  matrix shown in equation (2.3) where  $T$  is the time difference in minutes between the observed lines-of-bearing. (It is assumed that the lines-of-bearing are received simul-

taneously by both sensors.) Once the projected state estimate has been calculated, it is used to calculate the linearized observation matrix in equation (3.12).

The Kalman gain matrix serves to minimize the mean square estimation error and is an indication of how much emphasis or weight will be placed on the current observation. If  $P_{(k|k-1)}$  is small, the Kalman gain matrix will also be small due to the finite value of  $R_k$ . If the  $P_{(k|k-1)}$  is relatively large, the gain is approximately one. By rewriting the equation for the calculation of the state estimate, equation (3.36) as

$$\hat{\underline{x}}_{(k|k)} = (1 - G_k H_k) \hat{\underline{x}}_{(k|k-1)} + G_k \underline{z}_k \quad (3.38)$$

we can see how the Kalman gain matrix directly affects the weight placed on the current observation  $\underline{z}_k$ . A large gain, indicating a large error covariance, will place more weight on the current observation as the filter tries to correct the states. A small gain, indicating a small error covariance, places less emphasis on the new observation.

If the Kalman gain is expressed as

$$G_k = P_{(k|k-1)} H_k^T R_k^{-1} \quad (3.39)$$

it can be seen that the gain matrix is "proportional" to the uncertainty in the estimate  $P_{(k|k-1)}$  and "inversely proportional" to the measurement noise  $R_k$ . For a large  $R_k$  and a small  $P_{(k|k-1)}$ , the measurement noise ( $\underline{z}_k$ ) in equation (3.4) is due mainly to noise and only small corrections should be made in the state estimate. However, if  $R_k$  is small and  $P_{(k|k-1)}$  is large, the measurement noise contains considerable information about the errors in the estimates and therefore a strong correction should be made to the state estimates. [Ref. 5 : p. 127-8]

## E. MANEUVER AND DIVERGENCE DETECTION

The extended Kalman filter used in the tracking scenario is defined as an adaptive or self-learning filter due to its ability to manipulate the process parameters ( $\phi_k$ ,  $H_k$ ,  $R_k$ , and  $Q_k$ ) that change with time. If the model of the dynamic process under consideration is inaccurate, the filtered estimates tend to walk off from, or diverge from, the true estimates. As the filter locks on to these inaccurate estimates, the state error covariance matrix gets very small which in turn causes the filter gain to decrease. When the filter gain decreases, less weight is placed on the current observations and the filter is unable to make the corrections required to correct the state estimates. The divergence problem can be detected by monitoring the filter residual process.

The residual process of the extended Kalman filter is defined as the difference between the observation at time  $t_k$  and the output of the system model based on past inputs up to time  $t_k$ . The residuals are a measure of how well the model fits the data. From equation (3.36), the residual process is

$$z_k - H_k \hat{x}_{(k|k-1)} \quad (3.40)$$

There are several techniques used to compensate for divergence. Bennett [Ref. 7: p. 14-16], observes the three most recent residual values using a moving average filter and computing the standard deviation of the residual process. It is determined that the target has maneuvered if the standard deviation exceeds a maneuver detection threshold value. The window of the moving average filter is wide enough to absorb excessive bearing errors that are far outside the standard deviation but narrow enough to detect a target maneuver soon after it occurs. This detection threshold was chosen to achieve a 90% probability of detecting a maneuver with a 10% false alarm rate.

The maneuver and divergence technique implemented in this thesis is an adaptive noise estimation technique presented by Jazwinski [Ref. 8: pp. 311-315], and utilized by Olcovich [Ref. 9: pp. 30-33]. This technique examines the residual of each observation and compares the residual value to an adaptive gate where the adaptive gate is defined as three times the predicted residual standard deviation. Defining the variance of the residual [Ref. 8: p.271] as

$$r_{(k|k+1)} = H_k P_{(k|k-1)} H_k^T + R_k \quad (3.41)$$

The predicted residual standard deviation is

$$\sigma_k = \sqrt{r_{(k|k+1)}} = \sqrt{H_k P_{(k|k-1)} H_k^T + R_k} \quad (3.42)$$

and the adaptive gate becomes

$$GATE = 3\sigma_k \quad (3.43)$$

For each observation, the residual is compared to the adaptive gate. If the residual value is less than the value of the adaptive gate, the filter continues on and processes the next observation. If the residual value is greater than the adaptive gate, the divergence detection and compensation algorithm begins.

The state excitation matrix,  $Q_k$ , is increased by increasing the elements along the main diagonal of the  $Q'_k$  matrix given by equation (3.16). The old a priori value of the error covariance matrix,  $P_{(k-1)}$ , given by equation (3.34), is increased by adding the new state excitation matrix to it. A new filter gain,  $G_k$ , and a new predicted residual variance,  $r_{(k-1)}$ , are then calculated using equations (3.35) and (3.41) respectively. By increasing  $Q_k$  and adding it to  $P_{(k-1)}$ , we prevent the state error covariance from becoming overly optimistic while at the same time increasing the Kalman filter gain to appropriately weigh the current observations. The larger predicted residual variance increases the width of the adaptive gate and opens the filter window to a larger bearing deviation. If this bearing deviation exceeds the adaptive window for three consecutive iterations using the same observation, the filter determines that the target has maneuvered and the filter parameters are reset.

In order to efficiently implement this maneuver/divergence detection process, the value of  $Q_k$  that is added to  $P_{(k-1)}$  must be carefully evaluated. If  $Q_k$  is increased too much,  $P_{(k-1)}$  will grow without bound resulting in a highly unstable filter. This value of  $Q_k$  should be sufficiently high in order to open the adaptive gate wide enough to account for a random noisy bearing without indicating a target maneuver, and yet low enough so that a maneuvering bearing will be outside the filter window and the maneuver will be detected. A more sensitive filter, one with a narrow adaptive gate that would be exceeded rather frequently by noisy bearings, will give a higher number of "false alarms" or indications that the target has maneuvered when it actually has not. On the other hand, a less sensitive filter will tend to "miss" a target maneuver more often, due to the larger window of the adaptive gate. However, it will also provide fewer erroneous target maneuver indications. The idea is to design the adaptive gate parameters in order to optimize the number of actual target maneuver detections, to minimize the number of erroneous indications, and to prevent the filter from becoming unstable.

For the ship tracking scenario, the state excitation matrix  $Q_k$  was increased by increasing the coefficients along the main diagonal of the  $Q'_k$  matrix by a factor of 2.5. These coefficients account for the random course and speed changes of the target. The multiplicative constant of 2.5, found by trial and error, increases the width of the adaptive gate by three percent for each iteration.

The advantage of using this divergence algorithm over the moving average process used in Ref. 7, is that a target maneuver can be detected with one observation as opposed to three observations required in the previous filtering algorithm. This advantage also poses a serious defect in that the divergence/maneuver detection decision is based



on only one residual and, therefore, has little statistical significance. This can be corrected with the smoothing algorithm. [Ref. 8 : p. 313]

## F. SMOOTHING ALGORITHM

Smoothing is an off-line procedure that uses all the state estimates produced by an estimator and attempts to improve the accuracy of these estimates by using more measurements to produce the smoothed estimate. The estimator used in this thesis is the extended Kalman filter described above. The basic idea behind smoothing is that for a time interval from 0 to  $K$ , an estimate at time  $k$  based on all previous estimates up to time  $K$ , ( $\hat{x}_{(k|K)}$ ), will be more accurate than an estimate based only on the estimates up to time  $k$ , ( $\hat{x}_{(k|k)}$ ).

Meditch [Ref. 10: p. 193] categorizes smoothing algorithms into three particular groups.

*Fixed Point Smoothing* smooths the estimate  $\hat{x}_{(k|K)}$  at a fixed point  $k$  as  $K$  increases.

*Fixed Lag Smoothing* smooths the estimate  $\hat{x}_{(k-N|K)}$  for a fixed delay  $N$  as  $K$  increases.

*Fixed Interval Smoothing* smooths the estimate  $\hat{x}_{(k|K)}$  over the time interval from 0 to  $K$  where  $K$  is fixed and  $k$  varies from 0 to  $K$ .

This thesis uses a fixed-interval smoothing algorithm [Ref. 10: p. 216-224], to smooth the state estimates of the extended Kalman filter in the ship and storm tracking scenarios. This smoothing routine provides the optimal state estimate at each time  $k$  over a fixed interval from 0 to  $K$ . The smoothing algorithm is entered with the a priori and a posteriori estimates and their associated covariance matrices. The equations used in the smoothing algorithm are

$$A_k = P_{(k|k)} \Phi^T P_{(k+1|k)}^{-1} \quad (3.44)$$

$$\hat{\underline{x}}_{(k|N)} = \hat{\underline{x}}_{(k|k)} + A_k (\hat{\underline{x}}_{(k+1|N)} - \hat{\underline{x}}_{(k+1|k)}) \quad (3.45)$$

$$P_{(k|N)} = P_{(k|k)} + A_k (P_{(k+1|N)} - P_{(k+1|k)}) A_k^T \quad (3.46)$$

where

$A_k$  = smoothing filter gain matrix

$\hat{\underline{x}}_{(k|N)}$  = smoothed state estimate at time  $k$  based on  $N$  observations

$P_{(k|N)}$  = smoothed state error covariance matrix.



At the start of the smoothing routine, the last filtered estimate becomes the first smoothed estimate. The index  $k$  in equations (3.44-46) is decremented by one for each pass through the smoother with the beginning value of  $k$  equal to the number of data points to be smoothed, minus one ( $N - 1$ ). Consequently, the program makes  $N - 1$  passes through the smoothing algorithm.

## IV. COMPUTER SIMULATIONS

### A. GENERAL

The SHIPTRACK extended Kalman filter program used in Ref. 7 was originally implemented on an Apple Macintosh Plus microcomputer. This program was modified and adapted to run on an IBM PC. A complete listing of the SHIPSM.FOR extended Kalman filter and fixed interval smoothing algorithm is included in Appendix A. The general scenario used in all of the computer simulation cases is that of two tracking ships moving in the general direction of the target ship. The track data required by SHIPSM.FOR for each scenario was generated using the program [Ref. 7] TRACKDATA.FOR. This program calls for the initial course, speed, and position of the two tracking ships and the target ship, the time of each HFDF interception, and any course and speed changes of the target. (The course and speed of the tracking ships is held constant throughout each simulation run.) The atmospheric noise is added to the observed HFDF line-of-bearing in the TRACKDATA.FOR routine. It generates an output file called TRKDATA.DAT that contains the time of each observation, the position of each tracking ship at each observation, and the angle of reception of each HF intercept. This is the input file for the filter and smoothing algorithm. SHIPSM.FOR generates four output files. FILDATA.DAT and SMDATA.DAT contain the track information and the files ELLIP.DAT and ELLIPS.DAT contain the data required to plot the error ellipses for the filtered and the smoothed positions respectively. The error ellipses provide a graphical representation of the accuracy of the estimate.

The error ellipses generated [Ref. 7: pp. 16-17] by the filter and smoothing algorithm represent an area where the probability of the target's true position being within the ellipse is 68%. The error ellipses are plotted for every fourth position on the overall track plot for each scenario (if the ellipses are plotted for every point the plots become too cluttered to be interpreted accurately). A smoothed observation generates a smaller error ellipse than the filtered estimate. This is due to the smaller error variances for the smoothed estimate compared to the error variances calculated for the filtered estimates and reflect the higher degree of confidence placed in the accuracy of the smoothed estimate. The last filtered estimate is equal to the first smoothed estimate and, therefore, the smoothed and filtered error ellipse for this point overlap.

Graphical results were obtained using the Matlab graphics package and the plots included are representative of the results obtained from the different tracking scenarios. The first graph is a geographical plot that compares the observed track, or the raw data, with the filtered and smoothed track data and is used to demonstrate the effect of the Kalman filter and the smoothing algorithm on the noisy data. The following two graphs present the position errors and the variance in the  $x$  direction associated with the track data. The last plot is included to give the reader an idea of how accurate the filtered and the smoothed tracks are when compared to the target's true track.

The computer simulations consisted of nine targeting scenarios as listed below.

- Scenario #1--maneuver toward tracking ships, no measurement noise
- Scenario #2--no maneuver, white noise model
- Scenario #3--no maneuver, Hall noise model
- Scenario #4--maneuver toward tracking ships, white noise model
- Scenario #5--maneuver toward tracking ships, Hall noise model
- Scenario #6--maneuver away from tracking ships, white noise model
- Scenario #7--maneuver away from tracking ships, Hall noise model
- Scenario #8--2 maneuvers away from tracking ships, white noise model
- Scenario #9--2 maneuvers away from tracking ships, Hall noise model

Scenarios one thru seven were started with the target ship at a position of  $(-75,150)$ , tracking ship #1 at a position of  $(-30,0)$ , and tracking ship #2 at a position of  $(30,0)$ . For scenarios eight and nine, the target ship started at the origin and the tracking ships were located at the above positions. The tracking ships were set on a course of  $000^\circ$  at 10 knots for each scenario. The speed of the target ship was held constant at 15 knots throughout the simulations. The data was collected over a ten hour time frame with the HF intercepts recorded at 30 minute intervals for a total of 21 intercepts for each simulation. All times are given in minutes.

The percent improvement in the position error due to the Kalman filter and the smoothing algorithm, is given for the different scenarios. This percentage was calculated by taking the percent of improvement,  $(\pm)$ , for each observation and then averaging these percentages over the time interval of interest. These values give a relative indication of the effectiveness or ineffectiveness of the filter and the smoother for a particular scenario.

## B. SCENARIO #1

The first tracking scenario was used to verify that the Kalman filter and the smoothing algorithm would accurately track a maneuvering target in a noiseless environment. The results for this scenario are shown in Figures 5-8. In this case, the observed track equals the true track due to the absence of noise in the bearing measurements. The initial track error shown in Figure 6 is due to the error in the initial state estimates. When the target maneuvers at 300 minutes, the tracking error increases dramatically for the first observation after the turn, however, it returns to zero two observations later as the filter regains the target track.

The error ellipses in Figure 8 demonstrate graphically how the accuracy of the position estimates increases as the problem progresses. At time zero, the tracking ships are approximately 150 nm southeast of the target. The large distance in the  $y$  direction is reflected in the size and orientation of the major axis of the ellipse lying in a southeasterly direction. As the tracking ships move north, the magnitude of the major axis decreases and the direction of this axis rotates as the target ship passes in front of the advancing tracking ships and eventually to the east of at a range of approximately 10 nm. At the end of the scenario, the tracking ships are located northeast of the target.

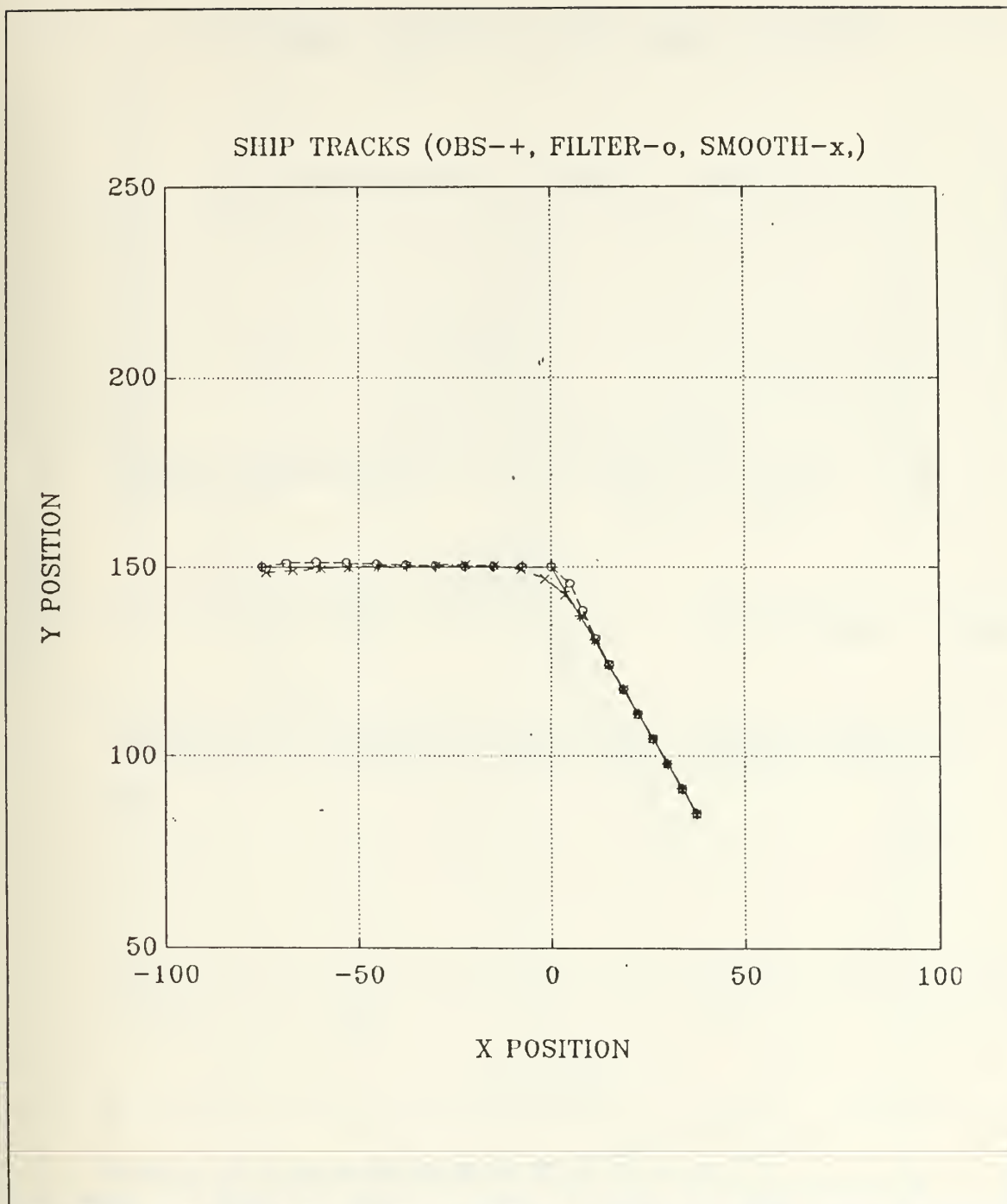


Figure 5. Processed Data vs Observed Results

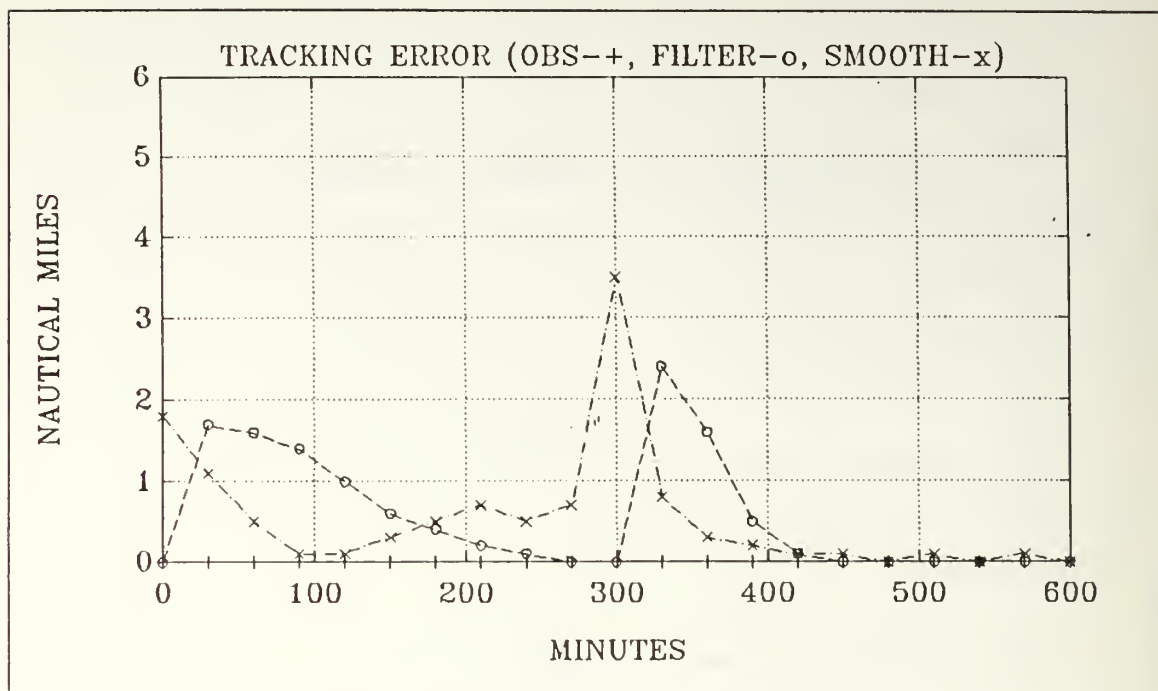


Figure 6. Position Error

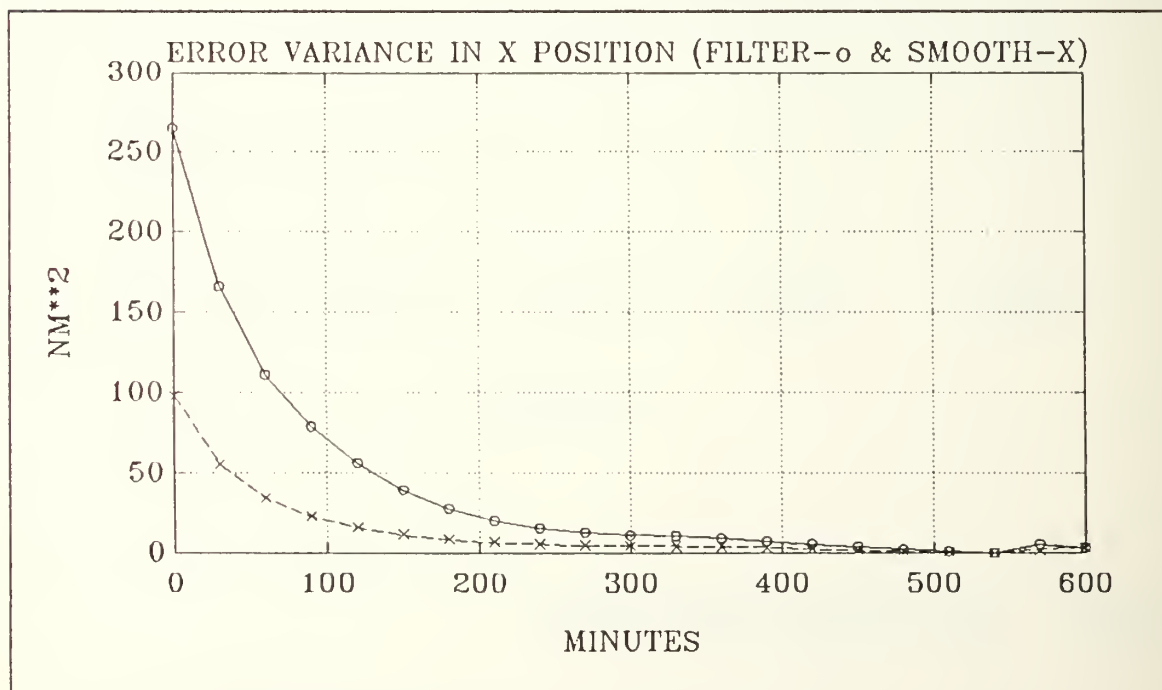


Figure 7. Variance of Position Error in the X Direction



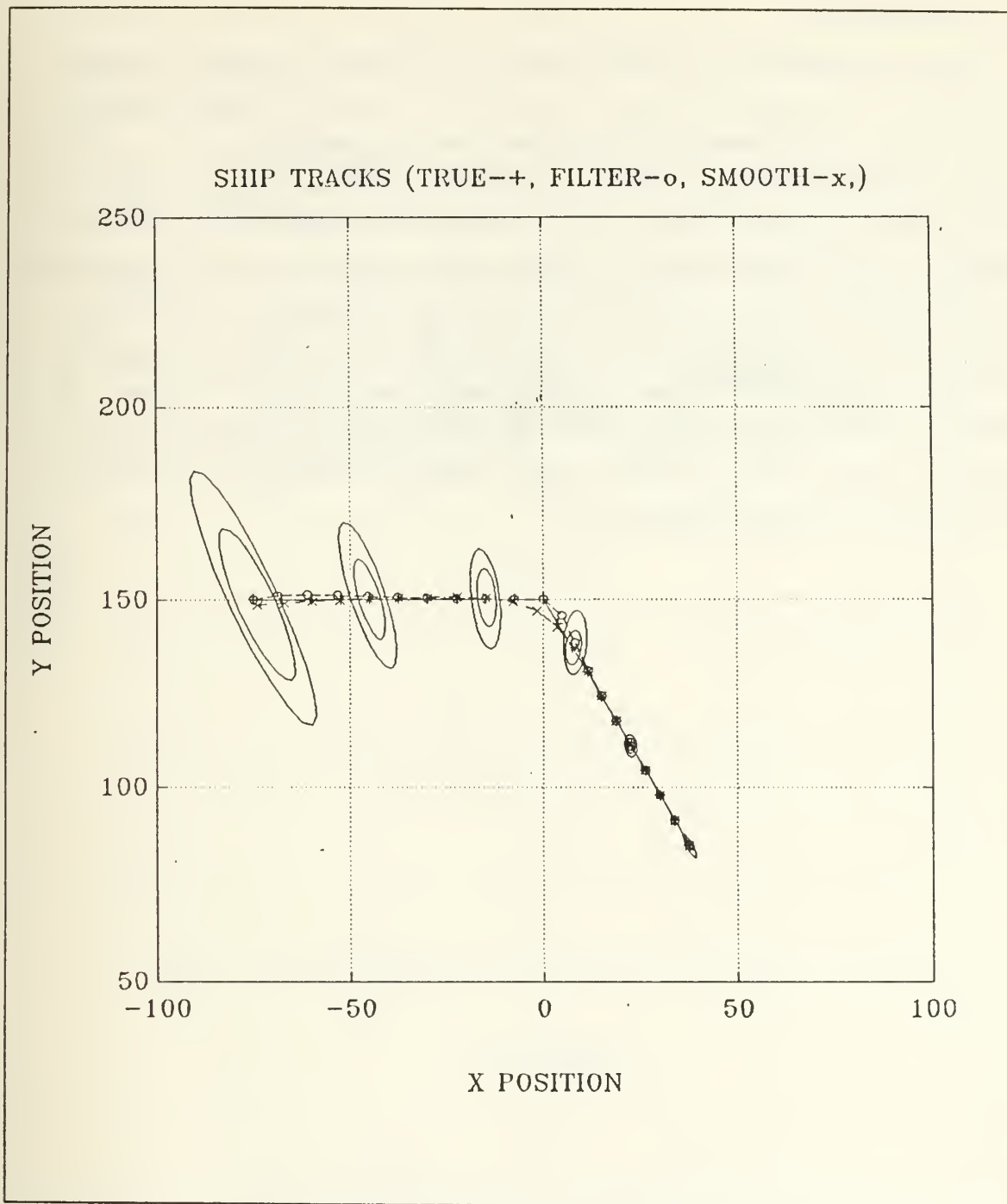


Figure 8. Scenario #1 Overall Track Results

### C. SCENARIO #2

In this case, the target is steaming due east at 15 knots for the entire simulation. The results for this scenario are shown in Figures 9-12. The HFDF lines-of-bearing are distorted using a white noise model to represent the atmospheric noise. The observed track, calculated by taking the intercept of the unfiltered lines-of-bearing, is shown in Figure 9. From this plot and the error plot of Figure 10, we can see how the extended Kalman filter and the fixed interval smoothing improve the overall track estimate and decrease the position error. The Kalman filter improves the position accuracy by an average of 22% and the smoother improves the position accuracy by an average of 53%. The filtered target speed is 19 knots and the smoothed target speed is 14.8 knots. The increased confidence in the accuracy of the smoothed estimates is reflected in the plot of the error variance in the  $x$  direction. Figure 12 shows the relationship of filtered and smoothed tracks to the true target track.

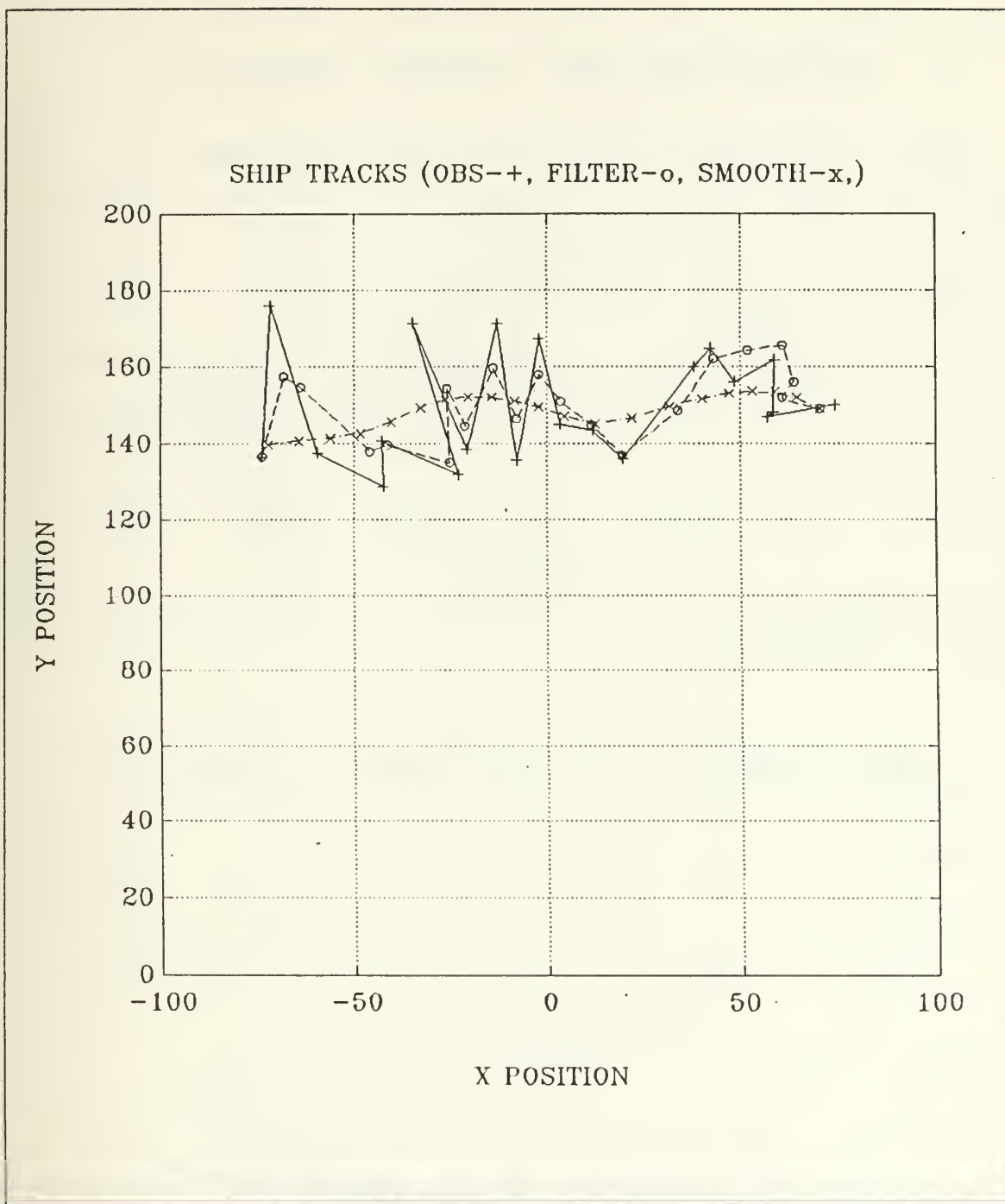


Figure 9. Processed Data vs Observed Results

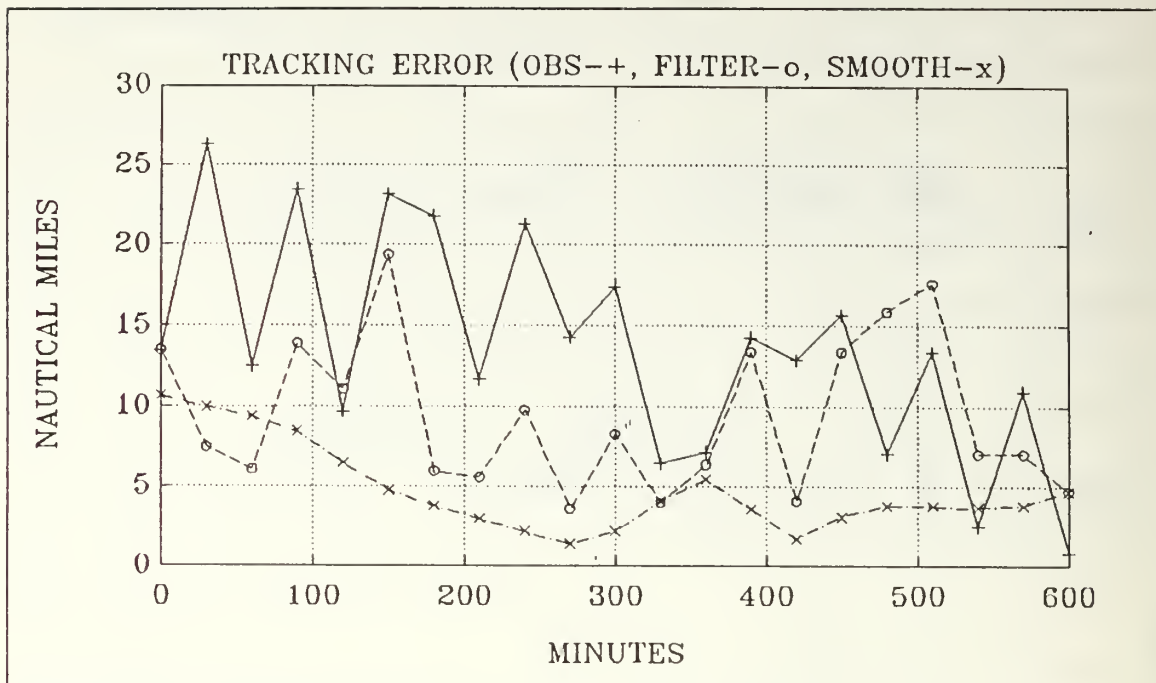


Figure 10. Position Error

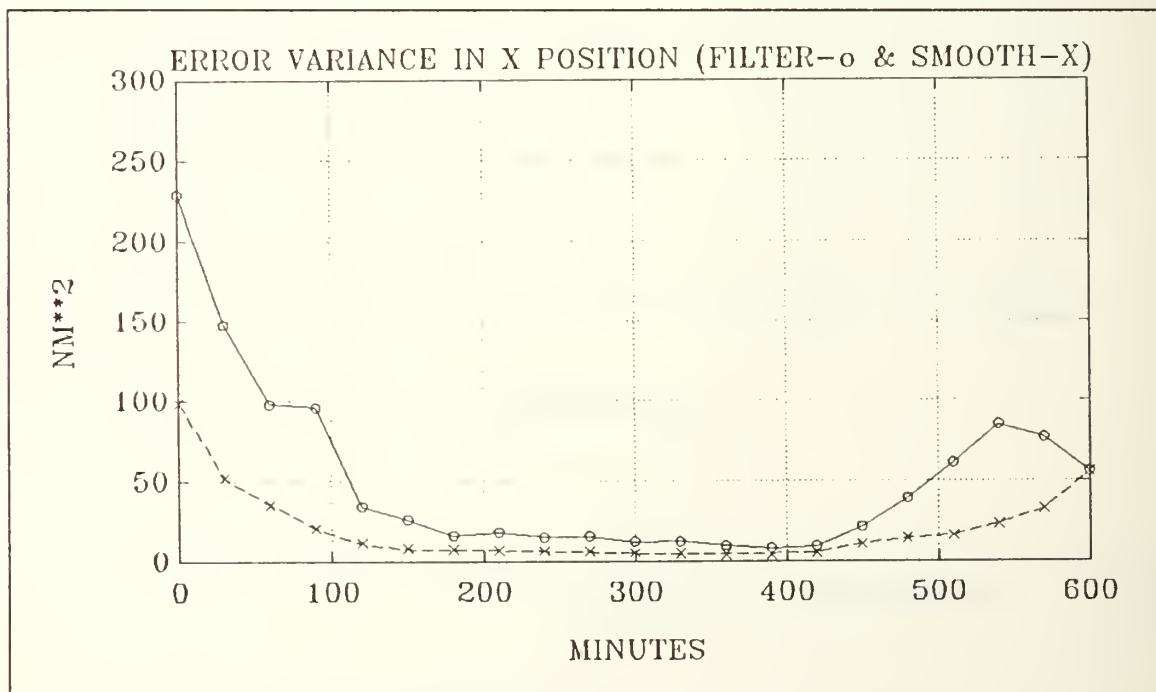


Figure 11. Variance of Position Error in the X Direction

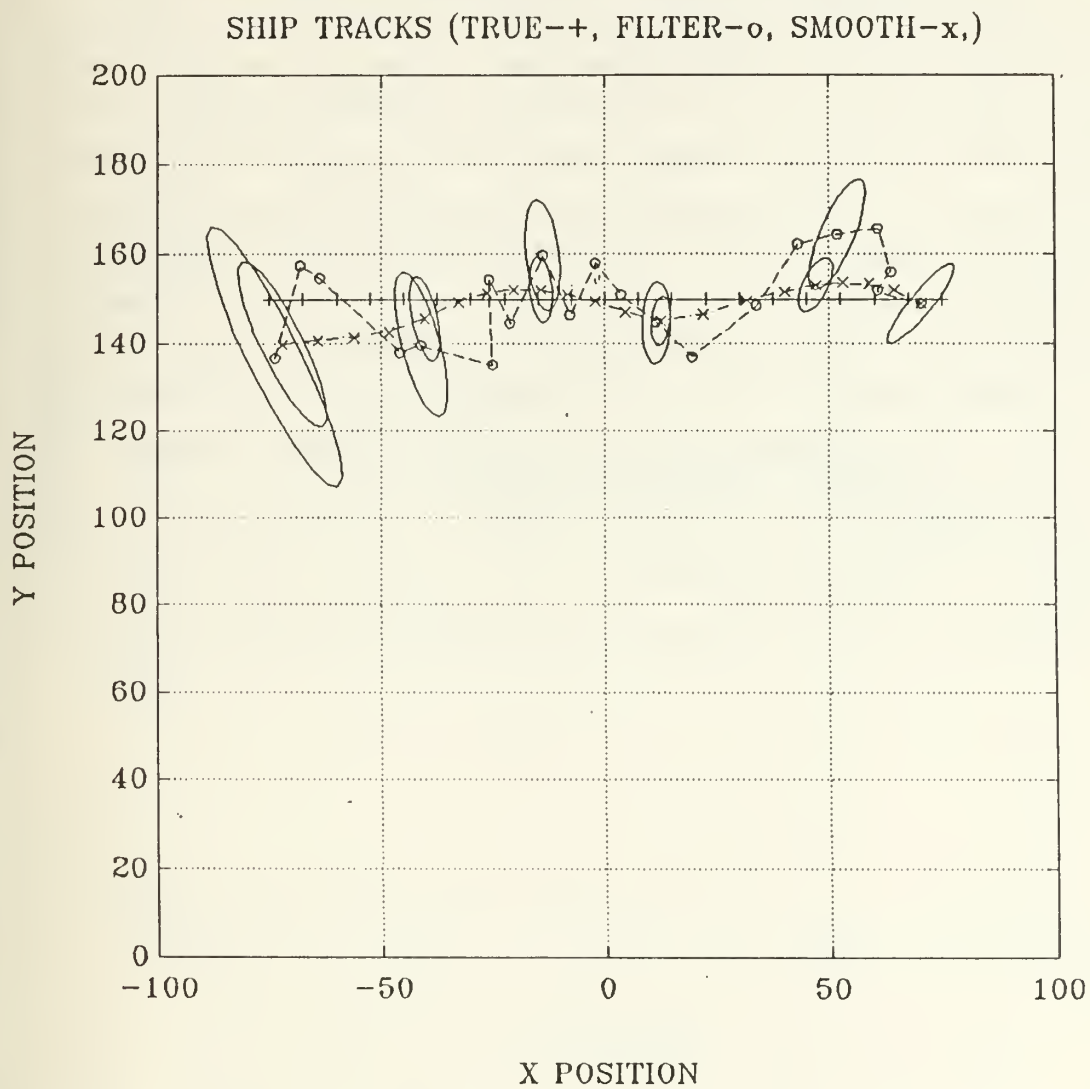


Figure 12. Scenario #2 Overall Track Results

#### D. SCENARIO #3

This scenario is the same as the previous one except that the white noise model is replaced by the Hall noise model. The results for this scenario are shown in Figures 13-16. The effects of the impulsive characteristics of this noise model are evident in the early part of this simulation. A "wild" bearing, due to a noise spike, occurs at time 90 resulting in a large position error. This causes the next three filtered estimates to be very inaccurate, however, the filter does begin to correct its track two observations after the noise spike occurred. It is interesting to see that the smoother just about eliminates the large tracking errors due to the erratic behavior of the Kalman filter. During the time interval from 90 to 240 minutes, the average position error of the filtered estimates is more than 850% worse than the observed position error while the average smoothed position error is less than 130% of the observed error. Even with this improvement, the position error is still greater than 20 nm and unacceptable for a long range missile attack. As the simulation progresses and the ships move toward each other, the track solution is refined and the track error remains inside of ten miles. The small noise spike at 570 minutes is completely smoothed by the smoothing algorithm. The average target speed estimated by the filter is 20.3 knots and the smoother refines that estimate to 17 knots.



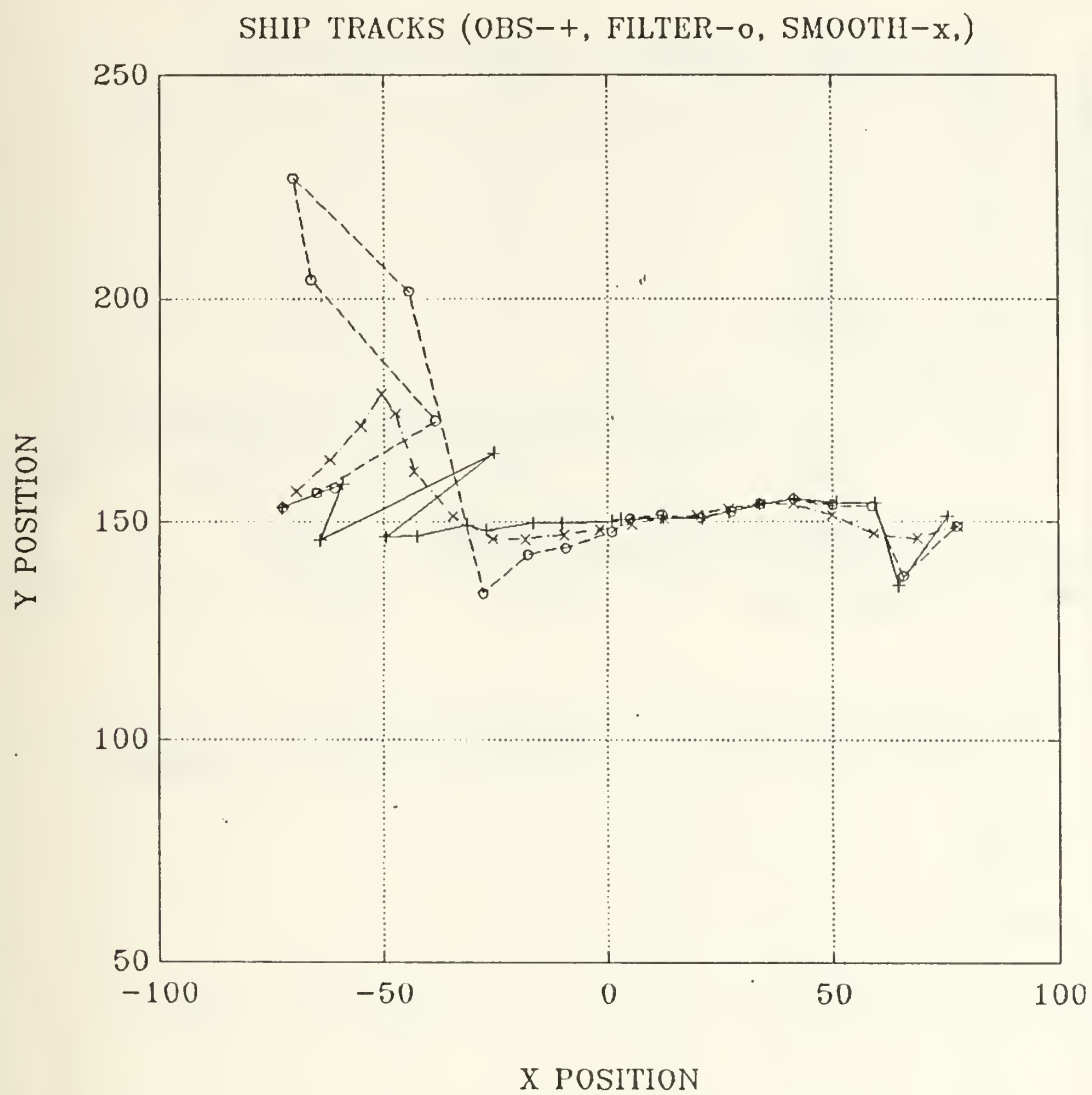


Figure 13. Processed Data vs Observed Results

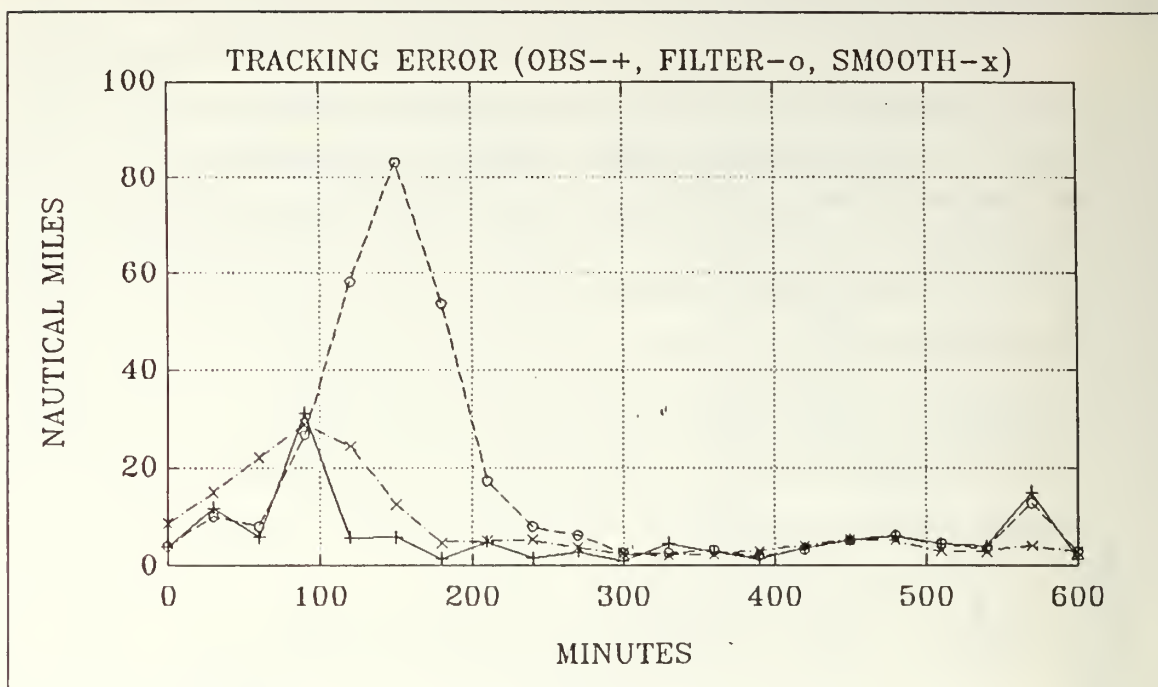


Figure 14. Position Error

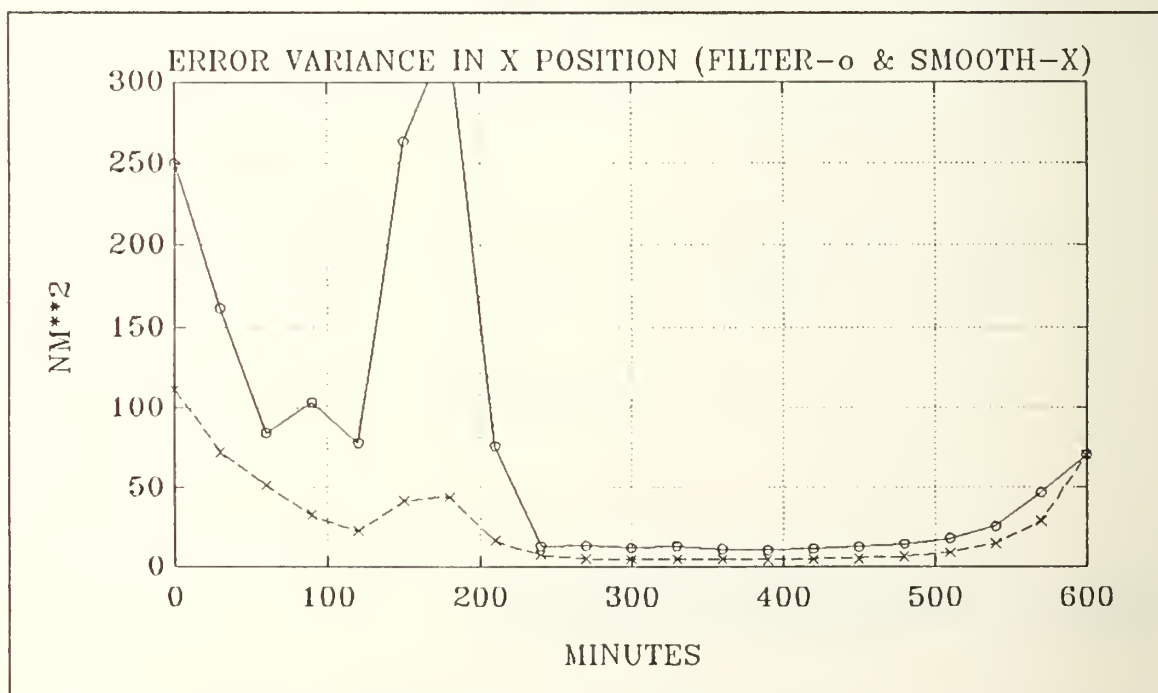


Figure 15. Variance of Position Error in the X Direction

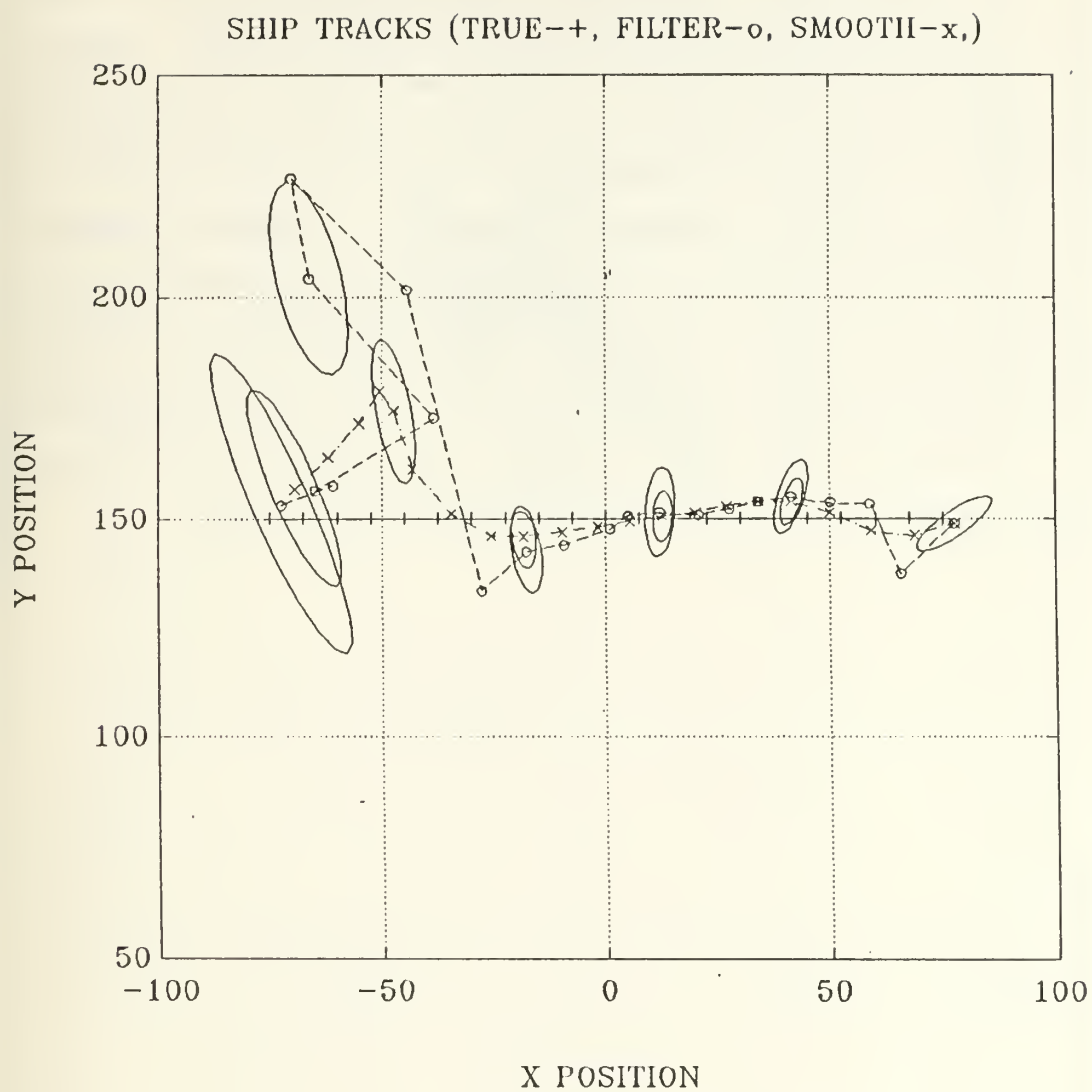


Figure 16. Scenario #3 Overall Track Results

#### E. SCENARIO #4

In this simulation, the target makes a  $60^\circ$  course change toward the advancing tracking ships five hours after the problem starts. The results for this scenario are shown in Figures 17-20. The atmospheric noise model in this case is white noise. As in Scenario 1, the initial error ellipses indicate the high degree of uncertainty in the position estimates, especially in the  $y$  direction where the range between the target ship and the tracking ships is the greatest. The average improvement in position error due to the filter for the entire simulation run was 24% and that due to the smoother was 28.5%. However, if we look at the first five hours of the problem, while the ships were still over 100 miles away from each other, the improvement due to the filter was 44.5% and the smoother improved the position accuracy by over 62%. After the target maneuvered, the vessels closed each other at a speed of 23 knots and the position error decreased rapidly. The Kalman filter tracked the target at an average speed of 16.5 knots throughout the problem and the smoothed speed estimate was 14.8 knots.

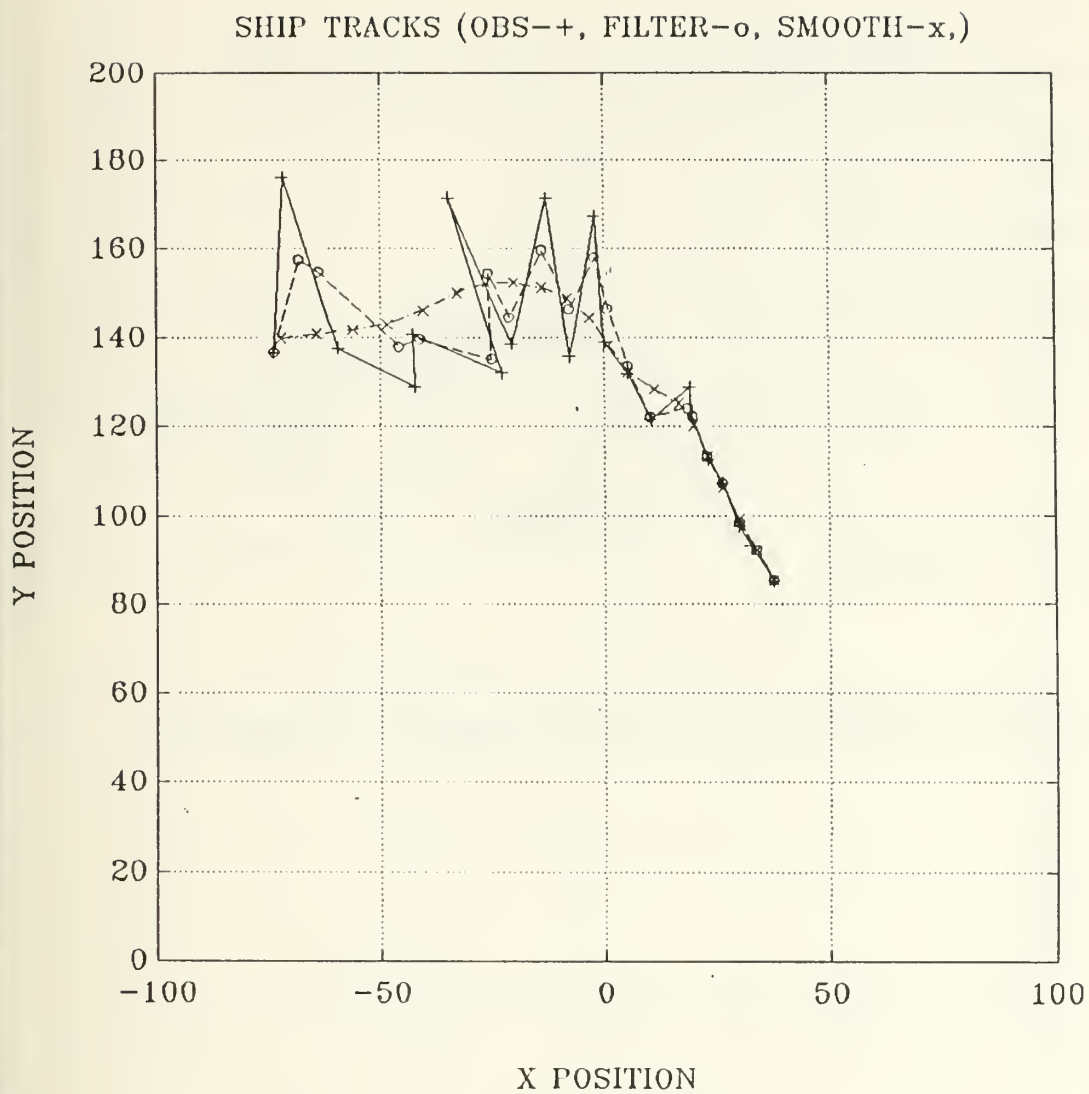


Figure 17. Processed Data vs Observed Results

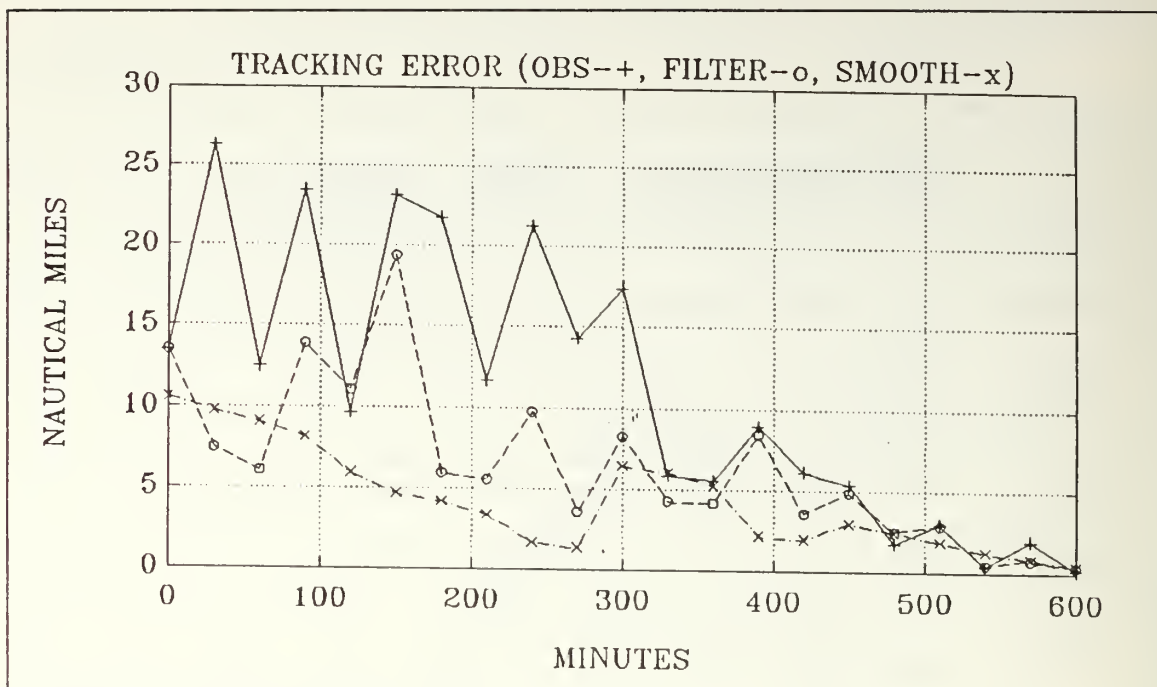


Figure 18. Position Error

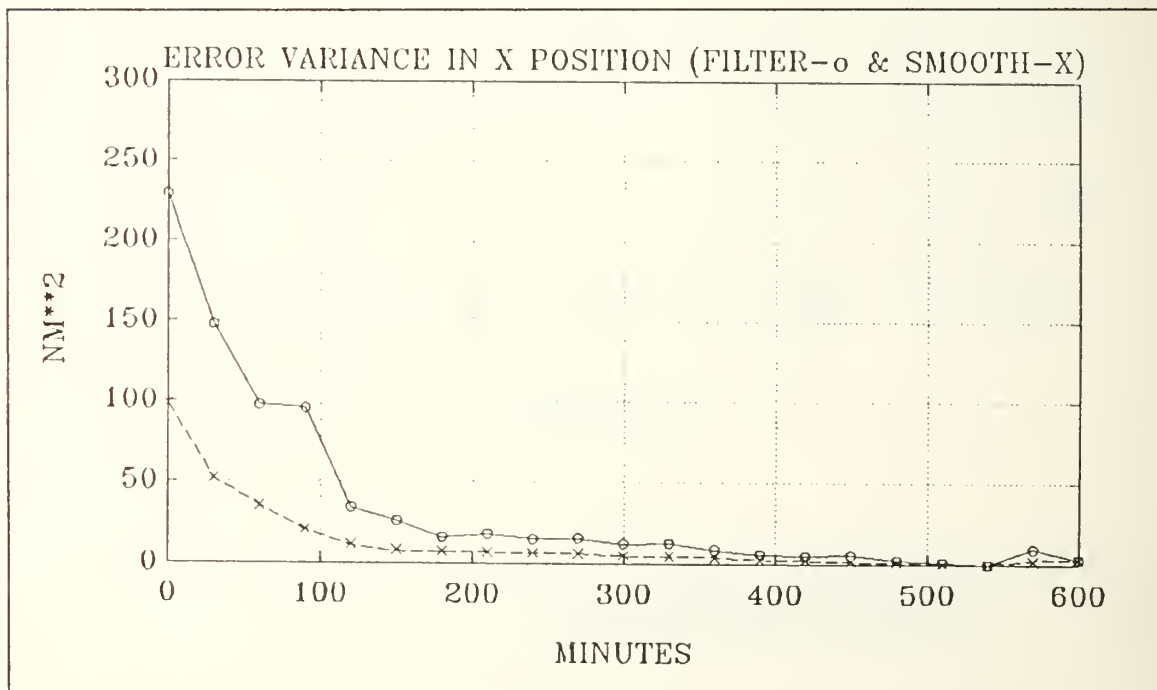


Figure 19. Variance of Position Error in the X Direction



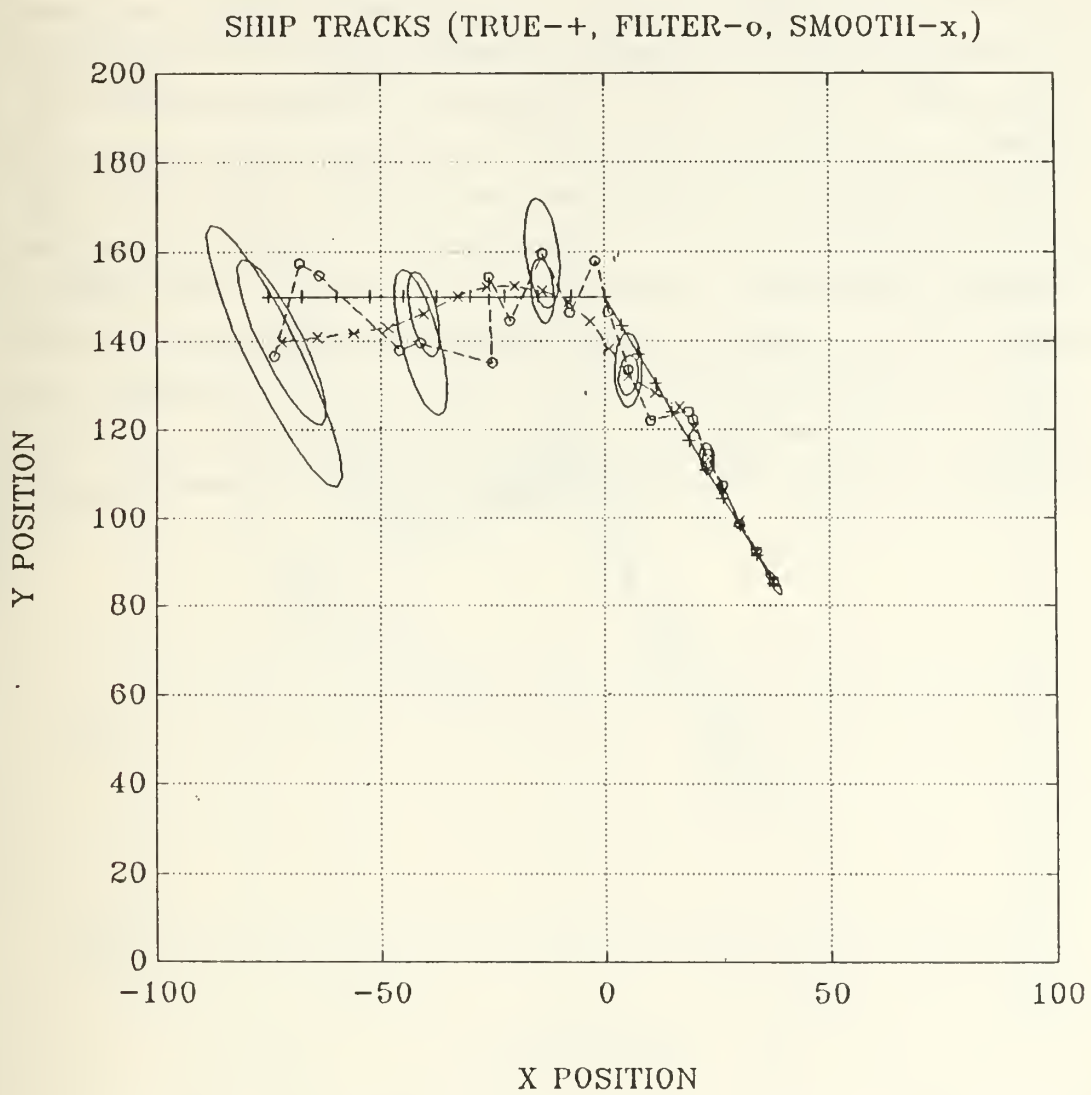


Figure 20. Scenario #4 Overall Track Results

## F. SCENARIO #5

The white noise model used in Scenario #4 is replaced by the Hall noise model for Scenario #5. The results for this scenario are shown in Figures 21-24. In this case, three noise spikes occur at observations one, three, and four as seen in Figure 21 and, therefore, the observed positions at these times are extremely inaccurate. The Kalman filter improved the position accuracy by 33% over these four observations while the improvement due to smoothing the estimates was 59%. A fourth noise spike occurred 270 minutes into the problem and although this was not as large as the first three spikes encountered, the filtered estimate is 46% better than the observed estimate and the smoothed estimate is 78% better. Due to the relatively low amplitude of the Hall noise model outside of the noise spikes, the filtered and smoothed position estimates show only a minor improvement in time frame from six to nine hours. The small noise spike at time 540 is pretty well smoothed out as seen in Figure 22. The average speed of the target estimated by the filter is 21 knots and the speed estimated by the smoother is 16.4 knots.

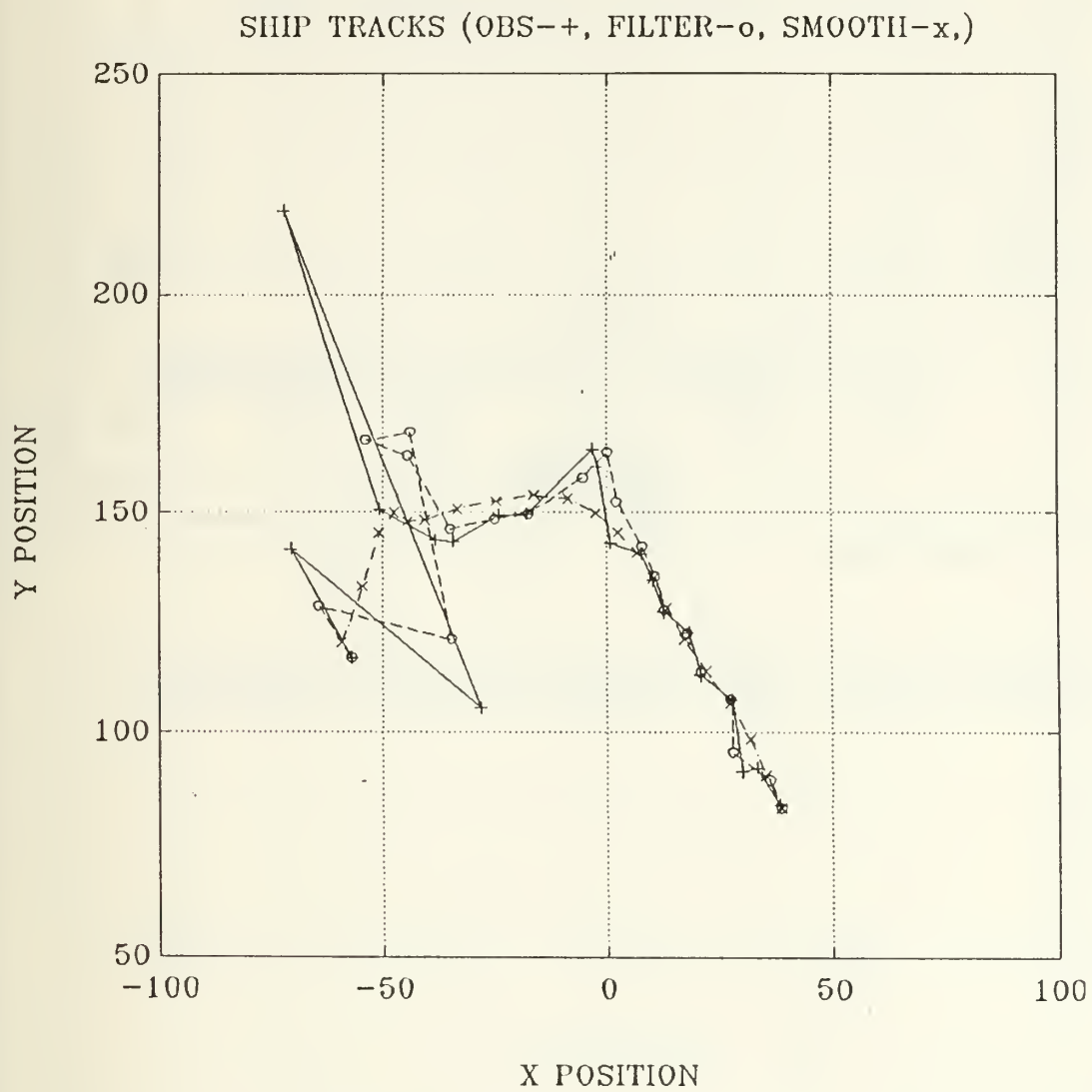


Figure 21. Processed Data vs Observed Results

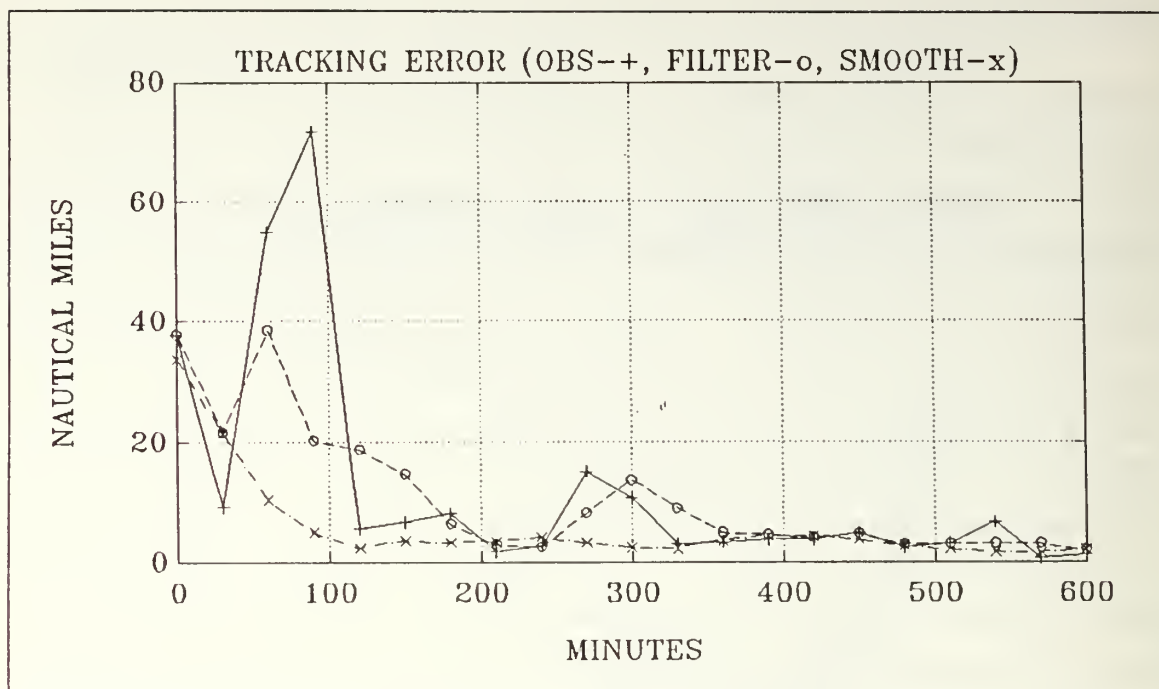


Figure 22. Position Error

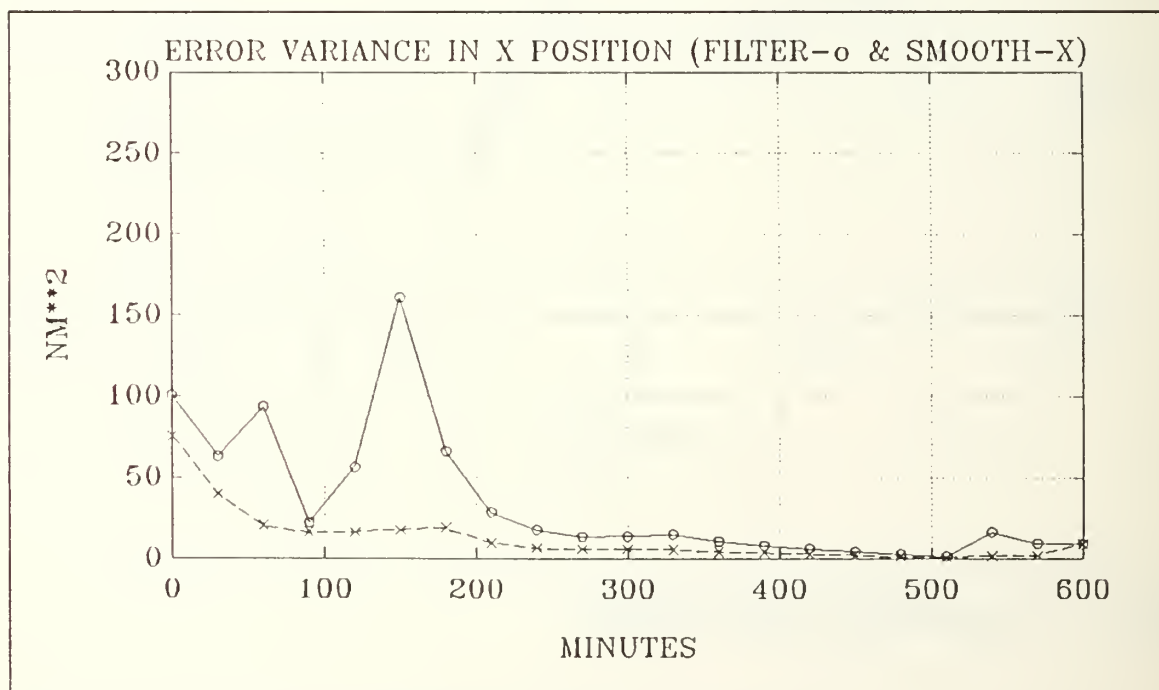


Figure 23. Variance of Position Error in the X Direction

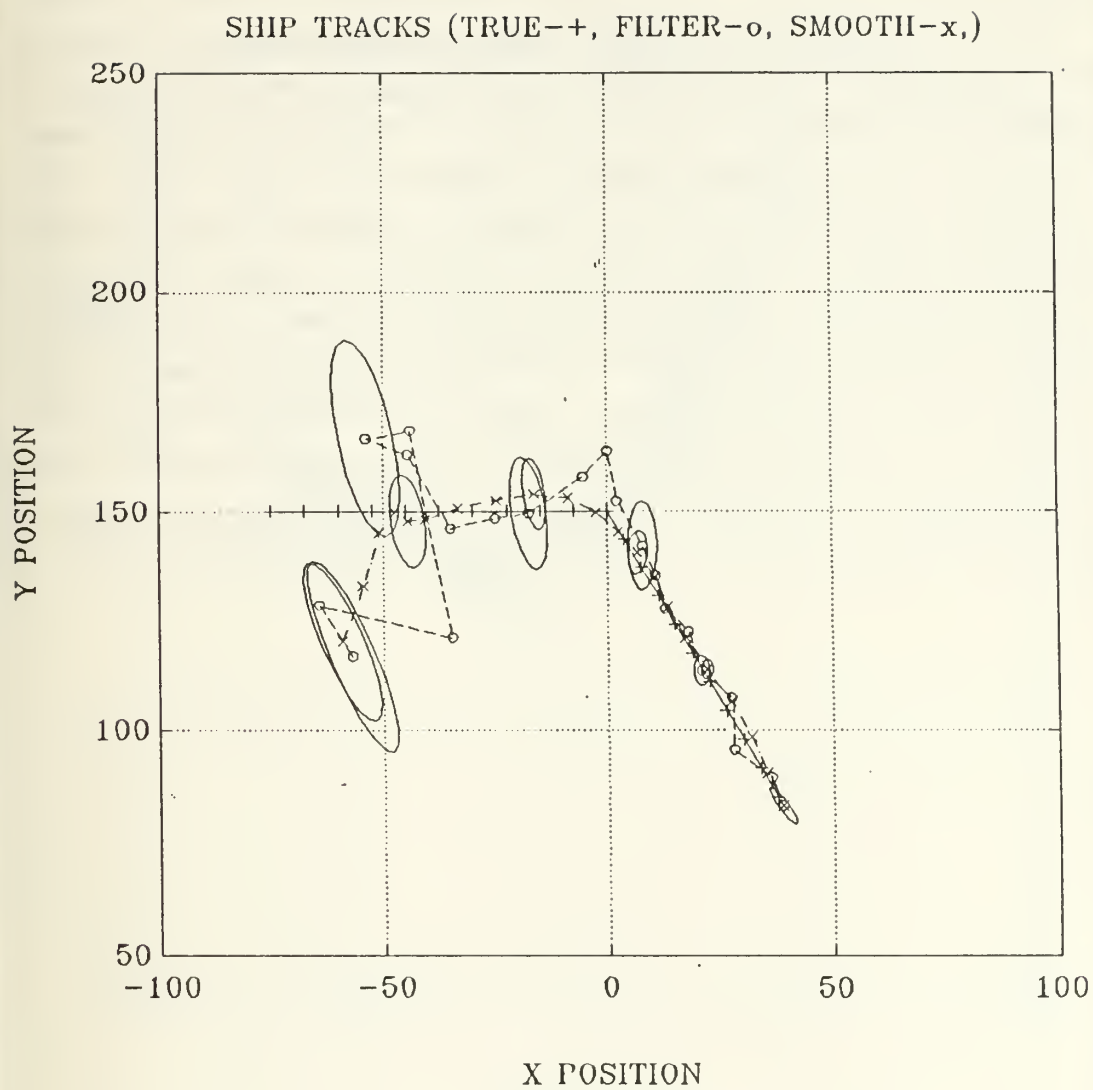


Figure 24. Scenario #5 Overall Track Results

## G. SCENARIO #6

This scenario depicts a  $60^\circ$  target maneuver to the northeast away from the two tracking ships heading due north. The results for this scenario are shown in Figures 25-28. The white noise model is used in this simulation and because the relative distance between the ships remains between 100 and 150 nm throughout the problem, the observed position error remains on the order of 10-20 nm. This case demonstrates a general improvement in the filtered and smoothed estimates over the entire track. The position accuracy was increased by 25% with Kalman filter and by 45% using the fixed interval smoothing routine. The smoother kept the track error at or below 8 nm for the entire track interval with the exception of the first three observations to be smoothed at times 600, 570, and 540. The average speed estimates for the filter and the smoother were 17.1 knots and 16.6 knots respectively. Figure 28 shows the orientation of the major axis lying in the north-south direction where the distance between the ships is the largest. The magnitude of this axis is the largest at the beginning and the end of the problem and at a minimum when the target maneuvers and ships are the closest together.



SHIP TRACKS (OBS-+, FILTER-o, SMOOTH-x,)

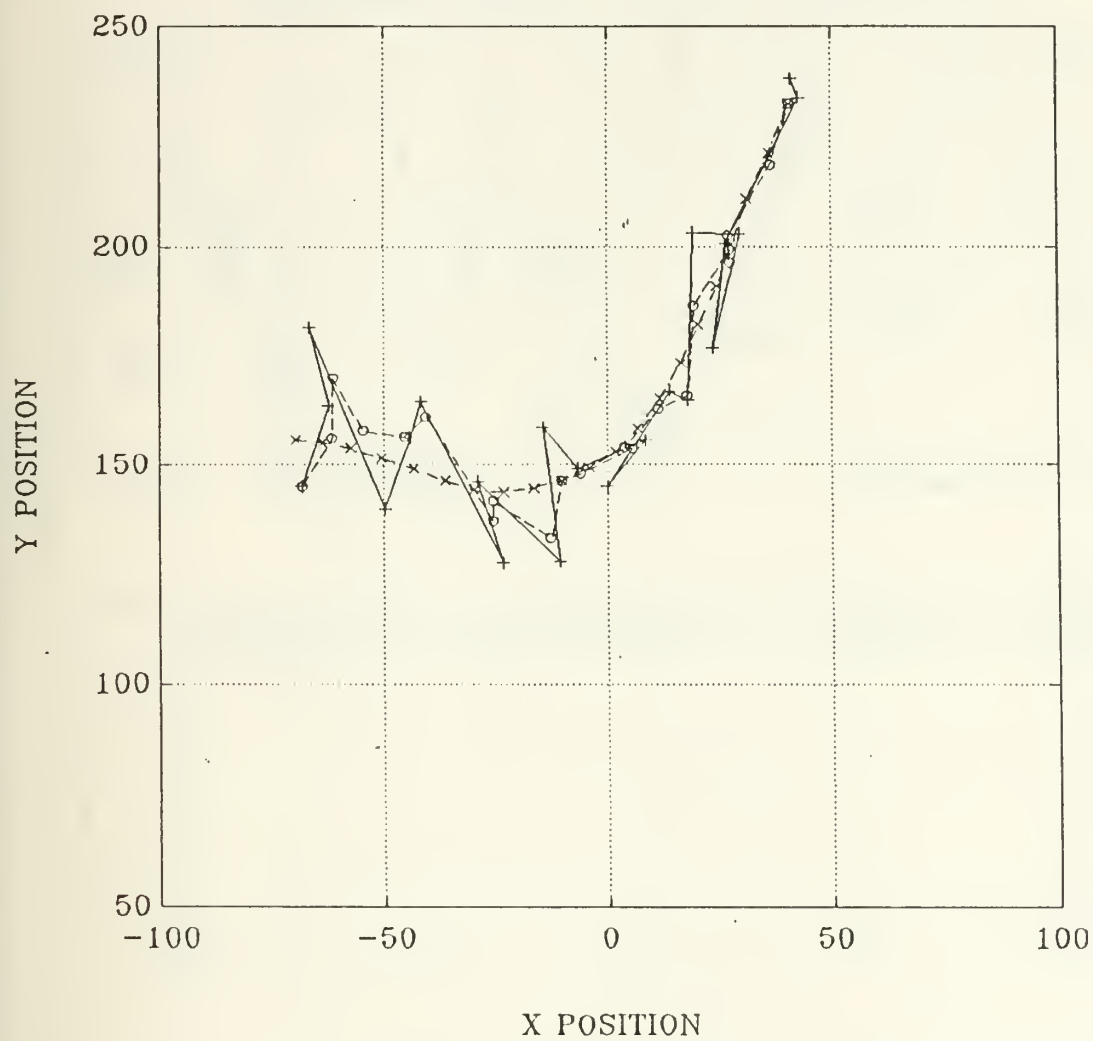


Figure 25. Processed Data vs Observed Results

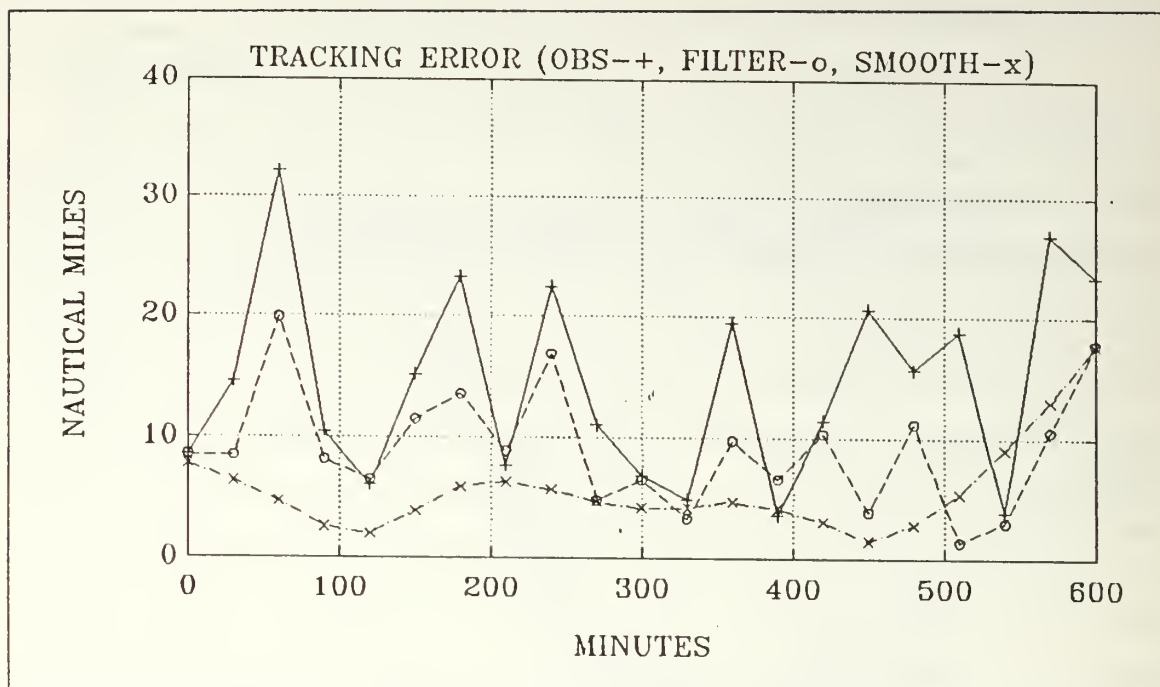


Figure 26. Position Error

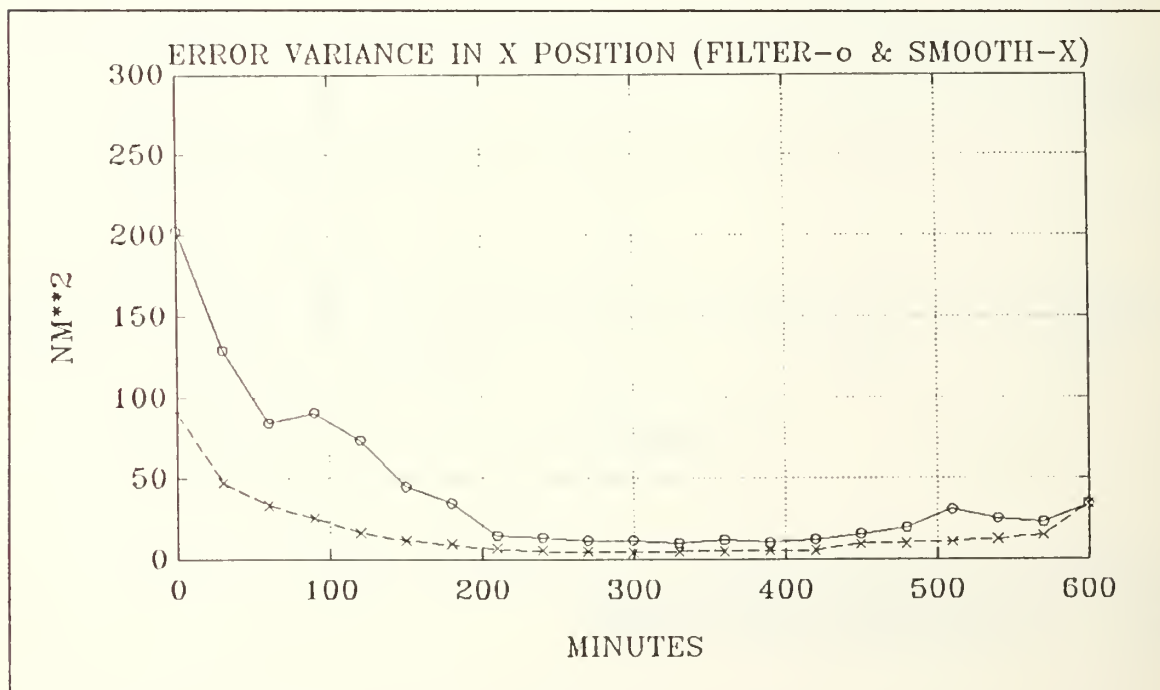


Figure 27. Variance of Position Error in the X Direction

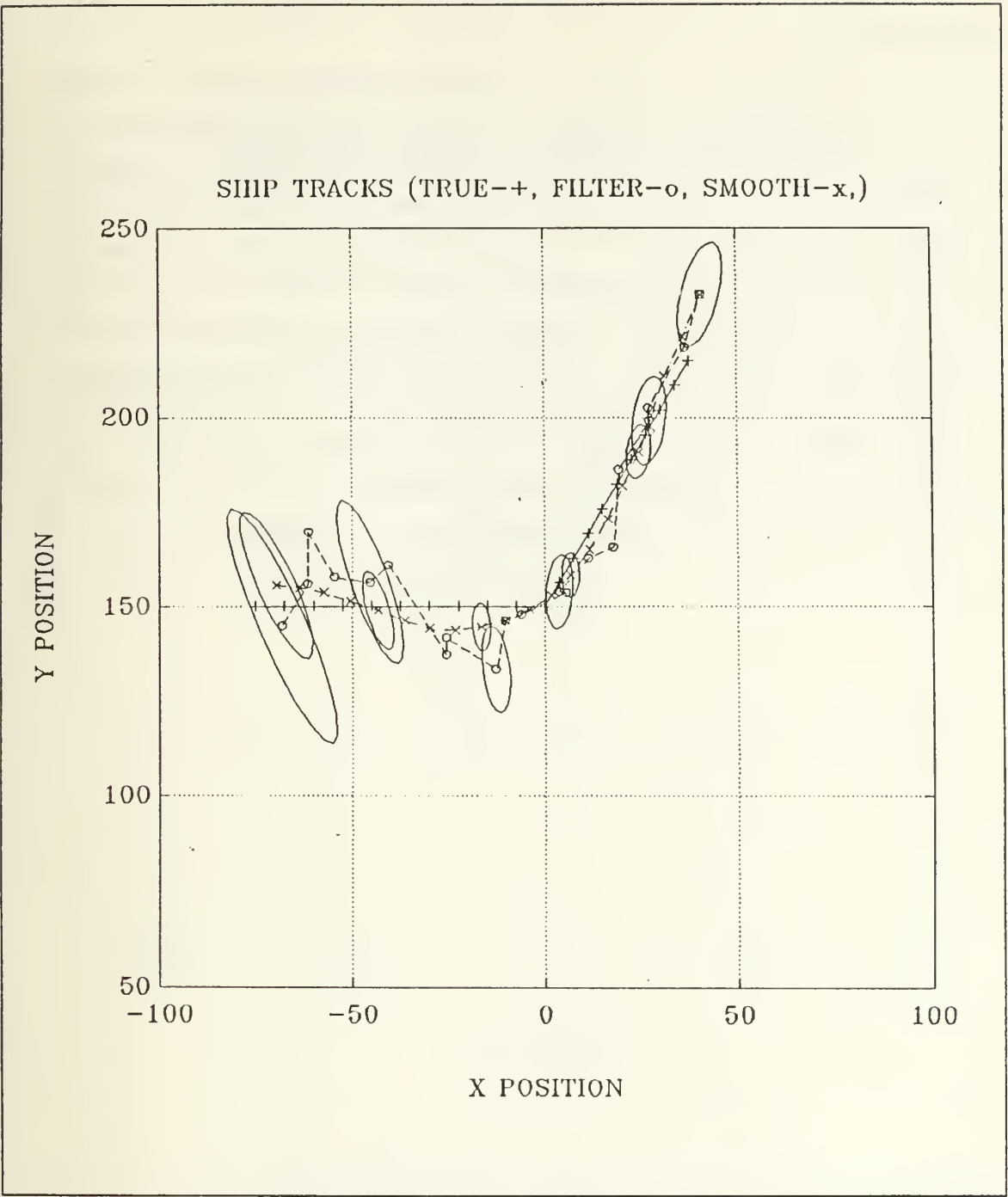


Figure 28. Scenario #6 Overall Track Results

## H. SCENARIO #7

In this case, the Hall model was used to model the atmospheric noise. The results for this scenario are shown in Figures 29-32. We can see three distinct noise spikes from the error plot in Figure 30 at 120, 330, and 510 minutes. For each of these times, the filtered estimate is better than the observed estimate and the smoothed estimate is the most accurate of all. At other times, however, the filtered and smoothed estimate are not the most accurate and in fact are sometimes (180, 360, & 450) much worse than the observed error. The advantage to be gained by using the Kalman filter and the smoothing routine in a case like this is the elimination of large, non-predictable errors caused by the impulsive characteristics of atmospheric noise. The smoothed position error remains between 2-11 nm throughout the problem while the filter position error has a range of 2-28 nm and the observed position error varies from 3-38 nm. Figure 32 shows the overall accuracy of the smoothed track compared to the target's true track.

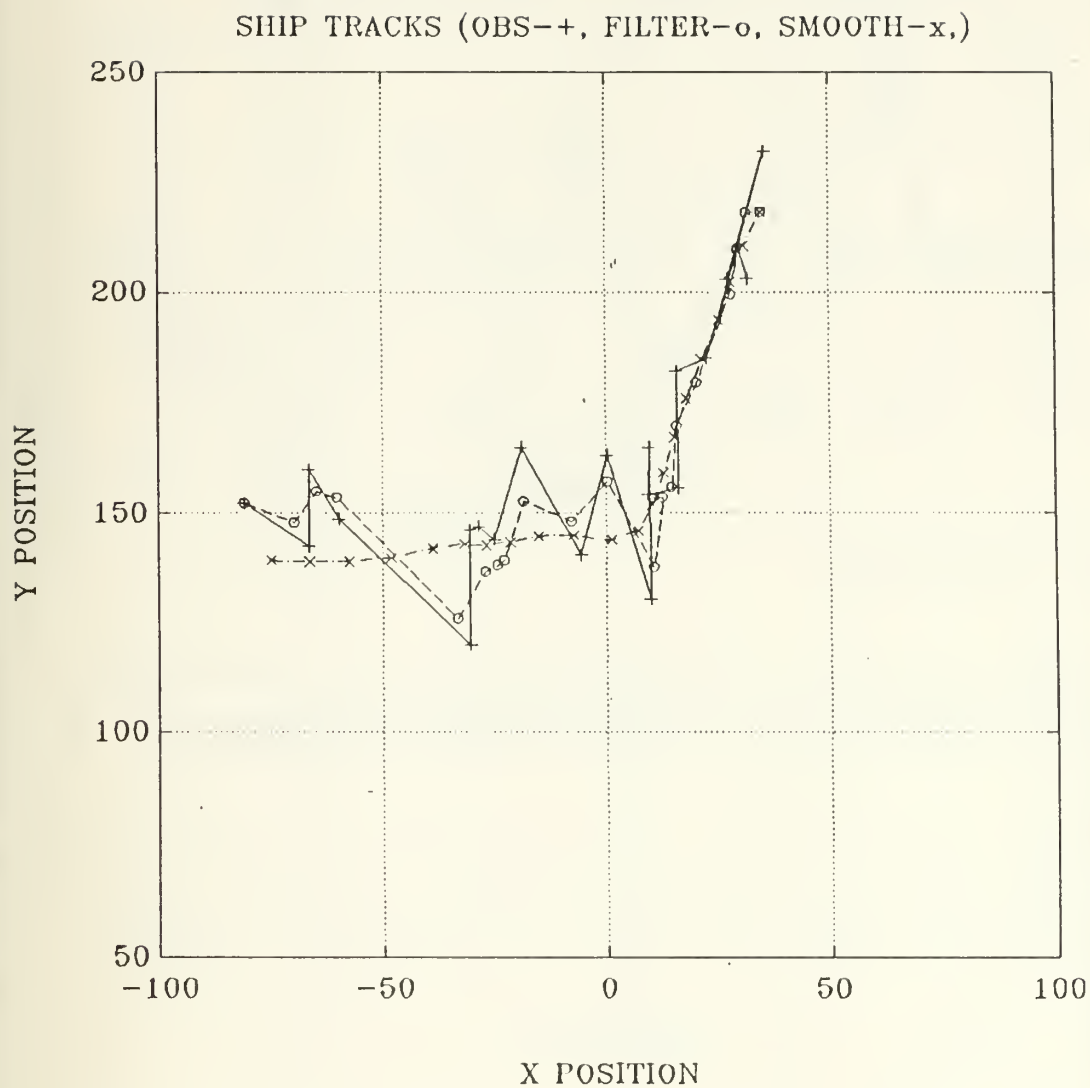


Figure 29. Processed Data vs Observed Results

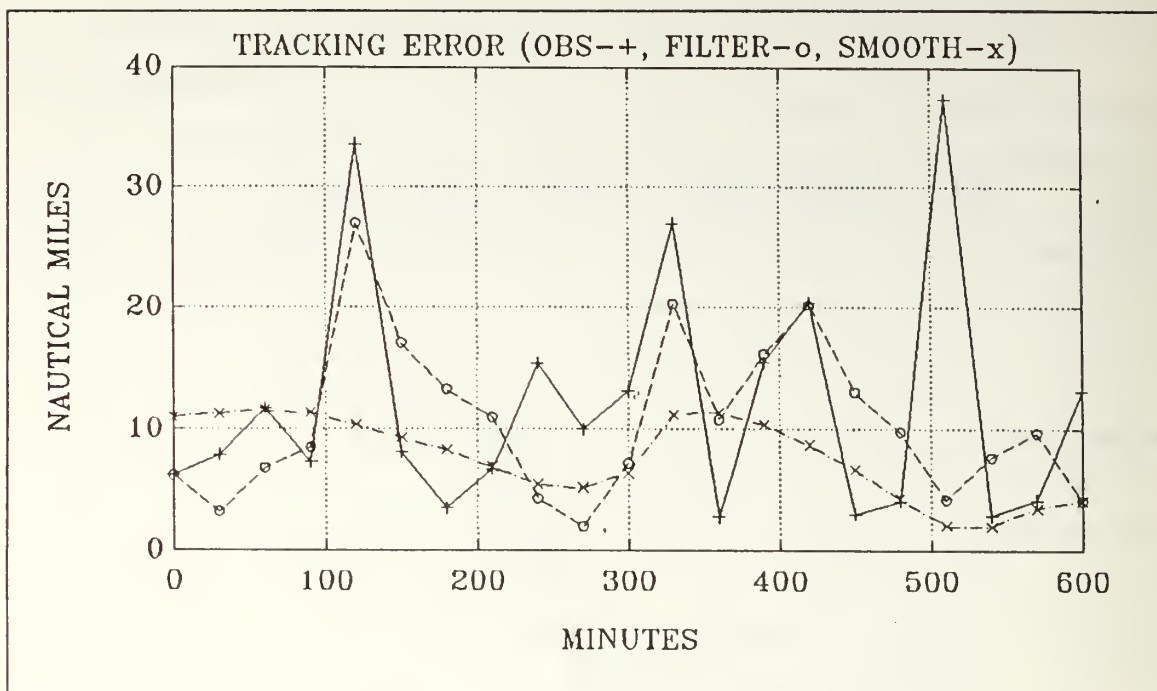


Figure 30. Position Error

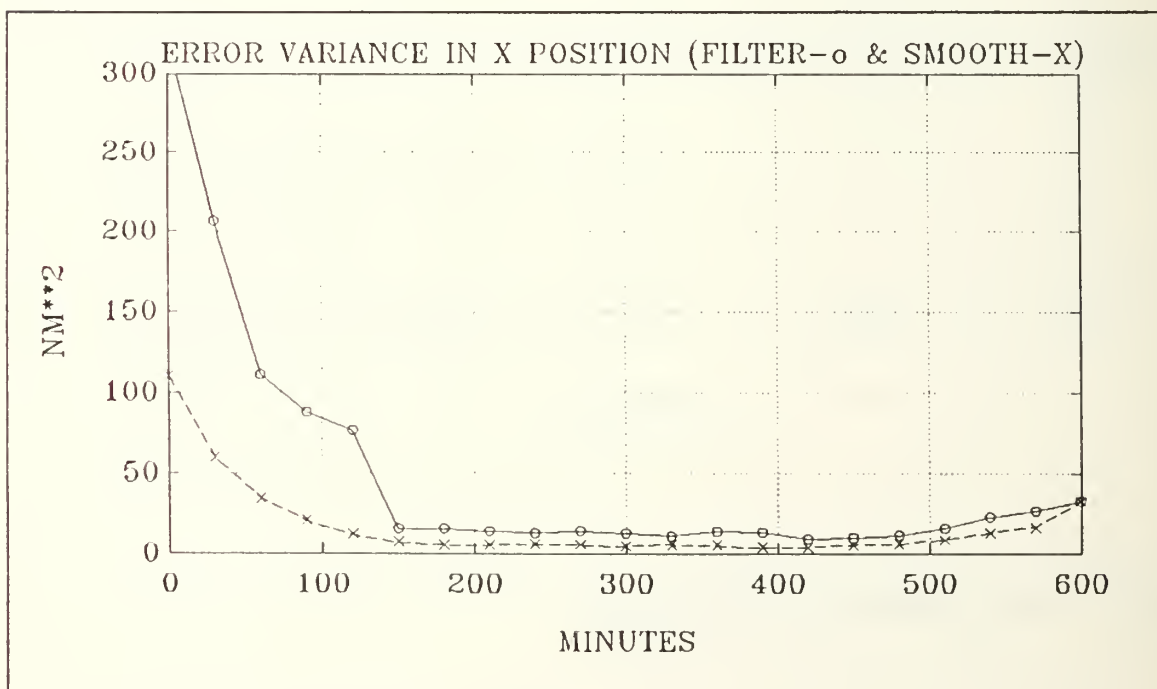


Figure 31. Variance of Position Error in the X Direction



SHIP TRACKS (TRUE-+, FILTER-o, SMOOTH-x,)

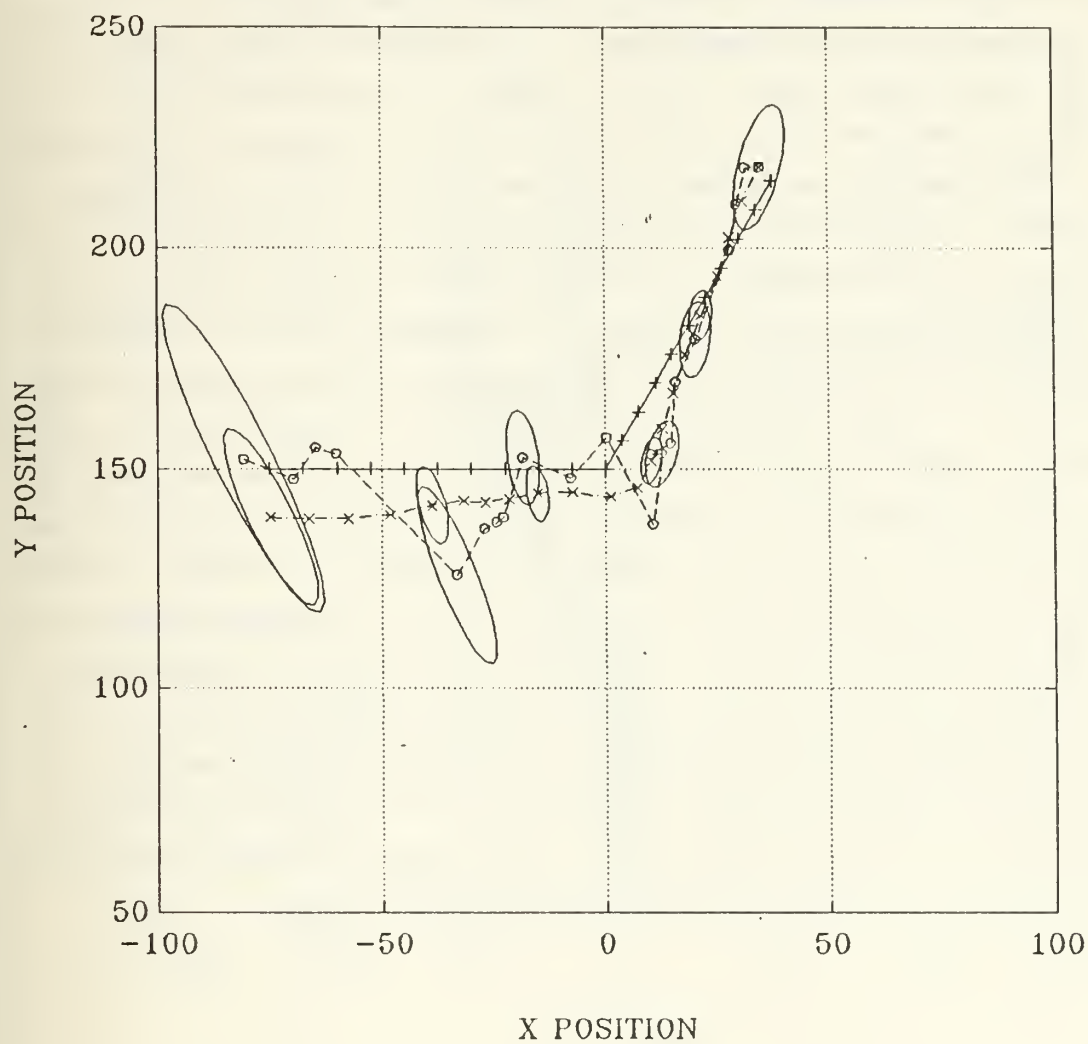


Figure 32. Scenario #7 Overall Track Results

## I. SCENARIO #8

This simulation uses the white noise model and includes two target maneuvers during the problem. The results for this scenario are shown in Figures 33-36. The target begins this scenario 150 nm due north and directly between the tracking ships on the  $y$  axis. The target's initial course is  $000^\circ$  at 15 knots. At time 180 the target turns northwest to a new course  $310^\circ$ . At time 390 the target turns again to a new course  $040^\circ$ . The tracking ships are heading due north at 10 knots. Due to the geometry of this scenario, the tracking routine is relatively accurate in the  $x$  direction with most of the position error in the  $y$  direction. The accuracy in the  $x$  direction is reflected in the small variance error values shown in Figure 35. For the first five hours of the problem the improvement in the position accuracy due to the filter and the smoother was about the same (40%). During the second half of the problem, two large observation errors are detected. In both instances the filter and the smoother improve on the position accuracy, however, because the observation error at 570 minutes is so large (140 nm), the position errors for the filtered estimates and consequently the smoothed estimates for the last two observations are also very large. The effect of these large bearing errors is that the smoothed target track gives the impression that target has maneuvered and turned north when it actually has not. This can be seen in Figure 36. The size of the major axis of the error ellipses generated by the filtered and smoothed estimates also increases when the estimated distance of the target from the tracking ships increases to more than 220 nm by the end of the problem. The average target speed computed by the Kalman filter is 32.3 knots and the smoothed speed is 23.5 knots.

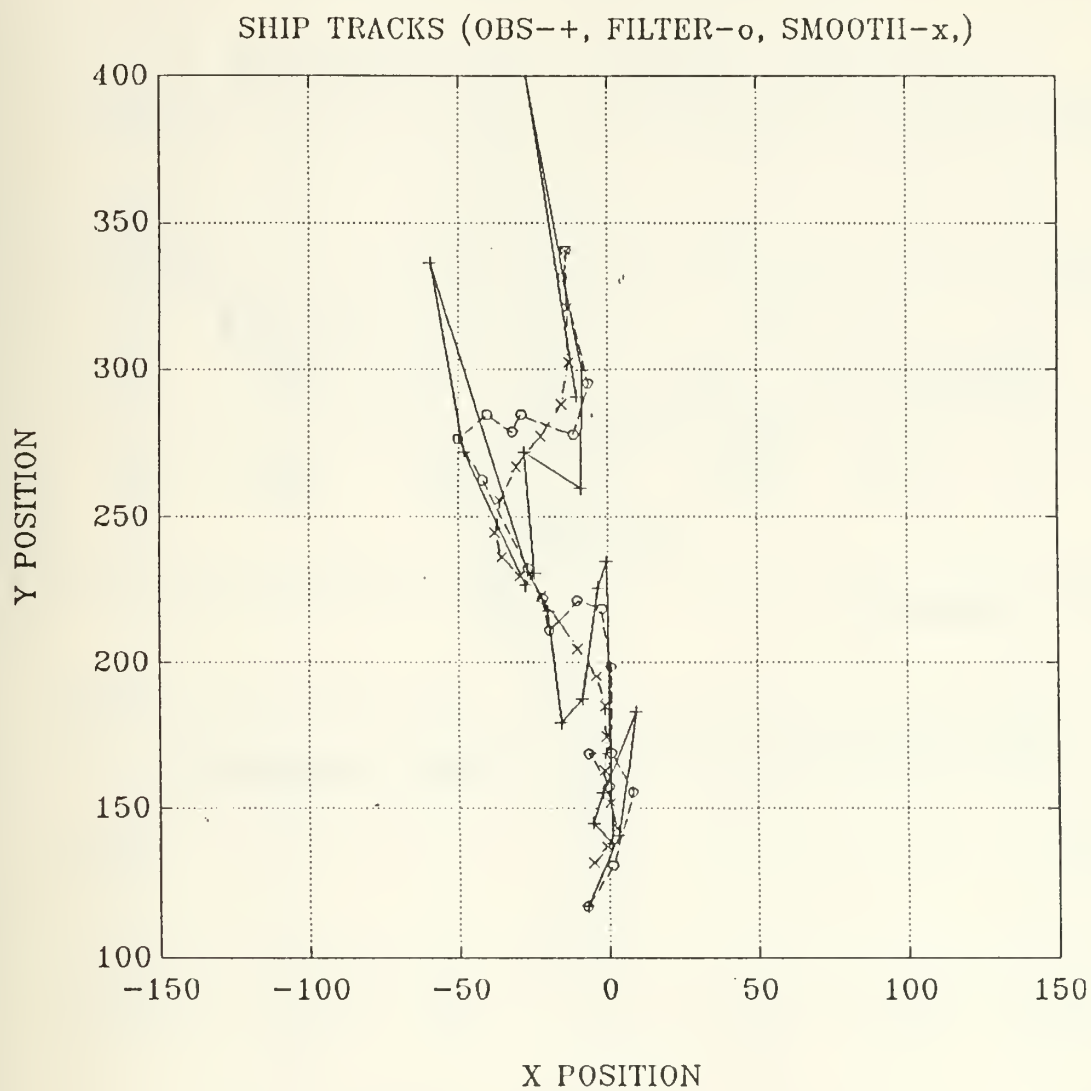


Figure 33. Processed Data vs Observed Results

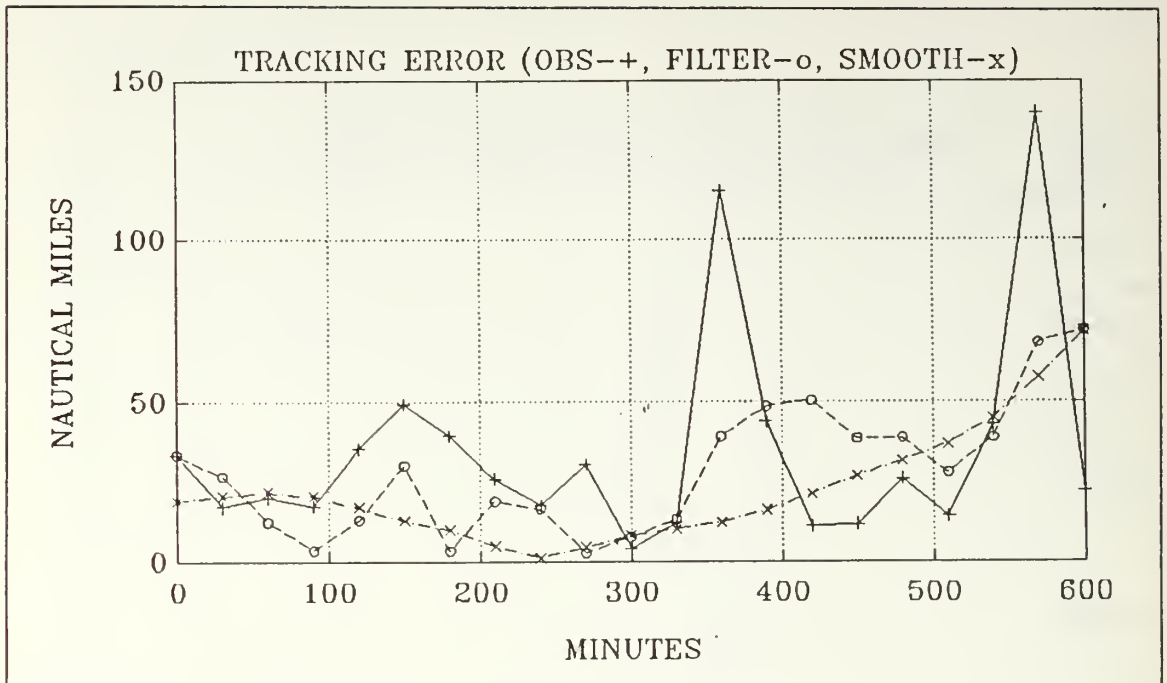


Figure 34. Position Error

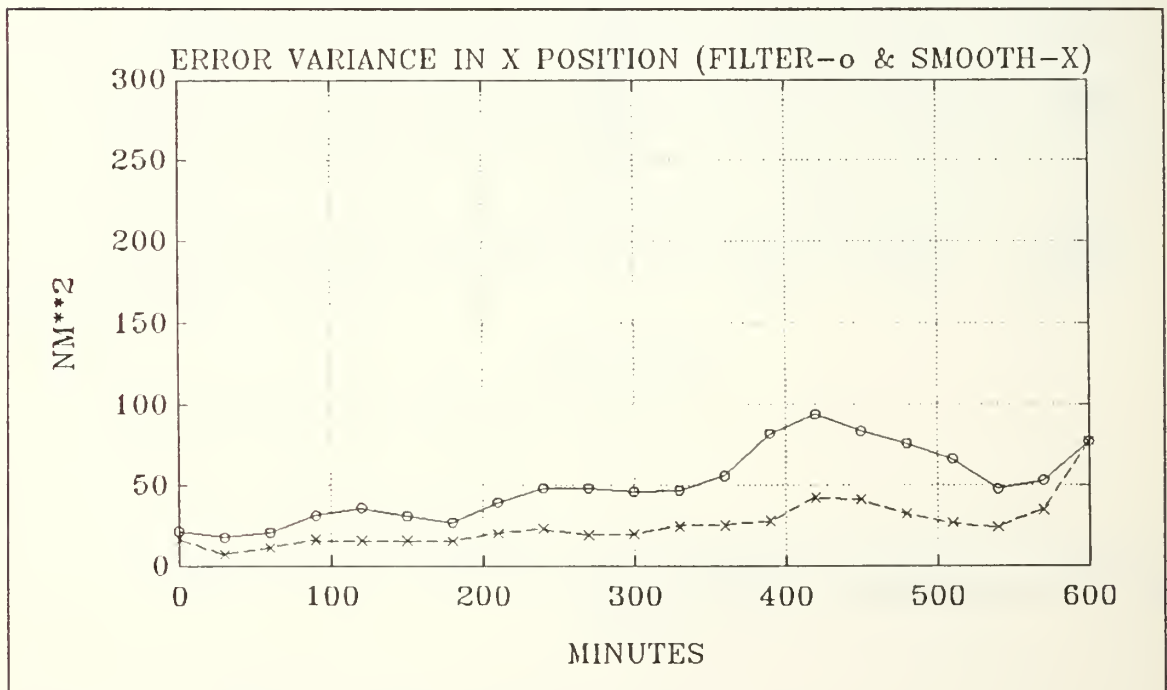


Figure 35. Variance of Position Error in the X Direction

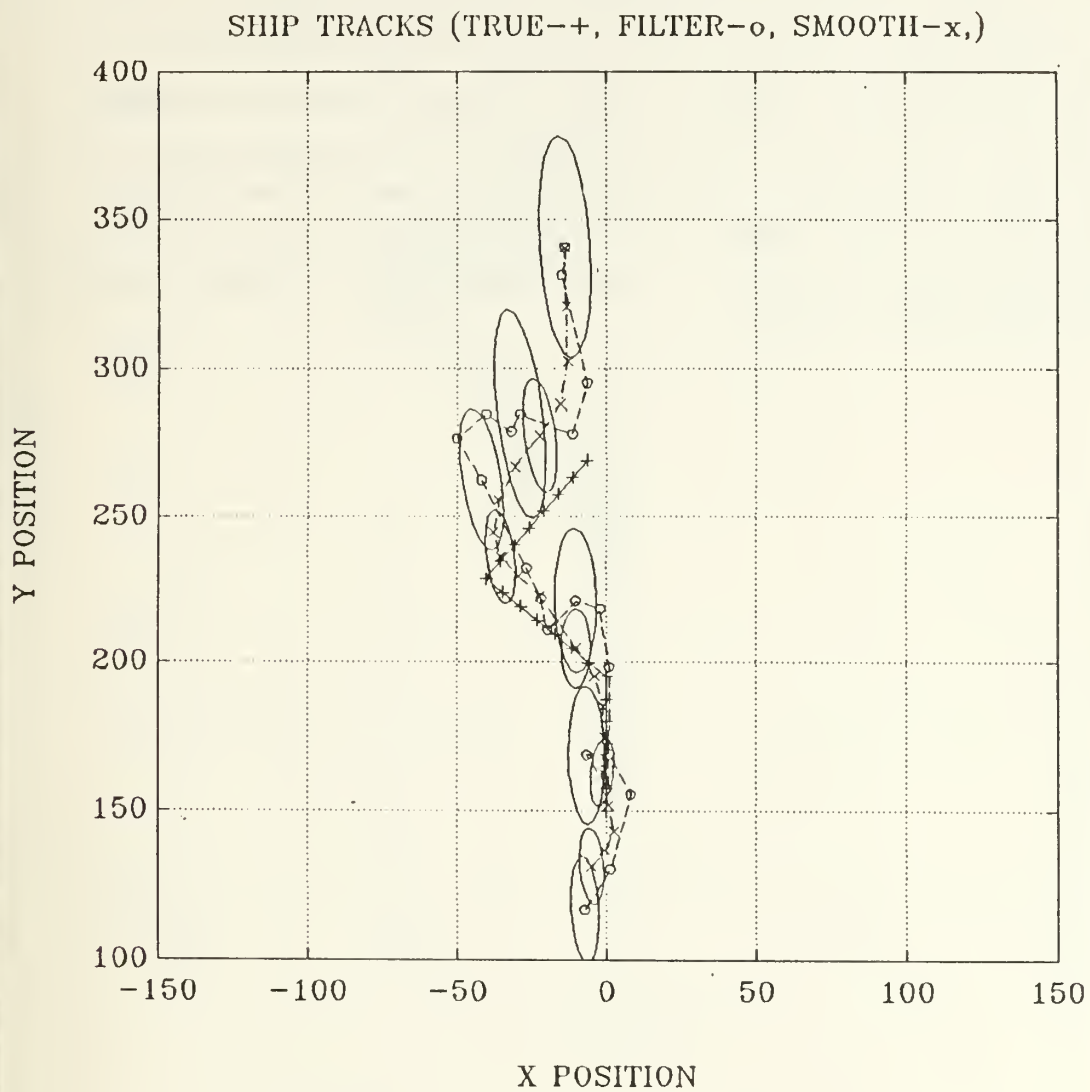


Figure 36. Scenario #8 Overall Track Results

## J. SCENARIO #9

Scenario #9 duplicates Scenario #8 with the Hall model used to approximate the atmospheric noise. The results for this scenario are shown in Figures 37-40. Figure 38 shows a large position error due to a noise spike 60 minutes into the problem. The filtered track for this scenario follows the target's true track, however, the position errors vary from 4 to 28 nm over a ten hour tracking period. The smoother improves the position accuracy of the tracker in this problem by an average of more than 60%. The smoothed track follows the target's real track for the entire track period with no major deviations as shown in Figure 40. The average filtered speed is 25 knots and the averaged smoothed speed is 16.5 knots.



# SHIP TRACKS (OBS-+, FILTER-o, SMOOTH-x,)

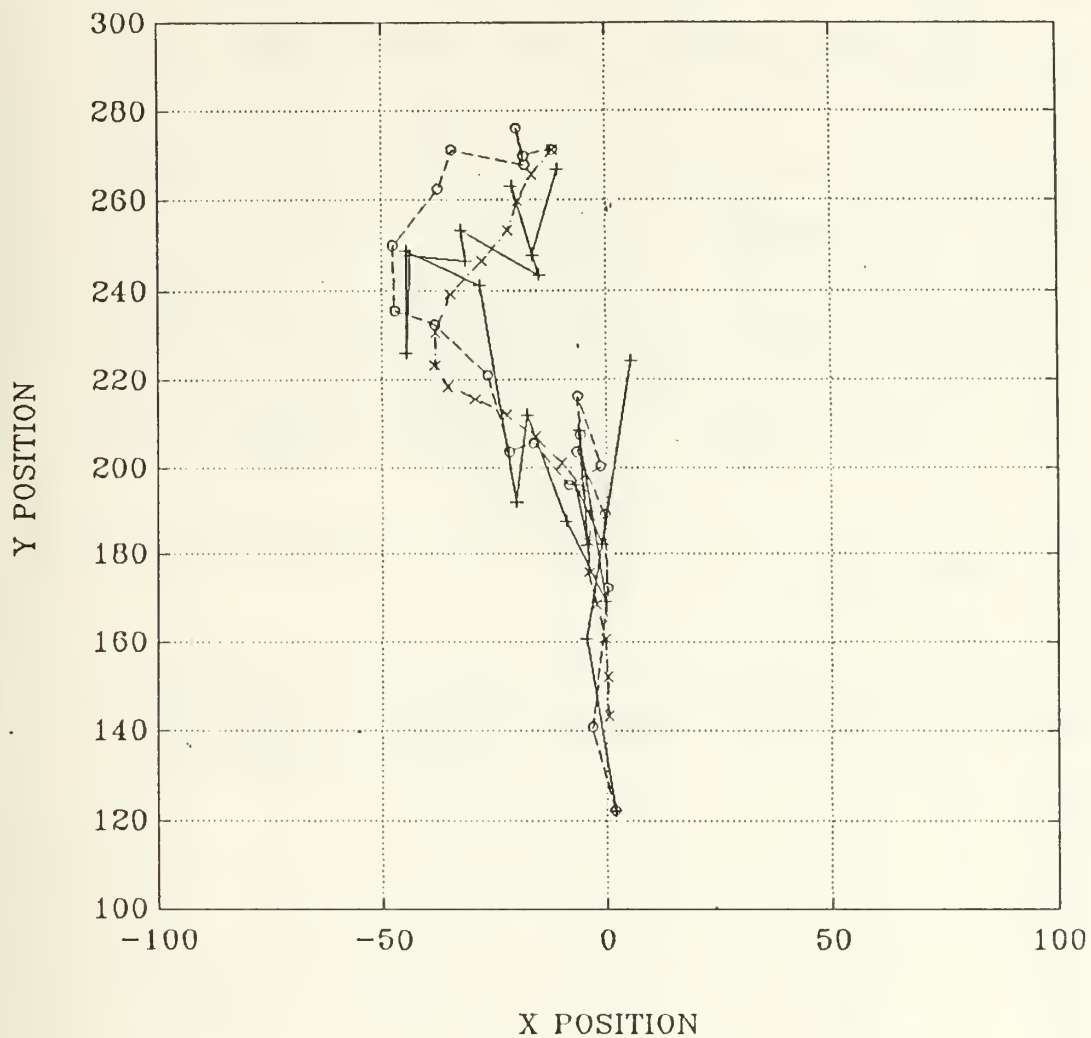


Figure 37. Processed Data vs Observed Results

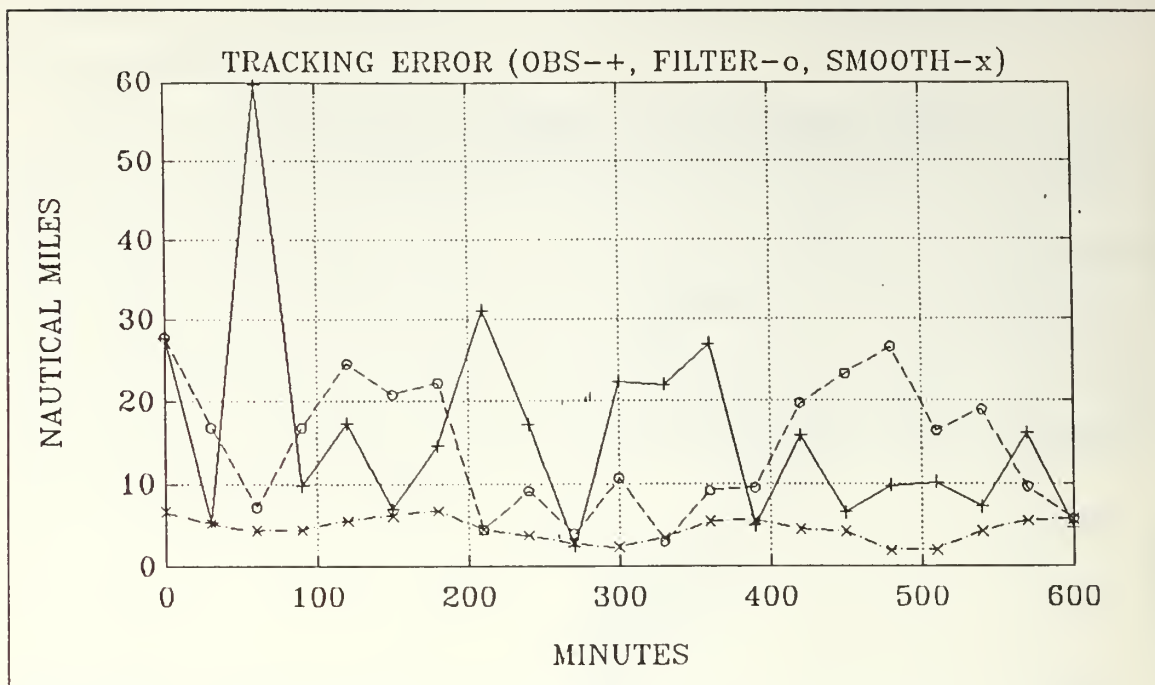


Figure 38. Position Error

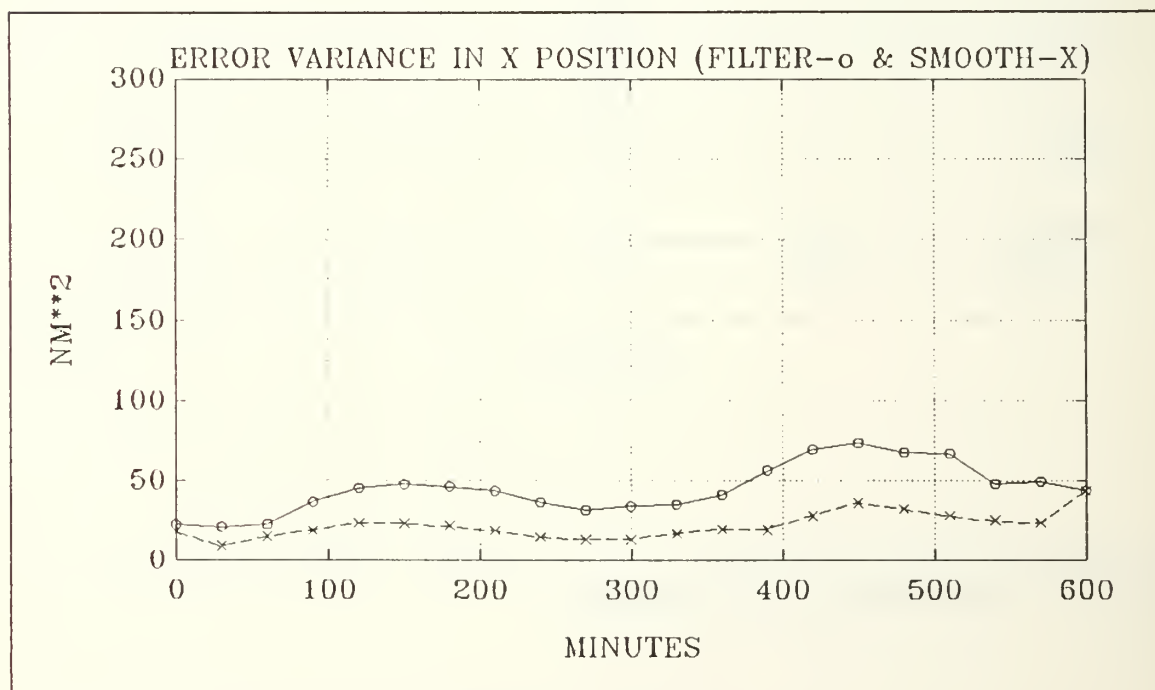


Figure 39. Variance of Position Error in the X Direction

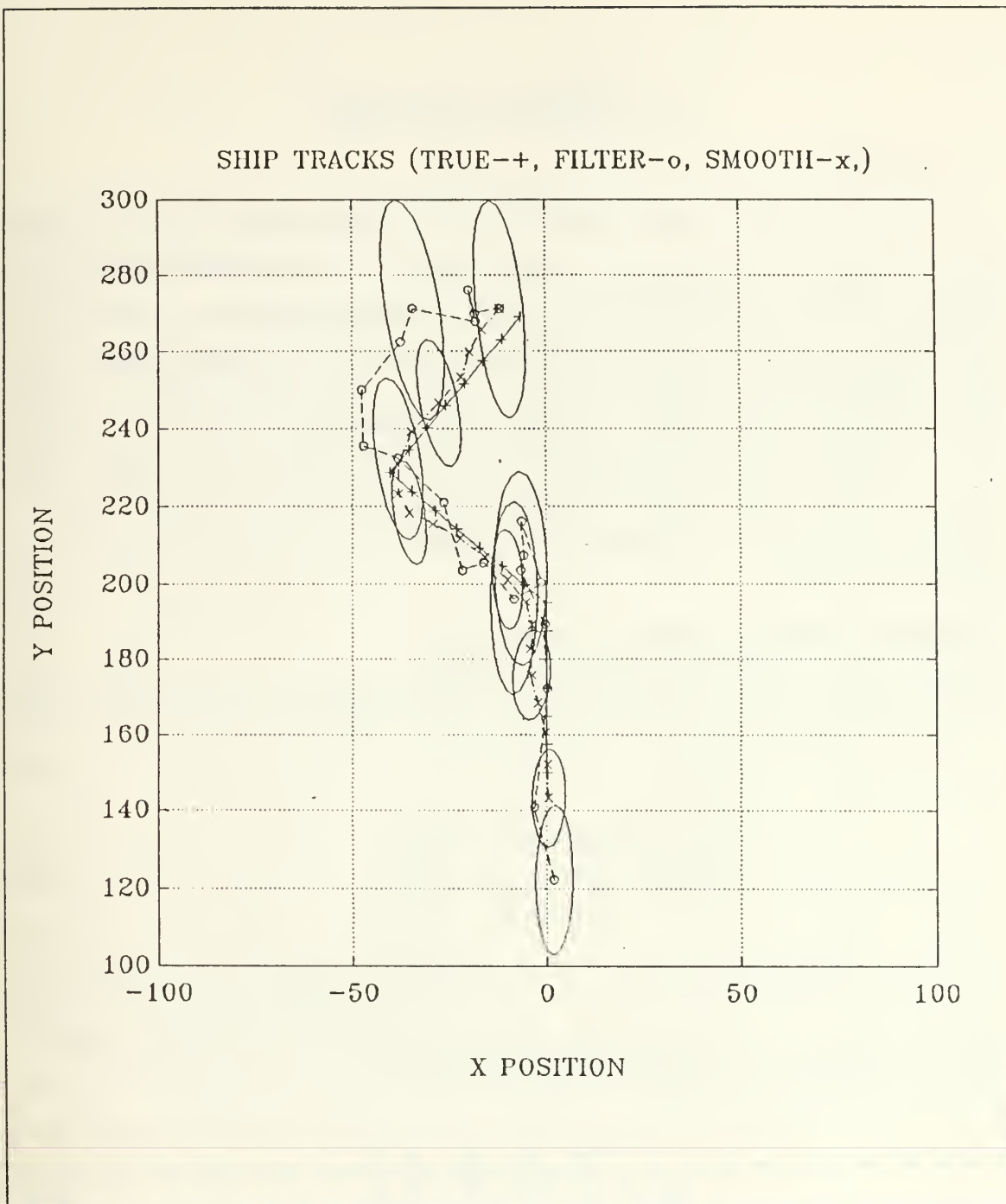


Figure 40. Scenario #9 Overall Track Results

## V. STORM TRACKING

### A. GENERAL

The storm tracking scenario parallels the ship tracking problem in that both problems develop a position, course, and speed solution for a "target" with similar system dynamics. Where the observations for the ship tracking problem were RDF lines-of-bearing that resulted in a nonlinear measurement equation (2.5), the observations for the storm tracking scenario are actual position coordinates given by latitude and longitude values. The storm tracks used in this thesis were obtained from data collected at the Joint Typhoon Warning Center located in Guam and run by the U.S. Navy and the U.S. Air Force. The position coordinates were obtained using aircraft, satellite, and radar reconnaissance assets.

### B. SYSTEM AND MEASUREMENT MODELS

The tropical storms were modeled as linear, time distance systems where the state relationships are given by

$$\begin{bmatrix} x \\ \dot{x} \\ y \\ \dot{y} \end{bmatrix}_{k+1} = \begin{bmatrix} 1 & T & 0 & 0 \\ 0 & 1 & 0 & 0 \\ 0 & 0 & 1 & T \\ 0 & 0 & 0 & 1 \end{bmatrix} \begin{bmatrix} x \\ \dot{x} \\ y \\ \dot{y} \end{bmatrix}_k + w_k \quad (5.1)$$

where  $w_k$  is a random forcing function with a covariance matrix given by the state excitation matrix,  $Q_k$ . This is basically a fictitious noise source that prevents the error covariance matrix from becoming singular.  $Q_k$  is defined as

$$Q_k = \begin{bmatrix} 0.1 & 0 & 0 & 0 \\ 0 & 0.1 & 0 & 0 \\ 0 & 0 & 0.1 & 0 \\ 0 & 0 & 0 & 0.1 \end{bmatrix} \quad (5.2)$$

The measurement model utilizes the linear measurement equation given by equation (2.6). Since the  $x$  and  $y$  position states are observed directly and given by the latitude and longitude position coordinates, the measurement equation can be written as

$$\begin{bmatrix} z_x \\ z_y \end{bmatrix}_{k+1} = \begin{bmatrix} 1 & 0 & 0 & 0 \\ 0 & 0 & 1 & 0 \end{bmatrix} \begin{bmatrix} x \\ \dot{x} \\ y \\ \dot{y} \end{bmatrix}_k + v_k \quad (5.3)$$

where the measurement noise  $v_k$  has a variance of  $\pm 1$  nm.

### C. STORM TRACKS

Typhoon Pat developed east of Taiwan in the western Pacific on 24 August 1985. The Typhoon Warning Period for this storm was from 27 August until 1 September. Over this six-day period the storm traveled 1337 nm with maximum wind speeds of over 95 knots. This storm caused significant damage in southwestern and northeastern Japan; primarily on the islands of Kyushu and Hokkaido. [Ref. 11: pp. 64-68]

Figure 41 shows the actual track of Typhoon Pat using the observed positions. The storm track shown in Figure 42 was constructed using the filtered and smoothed position estimates obtained from the Kalman tracker. The observed storm positions are fairly accurate and do not deviate from the overall track very much. Consequently, the filtered and smoothed storm positions do not show a great deal of improvement overall. In the areas of the track where the observed positions do vary, the smoother does improve the track accuracy. Specifically, these areas occur near 22° N, 126° E, and 37° N, 133° E.

The second storm track analyzed was that of Typhoon Tess that originated south-east of Guam on 30 August 1985. The warning period for this storm lasted from 1 September until 6 September. Tess traveled 1470 nm over its' seven-day lifespan on a track that took it over the Philippines, north of Luzon, and across the South China Sea moving inland 170 nm south of Hong Kong. Maximum wind speeds for this typhoon were over 75 knots. [Ref. 11: pp. 76-77]

The performance of the smoother on the track of Typhoon Tess was similar to that of Typhoon Pat. Figure 43 shows Tess's overall track and Figure 44 shows the track results obtained with the Kalman filter and the smoothing algorithm. The Kalman tracker and the smoother show some improvement in the track accuracy in the area of 15° N, 123° E and 18.5° N, 117° E.

The application of the Kalman filter tracker to the storm tracking problem would be very useful in attempting to predict the storm's track when all the position data is not available and the data that is available is not refined. Then, by using the filter and smoothing routine, a more accurate track of the storm's past history can be calculated allowing for a more accurate prediction of the storm's future track.

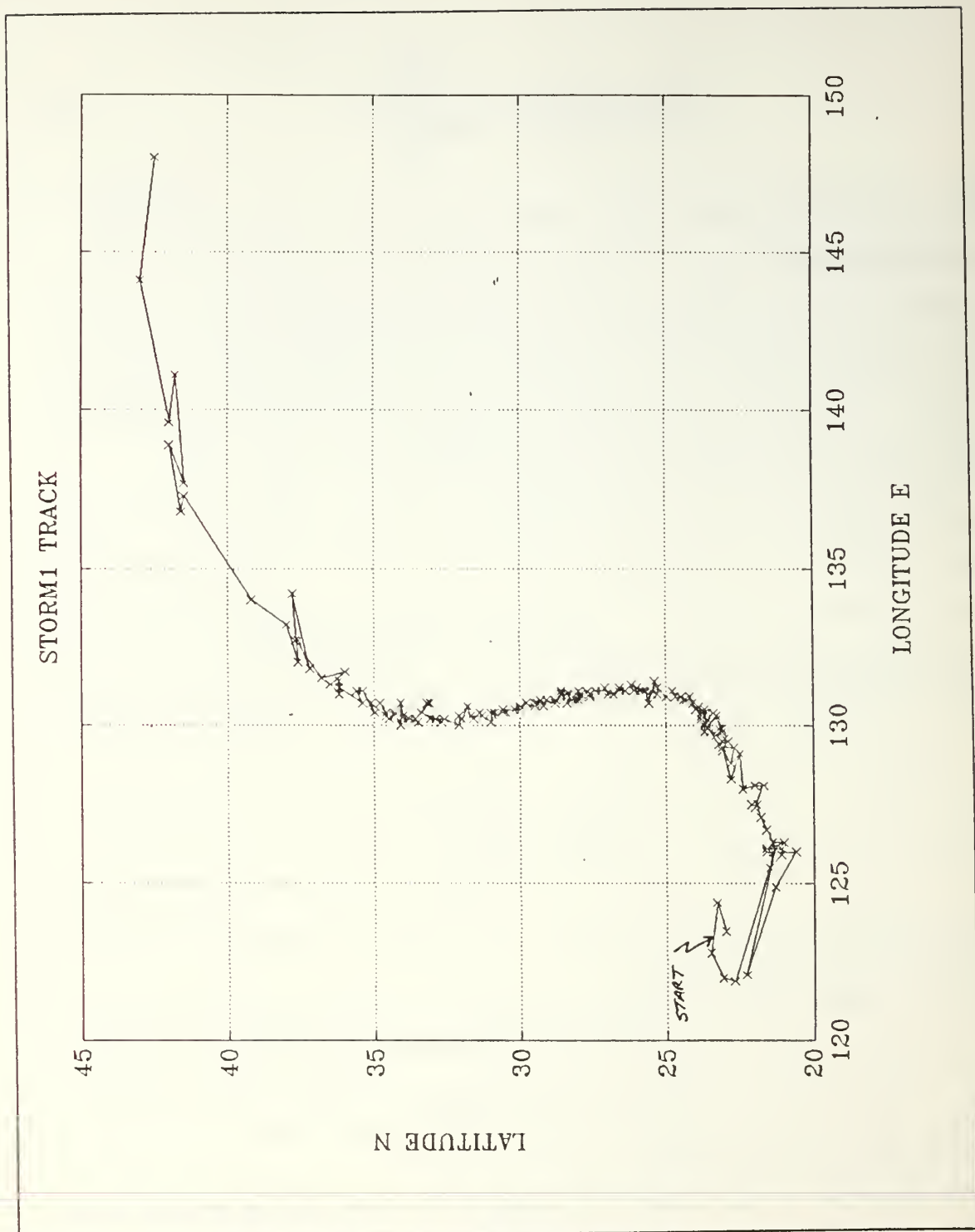


Figure 41. Storm Track of Typhoon Pat



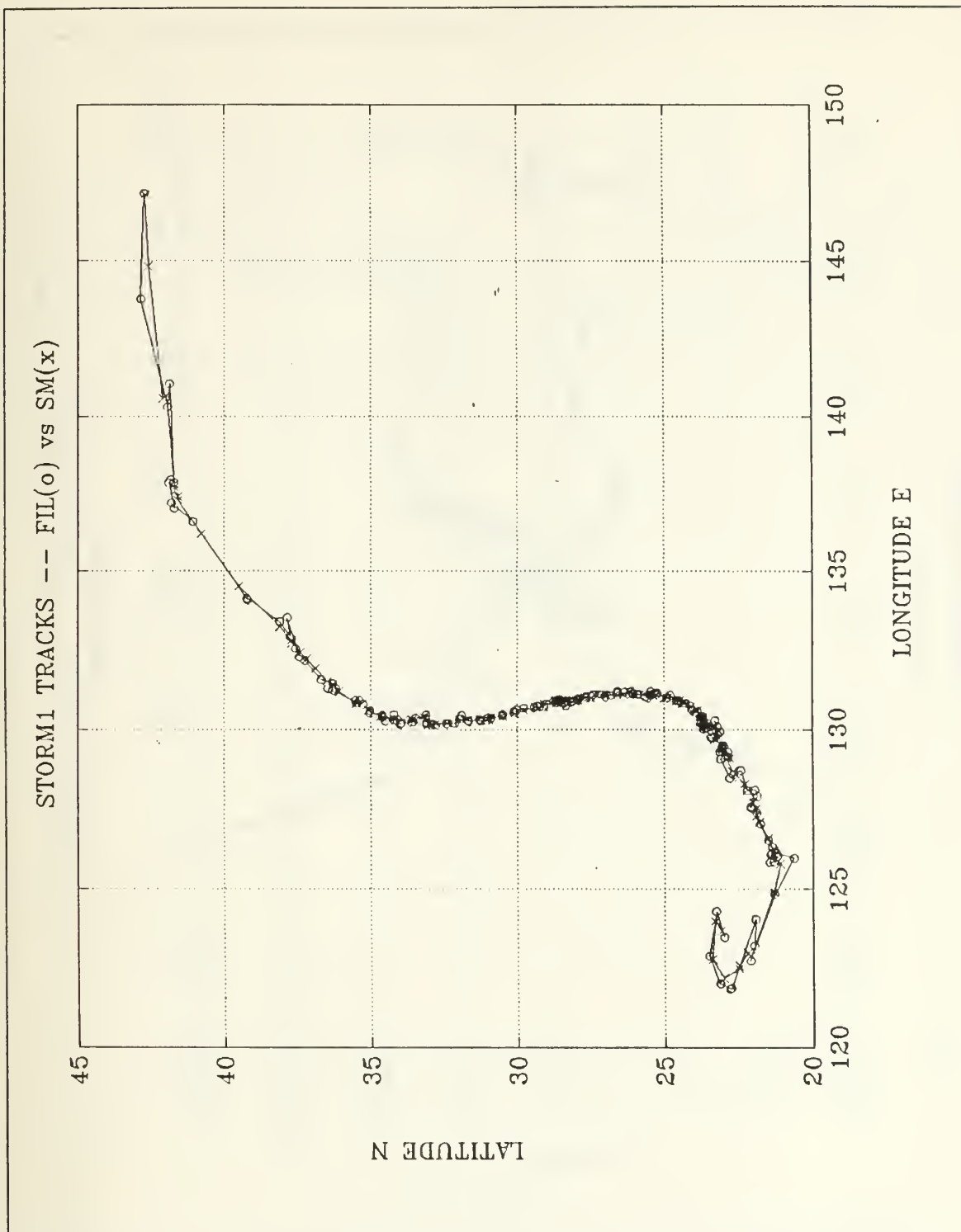


Figure 42. Filtered and Smoothed Track of Typhoon Pat

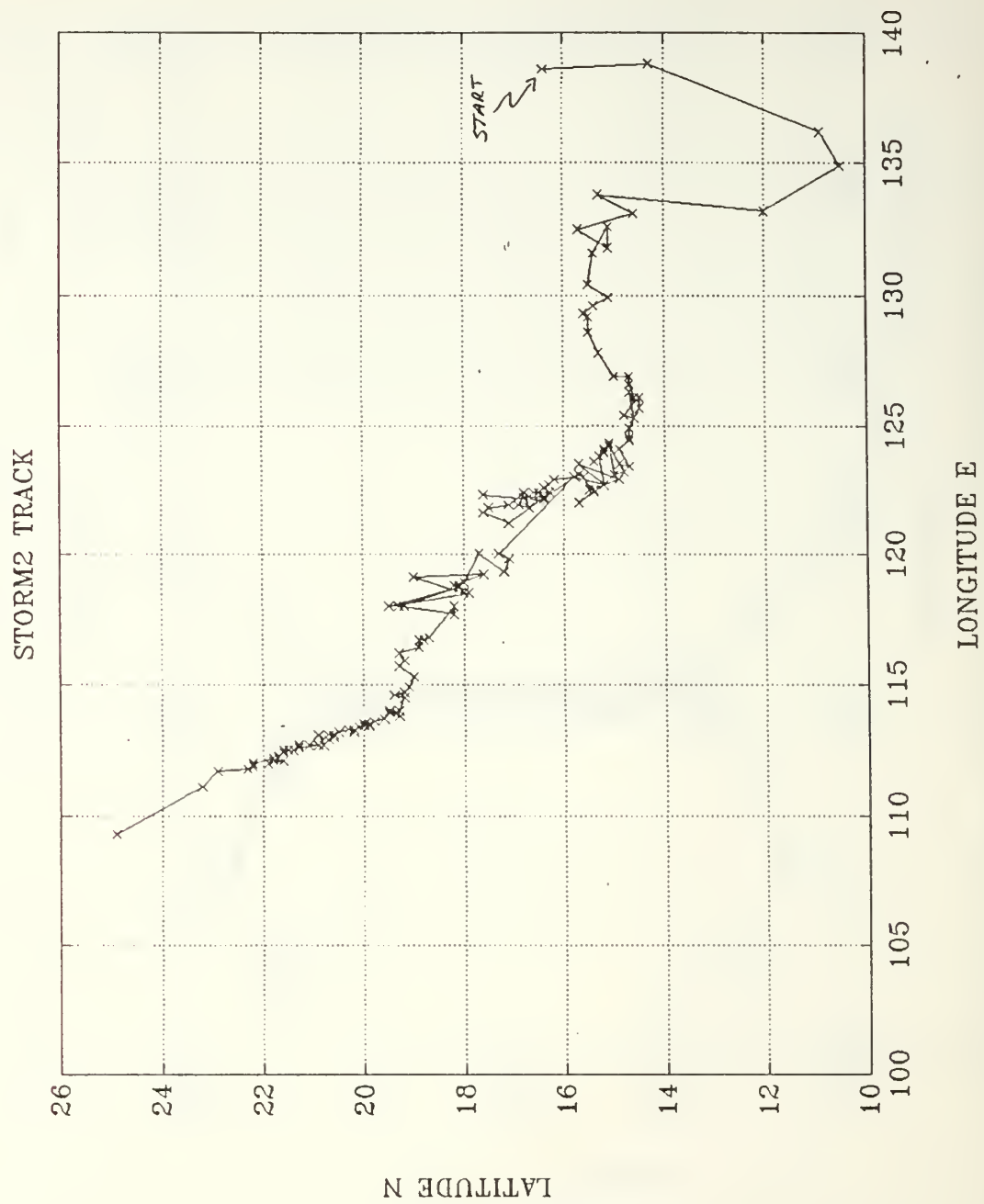


Figure 43. Storm Track of Typhoon Tess

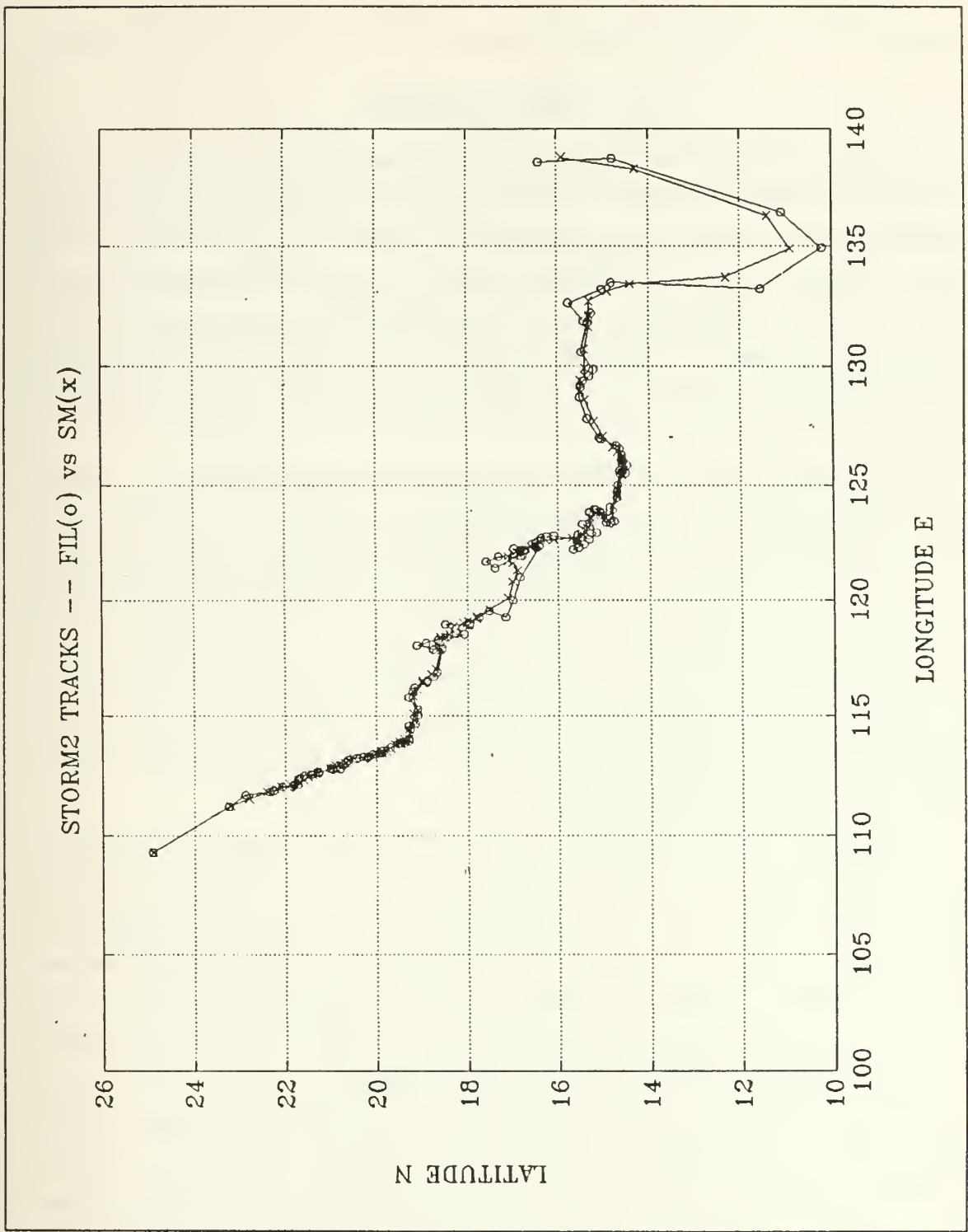


Figure 44. Filtered and Smoothed Track of Typhoon Tess

## VI. CONCLUSIONS

The purpose of this research was to improve the accuracy and maneuver detection capability of an extended Kalman filter tracking routine by implementing a fixed interval smoothing algorithm and a maneuver/divergence detection method that uses a noise variance estimator process. The Hall atmospheric noise model was compared with a white noise model in estimating the effects of atmospheric noise on the received HFDF lines-of-bearing. Several different targeting scenarios were simulated and the accuracy of the observed, the filtered, and the smoothed target tracks were analyzed and compared.

The fixed interval smoothing algorithm improved the position accuracy of the target in all the targeting scenarios simulated. Although the smoothed result was not always the most accurate for every observation, the smoother did improve the track accuracy by an average of 40-60 percent over the observed target positions and by an average of 20-30 percent over the filtered estimates. The effectiveness of the smoother increased as the target range increased. The cost of this improvement was the increased computer time required to run the smoothing routine and for the simulations conducted, this increase was on the order of approximately 60% or 6-7 seconds when the program was run on an IBM PS 2 Model 60 micro-computer.

The maneuver divergence detection scheme implemented worked well, however, because this process involves the addition of a time varying value of the state excitation matrix,  $Q$ , to the a priori error covariance matrix,  $P_{(k-1)}$ , there is a strong potential for the filter to go unstable. This was observed when a very large noise impulse was encountered causing the observed line-of-bearing to change by more than  $45^\circ$  over one observation. The major advantage gained in using this maneuver detection process is that a maneuver is detected one observation after it occurs.

A white noise model is a relatively accurate model of the atmospheric noise over an extended period of time, however, it fails to account for the impulsive nature of this noise process. The Hall noise model corrects for this deficiency and was used in several of the simulations. It was in the presence of these noise spikes that the operation of the smoother was at its best. In virtually all of the simulations conducted, the smoothing algorithm effectively eliminated the position errors due to a "wild" bearing caused by the impulse noise. The improvement in the position estimate due to the smoother was

commonly observed to be in the 75-85 percent range when a noise spike was encountered.

There are several areas of this problem to be investigated further. The first area of investigation involves the divergence detection algorithm. Although the process used in this thesis was able to detect a maneuver using one observation and accurately track a maneuvering target, there are many factors that must be modified to fit a particular noise environment and tracking scenario. These factors make this detection scheme undesirable if not impossible to implement in a real world, real time tracking problem. Another area for further research is adaptation of this tracking algorithm to a multiple target environment. This is an area where some work has been done and would be of great value in a ship tracking targeting scenario. In this type of problem, the ability to identify a high value target in a convoy or battlegroup is very important as well as the ability to identify any background shipping that is not to be attacked. The trend toward increased emphasis on passive tracking and targeting techniques will make this area of research highly interesting and very useful in the future.

## APPENDIX A. SHIPSM.FOR

This is a listing of the SHIPSM.FOR program used to generate the data for the target tracks presented in this thesis. In order to run this program, the TRKDATA.DAT file must be available. This file is created by running the TRACK.FOR program located in Appendix B.

C SHIPSM.FOR

C\*\*\*\*\* TO RUN \*\*\*\*\*

C

C 1) RUN TRACK

C 2) RUN SHIPSM

C

C\*\*\*\*\* FOR GRAPHICAL OUTPUT \*\*\*\*\*

C 3) COPY ELLIP, ELLIPS ,FILDATA ,& SMDATA --> MATLAB SUB-DIR.

C 4) BEGIN MATLAB --> RUN SHIP

C

C \*\*\*\*\*

C THIS PROGRAM EMPLOYS AN ADAPTIVE EXTENDED KALMAN FILTER WITH A  
C FIXED INTERVAL SMOOTHING ALGORITHM TO TRACK A MANEUVERING SURFACE SHIP  
C TARGET USING BEARINGS-ONLY RADIO DIRECTION-FINDING MEASUREMENTS FROM  
C SEVERAL SPATIALLY DISTRIBUTED SENSORS.

C \*\*\*\*\*

C \*\*\*VARIABLE DEFINITIONS\*\*\*

C	AK	=	SMOOTHING FILTER GAIN MATRIX
C	AKT	=	TRANPOSE OF AK
C	BRG	=	MEASURED TARGET BEARING IN RADIANS
C	BRKKM1	=	PREDICTED TARGET BEARING MEASUREMENT IN RADIANS
C			BRG(K K-1)
C	DBRG	=	MEASURED TARGET BEARING IN DEGREES
C	DT	=	TIME DELAY BETWEEN OBSERVATIONS, T(K) - T(K1)
C	DTOR	=	DEGREE TO RADIAN CONVERSION FACTOR
C	E1,E2	=	MEASUREMENT RESIDUAL, Z(K) - H(X(K K-1))
C	E1M1,E2M1	=	MEASUREMENT RESIDUAL AT PREVIOUS OBSERVATION
C	E1M2,E2M2	=	MEASUREMENT RESIDUAL TWO OBSERVATIONS PREVIOUS
C	FAC1	=	RECIPROCAL OF VARE
C	G	=	KALMAN GAIN VECTOR
C	GATE	=	3*PREDICTED RESIDUAL STANDARD DEVIATION
C	H	=	MEASUREMENT MATRIX
C	HDG	=	ESTIMATED TARGET HEADING IN DEGREES
C	HT	=	TRANPOSE OF H
C	I	=	COUNTER
C	IMAT	=	4 X 4 IDENTITY MATRIX
C	J	=	COUNTER
C	K	=	ITERATION INTERVAL
C	LPKK	=	STATE COVARIANCE MATRIX AFTER PREVIOUS OBSERVAT



C	LPKKM1	=	A PRIORI STATE COVARIANCE ESTIMATE
C	LXKK	=	STATE ESTIMATE AFTER PREVIOUS OBSERVATIONS
C	LXKKM1	=	A PRIORI STATE ESTIMATE
C	PHI	=	DISCRETE-TIME STATE TRANSITION MATRIX
C	PHIT	=	TRANPOSE OF PHI
C	PI	=	3.141592654
C	PKK	=	ESTIMATION ERROR COVARIANCE MATRIX, P(K K)
C	PKKS	=	SMOOTHED ERROR COVARIANCE MATRIX
C	PKKM1	=	PREDICTED ESTIMATION ERROR COVARIANCE MATRIX, P(
C	PKKM1S	=	PREDICTED ERROR COVARIANCE MATRIX FOR SMOOTHING,
C	IPKKM1S	=	INVERSE OF PKKM1S
C	PSS	=	ERROR COVARIANCE MATRIX FOR SMOOTHING, P(K K)
C	Q	=	STATE EXCITATION MATRIX
C	R	=	MEASUREMENT NOISE COVARIANCE
C	RANGE	=	DISTANCE FROM SENSOR TO A PRIORI TARGET POSITION
C	RTOD	=	RADIAN TO DEGREE CONVERSION FACTOR
C	SPD	=	ESTIMATED TARGET SPEED IN KNOTS
C	TEMP	=	TEMPORARY STORAGE MATRICES USED IN MATRIX
C			OPERATIONS
C	VARE	=	VARIANCE OF RESIDUALS PROCESS
C	XDIFF	=	DISTANCE IN X DIRECTION FROM SENSOR TO A PRIORI
C			TARGET POSITION
C	XKK	=	ESTIMATED TARGET STATE VECTOR, X(K K)
C	XKKS	=	SMOOTHED TARGET STATE VECTOR
C	XKKM1	=	PREDICTED TARGET STATE VECTOR, X(K K-1)
C	XKKM1S	=	PREDICTED TARGET STATE VECTOR FOR SMOOTHING, X(K
C	XPOS	=	ESTIMATED TARGET POSITION IN X DIRECTION
C	XS	=	SENSOR POSITION IN X DIRECTION
C	XSS	=	TARGET STATE VECTOR FOR SMOOTHING, X(K K)
C	XT	=	TRUE TARGET POSITION IN X DIRECTION
C	YDIFF	=	DISTANCE IN Y DIRECTION FROM SENSOR TO A PRIORI
C			TARGET POSITION
C	YPOS	=	ESTIMATED TARGET POSITION IN Y DIRECTION
C	YS	=	SENSOR POSITION IN Y DIRECTION
C	YT	=	TRUE TARGET POSITION IN Y DIRECTION
C	ZX	=	OBSERVED POSITION IN X DIRECTION
C	ZY	=	OBSERVED POSITION IN Y DIRECTION

#### C VARIABLE DECLARATIONS

```

REAL*4 XKK(4,1),XKKM1(4,1),LPKKM1(4,4),LXKKM1(4,1),PHI(4,4)
REAL*4 H(1,4),G(4,1),TEMP1(1,4),TEMP2(1,1),TEMP3(4,1)
REAL*4 TEMP4(4,4),TEMP5(4,4),PKK(4,4),PKKM1(4,4),HT(4,1)
REAL*4 LXKK(4,1),LPKK(4,4),XS(10),YS(10),DBRG(10),BRG(10)
REAL*4 TEMP6(4,4),PHIT(4,4),IMAT(4,4),TEMP7(4,4),XT,YT
REAL*4 GATE(2),VARE(2),E(2),TEMP8(4,1),XE(1000),YE(1000)
REAL*4 GATE1,GATE2
REAL*4 DT,XDIFF,YDIFF,RANGE,XS1,YS1,BRG1,BRKKM1,Q(4,4)
REAL*4 OBSERR(50),FAC1,SIGTH2,SIGVT2,R,ETOTAL,EAVG,RTOD
REAL*4 X2,YS2,BRG2,ZX,ZY,M1,E1,E1M1,E1M2,DTOR,TRKERR(50)
REAL*4 M2,E2,E2M1,E2M2,G11,G13,G21,G23,ZXM1,ZYM1,TEMP9(4,2)
REAL*4 XKKS(4,1,50),PKKS(4,4,50),SPD(50),SSPD(50),PMMS(4,4,50)
REAL*4 XNNM1(4,1),XSS(4,1),XKKM1S(4,1),XMMS(4,1,50)
REAL*4 PNNM1(4,4),PSS(4,4),PKKM1S(4,4),IPKKM1S(4,4)
REAL*4 AK(4,4),AKT(4,4),II(4,4),STRKERR(50),DTS(50)
REAL*4 TEMP1S(4,4),TEMP2S(4,1),TEMP3S(4,1)
REAL*4 TEMP4S(4,4),TEMP5S(4,4),TEMP6S(4,4)

```



```

REAL*4 XP(21),YP(21),XPS(21),YPS(21)

INTEGER*2 TIME,TIMEM1,NP,GTCTR

C OPEN OUTPUT DATA FILES
OPEN(UNIT=2,FILE='TRKDATA.DAT',STATUS='OLD')
OPEN(UNIT=3,FILE='OUTDATA.DAT',STATUS='NEW')
OPEN(UNIT=4,FILE='TRUDATA.DAT',STATUS='NEW')
OPEN(UNIT=5,FILE='FILDATA.DAT',STATUS='NEW')
OPEN(UNIT=6,FILE='SMDATA.DAT',STATUS='NEW')
OPEN(UNIT=7,FILE='ELLIP.DAT',STATUS='NEW')
OPEN(UNIT=8,FILE='ELLIPS.DAT',STATUS='NEW')
OPEN(UNIT=9,FILE='RESULTS.DAT',STATUS='NEW')
OPEN(UNIT=10,FILE='RESIDU.DAT',STATUS='NEW')

C RADIAN/DEGREE CONVERSION FACTORS
RTOD=57.29577951
DTOR=0.01745293

C COMPUTE 4X4 IDENTITY MATRIX
DO 5 I=1,4
DO 5 J=1,4
IF (I.EQ.J) THEN
    IMAT(I,J)=1.0
ELSE
    IMAT(I,J)=0.0
ENDIF
5 CONTINUE

C INITIALIZE TIME COUNTER
TIMEM1=0
NP=1
GTCTR=0

C COMPUTE BEARING MEASUREMENT COVARIANCE
C BEARING ERROR STANDARD DEVIATION = 3 DEGREES
R=(3*DTOR)**2

C *****

C READ IN OBSERVATION PACKET (TIME, # OF SENSORS)
C DT=TIME(K)-TIME(K-1)

WRITE(*,*)'FILTERING TRACK DATA WITH KALMAN FILTER'
WRITE(*,*)'****=====***'
810 READ(2,1001,END=800)TIME,XT,YT,XS(1),YS(1),DBRG(1),
* XS(2),YS(2),DBRG(2)
1001 FORMAT(I4,8F9.4)

DO 200 L=1,2
    IF (DBRG(L).GT.180.0) DBRG(L)=DBRG(L)-360
    BRG(L)=DBRG(L)*DTOR
200 CONTINUE

IF (TIME.LT.0) GOTO 800

```

```

DT=TIME-TIMEM1
DTS(NP)=DT

CALL FINDPHI(PHI,DT)

XS1=XS(1)
YS1=YS(1)
XS2=XS(2)
YS2=YS(2)
BRG1=BRG(1)
BRG2=BRG(2)

CALL MP(XS1,YS1,XS2,YS2,BRG1,BRG2,ZX,ZY)

IF(TIME.EQ.0) THEN
C      CALL INIT(XS1,YS1,XS2,YS2,BRG1,BRG2,XKK,PKK)
      WRITE(3,*)'X(0|0,0): '
      DO 601 I=1,4
C          LXKK(I,1)=XKK(I,1)
C          WRITE(3,*)XKK(I,1)
601      CONTINUE

C      WRITE(3,*)'P(0|0,0): '
      DO 602 I=1,4
          DO 602 J=1,4
C              LPKK(I,J)=PKK(I,J)
C              WRITE(3,401)PKK(I,J)
401          FORMAT(4F14.4)
602      CONTINUE

      ENDIF

C PROJECT AHEAD STATE AND ERROR COVARIANCE ESTIMATES
C      X(K+1|K) = PHI * X(K|K)
      CALL MATMUL(PHI,XKK,4,4,1,XKKM1)

C      WRITE(3,*)'X(' ,TIME,'|',TIMEM1,',0): '
      DO 603 I=1,4
C          WRITE(3,*)XKKM1(I,1)
C          LXKKM1(I,1)=XKKM1(I,1)
603      CONTINUE

C      P(K+1|K) = (PHI * P(K|K) * PHIT) + Q

      CALL MATRAN(PHI,PHIT,4,4)
      CALL MATMUL(PHI,PKK,4,4,4,TEMP6)
      CALL MATMUL(TEMP6,PHIT,4,4,4,TEMP4)
      CALL GETQ(DT,XKKM1,Q,1)
      CALL MATADD(TEMP4,Q,4,4,1,PKKM1)
      DO 408 I=1,4
          DO 408 J=1,4
C              LPKKM1(I,J)=PKKM1(I,J)
408      CONTINUE

```

```

        WRITE(3,*)'P(' ,TIME,'|',TIMEM1,',0): '
        DO 398 I=1,4
            WRITE(3,*)(PKKM1(I,J),J=1,4)
398      CONTINUE
        WRITE(3,*)'Q(' ,TIME,'|',TIMEM1,',0): '
        DO 604 I=1,4
            WRITE(3,*)(Q(I,J),J=1,4)
402      FORMAT(4F14.4)
604      CONTINUE

204      CONTINUE
        DO 210 L=1,2

C CALCULATE RANGE TO TARGET
        XDIFF=XKKM1(1,1)-XS(L)
        YDIFF=XKKM1(3,1)-YS(L)
        RANGE=SQRT(XDIFF**2+YDIFF**2)

C UPDATE H MATRIX WITH LATEST STATE ESTIMATES
        H(1,1)=YDIFF/RANGE**2
        H(1,2)=0.0
        H(1,3)=-XDIFF/RANGE**2
        H(1,4)=0.0
C        WRITE(3,*)'H MATRIX: '
C        WRITE(3,*)(H(1,I),I=1,4)

C COMPUTE OBSERVATION RESIDUAL
        BRKKM1=ATAN2(XDIFF,YDIFF)
        E(L)=BRG(L)-BRKKM1
C        WRITE(3,*)'MEASURED BEARING = ',BRG(L)
C        WRITE(3,*)'PREDICTED BEARING = ',BRKKM1
C        WRITE(3,*)'BEARING RESIDUAL OF SENSOR ',L,' = ',E(L)

C COMPUTE VARIANCE OF RESIDUALS SEQUENCE
C AND ADAPTIVE GATE VALUE
C        VAR(E)=H*PKKM1*HT+R
        CALL MATRAN(H,HT,1,4)
        CALL MATMUL(H,PKKM1,1,4,4,TEMP1)
        CALL MATMUL(TEMP1,HT,1,4,1,TEMP2)
        VARE(L)=TEMP2(1,1)+R
        WRITE(3,*)'VARIANCE OF RESIDUALS = ',TIME,VARE(L)
        GATE(L)=3.0*SQRT(VARE(L))
        DO 399 I=1,4
            WRITE(3,*)(PKKM1(I,J),J=1,4)
399      CONTINUE

C COMPUTE KALMAN GAIN MATRIX
C        G=PKKM1*HT*(H*PKKM1*HT+R)**-1
        CALL MATRAN(H,HT,1,4)
        CALL MATMUL(PKKM1,HT,4,4,1,TEMP3)
C        WRITE(3,*)'PKKM1*HT ='

```

```

C          DO 414 I=1,4
C          WRITE(3,*)TEMP3(I,1)
414        CONTINUE

          FAC1=1/VARE(L)
          CALL MATSCL(FAC1,TEMP3,4,1,G)
C          WRITE(3,*)'G ='
          DO 613 I=1,4
            WRITE(3,*)G(I,1)
613        CONTINUE

          IF (L.EQ.1) THEN
            G11=G(1,1)
            G13=G(3,1)
          ELSE
            G21=G(1,1)
            G23=G(3,1)
          ENDIF

C COMPUTE UPDATED ERROR COVARIANCE MATRIX
C          P(K|K) = (I - G*H) * P(K|K-1)
C          CALL MATMUL(G,H,4,1,4,TEMP4)
C          WRITE(3,*)'G*H ='
C          DO 419 I=1,4
C            WRITE(3,418)(TEMP4(I,J),J=1,4)
418          FORMAT(4F14.4)
419        CONTINUE

          CALL MATSUB(IMAT,TEMP4,4,4,TEMP5)
C          WRITE(3,*)'I-G*H ='
C          DO 413 I=1,4
C            WRITE(3,415)(TEMP5(I,J),J=1,4)
415          FORMAT(4F14.4)
413        CONTINUE
          CALL MATMUL(TEMP5,PKKM1,4,4,4,PKK)

C          WRITE(3,*)'P(' ,TIME,'|',TIME,',',',L,'):'
C          DO 606 I=1,4
C            WRITE(3,406)(PKK(I,J),J=1,4)
406          FORMAT(4F14.4)
606        CONTINUE

C SAVE LATEST RESIDUALS & ADAPTIVE GATES
          E1=E(1)
          E2=E(2)
          GATE1=GATE(1)
          GATE2=GATE(2)

          WRITE(10,900)TIME,ABS(E1),ABS(E2),GATE1,GATE2
900        FORMAT(I4,4F10.5)

C COMPARE BEARING ERRORS TO MANEUVER DETECTION GATES
          IF (ABS(E(L)).GT.(GATE(L))) THEN
            GTCTR=GTCTR+1

```

```

WRITE(*,*)'*** MANEUVER DETECTION GATE EXCEEDED ***'
WRITE(*,*)'TIME',TIME
C WRITE(3,*)'*** MANEUVER DETECTION GATE EXCEEDED ***'
C WRITE(3,*)'TIME',TIME
CALL GETQ(DT,XKKM1,Q,0)
C CALL MATADD(PKKM1,Q,4,4,1,PKKM1)
IF (GTCTR.EQ.3) THEN
    GTCTR=0
    WRITE(*,*)'*** MANEUVER DETECTION ***'
    WRITE(*,*)'TIME',TIME
    C WRITE(3,*)'*** MANEUVER DETECTION ***'
    C WRITE(3,*)'TIME',TIME
    CALL REINIT(DT,ZX,ZY,ZXM1,ZYM1,LPKKM1,XKKM1,PKKM1)
    CALL GETQ(DT,XKKM1,Q,1)
ELSE
    GOTO 204
ENDIF
ENDIF
GTCTR=0

C COMPUTE UPDATED ESTIMATE
C  $X(K|K) = X(K|K-1) + G * E$ , WHERE  $E = Z(K) - H(K)*X(K|K-1)$ 
XKK(1,1)=XKKM1(1,1)+(G(1,1)*E(L))
XKK(2,1)=XKKM1(2,1)+(G(2,1)*E(L))
XKK(3,1)=XKKM1(3,1)+(G(3,1)*E(L))
XKK(4,1)=XKKM1(4,1)+(G(4,1)*E(L))

C WRITE(3,*)'X(' ,TIME,'|',TIME,',',',L,'):'
DO 605 I=1,4
C WRITE(3,*)XKK(I,1)
605 CONTINUE

C IF MORE MEASUREMENTS,
IF (L.LT.2) THEN
C USE UPDATED STATE AND ERROR COVARIANCE ESTIMATES
C FOR NEXT MEASUREMENT
DO 150 I=1,4
DO 150 J=1,4
    PKK1(I,J)=PKK(I,J)
    XKKM1(I,1)=XKK(I,1)
150 CONTINUE
ENDIF
210 CONTINUE

C THESE STATEMENTS ARE FOR THE SMOOTHING ALGORITHM

DO 620 I=1,4
    XKKS(I,1,NP)=XKK(I,1)
620 CONTINUE

DO 630 I=1,4
    DO 630 J=1,4
        PKKS(I,J,NP)=PKK(I,J)
630 CONTINUE

```

```

C COMPUTE TRUE TRACKING AND OBSERVATION ERRORS
  TRKERR(NP)=SQRT((XT-XKK(1,1))**2+(YT-XKK(3,1))**2)
  OBSERR(NP)=SQRT((XT-ZX)**2+(YT-ZY)**2)

C COMPUTE ERROR ELLIPSE DATA
  CALL ELLIP(XKK(1,1),XKK(3,1),PKK(1,1),PKK(3,3),PKK(1,3),XP,YP)
  DO 640 IE=1,21
    WRITE(7,*)XP(IE),YP(IE)
640    CONTINUE

C COMPUTE ESTIMATED X-Y POSITION, COURSE, AND SPEED
  XPOS=XKK(1,1)
  YPOS=XKK(3,1)
  IF (XKK(2,1).EQ.0 .AND. XKK(4,1).EQ.0) THEN
    HDG=0.0
  ELSE
    HDG=RTOD*ATAN2(XKK(2,1),XKK(4,1))
  ENDIF
  IF (HDG.LT.0.0) HDG=HDG+360
  SPD(NP)=60*SQRT(XKK(2,1)**2+XKK(4,1)**2)
C  WRITE(*,*)'FILTERED DATA FOR DATA POINT',NP
  WRITE(3,*)'FILTERED DATA FOR DATA POINT',NP
C  WRITE(*,*)'TIME      X POS    Y POS    HEADING    SPEED'
  WRITE(3,*)'TIME      X POS    Y POS    HEADING    SPEED'
C  WRITE(*,1002)TIME,XPOS,YPOS,HDG,SPD(1)
  WRITE(3,1002)TIME,XPOS,YPOS,HDG,SPD(1)
  .  WRITE(4,1003)TIME,XT,YT
    WRITE(5,1004)TIME,NP,XPOS,YPOS,ZX,ZY,TRKERR(NP),OBSERR(NP),
      *      PKK(1,1),PKK(3,3),XT,YT
C  WRITE(5,*)TIME,XT,YT,XPOS,YPOS,ZX,ZY,LXKKM1(1,1),LXKKM1(3,1),
C  *      ABS(M1),GATE1(1),ABS(M2),GATE1(2),
C  *      G11,G13,G21,G23,TRKERR,OBSERR
1002  FORMAT(I4,8F8.1,8F8.5,2F8.1)
1003  FORMAT(I4,2F8.1)
1004  FORMAT(2I4,10F8.1)
1005  FORMAT(I4,4F8.1)

C UPDATE DATA COUNTER
  NP=NP+1

  TIMEM1=TIME

  ZXM1=ZX
  ZYM1=ZY

  GOTO 810

800  NP=NP-1
C THIS IS WHERE THE SMOOTHING ALGORITHM STARTS
C FIXED INTERVAL SMOOTHING
  WRITE(*,*)'SMOOTHING FILTERED DATA WITH A'
  WRITE(*,*)'FIXED INTERVAL SMOOTHING ALGORITHM'

```



```

WRITE(*,*)'*****'
C   WRITE(*,*)'***** SMOOTHING STARTS HERE *****'
   WRITE(3,*)'***** SMOOTHING STARTS HERE *****'

DO 1000 KK=1,NP-1
  K=NP-KK

  DT=DTS(K+1)

  TIME=TIMEM1-DT
  CALL FINDPHI(PHI,DT)

  DO 901 I=1,4
    XSS(I,1)=XKKS(I,1,K)
901  CONTINUE

  DO 902 I=1,4
    DO 902 J=1,4
      PSS(I,J)=PKKS(I,J,K)
902  CONTINUE

C   CALCULATE THE PREDICTED STATE AND ERROR COVARIANCE MATRICES
C    $X(K+1|K) = \Phi \cdot X(K|K)$ 
   CALL MATMUL (PHI,XSS,4,4,1,XKKM1S)
C    $P(K+1|K) = \Phi \cdot P(K|K) \cdot \Phi^T + Q$ 
   CALL MATRAN (PHI,PHIT,4,4)
   CALL MATMUL(PHI,PSS,4,4,4,TEMP6)
   CALL MATMUL(TEMP6,PHIT,4,4,4,TEMP4)
   CALL GETQ(DT,XKKM1S,Q,1)
   CALL MATADD(TEMP4,Q,4,4,1,PKKM1S)

C   CALCULATE THE SMOOTHING FILTER GAIN MATRIX
C    $AK = P(K|K) \cdot \Phi^T \cdot INV^0 P(K+1|K)$ 
   CALL MATINV (PKKM1S,4,IPKKM1S)
   CALL MATMUL (PKKM1S,IPKKM1S,4,4,4,II)
   CALL MATMUL (PSS,PHIT,4,4,4,TEMP1S)
   CALL MATMUL (TEMP1S,IPKKM1S,4,4,4,AK)

  DO 904 I=1,4
    XNNM1(I,1)=XKKS(I,1,K+1)
904  CONTINUE

C   CALCULATE THE SMOOTHED STATE ESTIMATE
C    $XKKS = X(K|K) + AK \cdot (X(K+1|N) - X(K+1|K))$ 
   CALL MATSUB (XNNM1,XKKM1S,4,1,TEMP2S)
   CALL MATMUL (AK,TEMP2S,4,4,1,TEMP3S)
   CALL MATADD (XSS,TEMP3S,4,1,K,XKKS)

  DO 906 I=1,4
    DO 906 J=1,4
      PNNM1(I,J)=PKKS(I,J,K+1)
906  CONTINUE

C   CALCULATE THE SMOOTHED COVARIANCE MATRIX
C    $PKKS = P(K|K) + AK \cdot [P(K+1|N) - P(K+1|K)] \cdot AK^T$ 

```



```

CALL MATSUB (PNNM1,PKKM1S,4,4,TEMP4S)
CALL MATRAN (AK,AKT,4,4)
CALL MATMUL (AK,TEMP4S,4,4,4,TEMP5S)
CALL MATMUL (TEMP5S,AKT,4,4,4,TEMP6S)
CALL MATADD (PSS,TEMP6S,4,4,K,PKKS)

C COMPUTE ESTIMATED X-Y POSITION, COURSE, AND SPEED
  SXPOS=XKKS(1,1,K)
  SYPOS=XKKS(3,1,K)
  IF (XKKS(2,1,K).EQ.0 .AND. XKKS(4,1,K).EQ.0) THEN
    SHDG=0.0
  ELSE
    SHDG=RTOD*ATAN2(XKKS(2,1,K),XKKS(4,1,K))
  ENDIF
  IF (SHDG.LT.0.0) SHDG=SHDG+360
  SSPD(K)=60*SQRT(XKKS(2,1,K)**2+XKKS(4,1,K)**2)
C  WRITE(*,*)'SMOOTHED DATA FOR DATA POINT',K
  WRITE(3,*)'SMOOTHED DATA FOR DATA POINT',K
C  WRITE(*,*)'TIME   X POS   Y POS   HEADING   SPEED'
  WRITE(3,*)'TIME   X POS   Y POS   HEADING   SPEED'
C  WRITE(*,1010)TIME,SXPOS,SYPOS,SHDG,SSPD(K)
  WRITE(3,1010)TIME,SXPOS,SYPOS,SHDG,SSPD(K)
C  WRITE(*,1020)NP,K,XKKS(1,1,K),XKKS(3,1,K),PKKS(1,1,K)
1010  FORMAT(I4,8F8.1,8F8.5,2F8.1)
1020  FORMAT(2I4,3F8.1)

      TIMEM1=TIME
1000  CONTINUE

      REWIND 4

C CALCULATE THE SMOOTHED TRACKING ERROR
  WRITE(9,*)'ERROR DATA FOR DATA POINT TRACKING ROUTINE'
  WRITE(9,*)'K   OBSERR  TRKERR  STRKERR  FILSPD  SMSPD'
  DO 1100 K=1,NP
    SXPOS=XKKS(1,1,K)
    SYPOS=XKKS(3,1,K)
    READ(4,1110)TIME,XT,YT
    STRKERR(K)=SQRT((XT-XKKS(1,1,K))**2+(YT-XKKS(3,1,K))**2)
C COMPUTE ERROR ELLIPSE DATA
    CALL ELLIP(XKKS(1,1,K),XKKS(3,1,K),
      *      PKKS(1,1,K),PKKS(3,3,K),PKKS(1,3,K),XPS,YPS)
    DO 1050 IE=1,21
      WRITE(8,*)XPS(IE),YPS(IE)
1050  CONTINUE
      WRITE(6,1120)K,SXPOS,SYPOS,STRKERR(K),
      *      PKKS(1,1,K),PKKS(3,3,K)
      WRITE(9,1130)K,OBSERR(K),TRKERR(K),STRKERR(K),SPD(K),SSPD(K)
1100  CONTINUE
1110  FORMAT(I4,2F8.1)
1120  FORMAT(I4,5F8.1)
1130  FORMAT(I4,5F8.1)

      CLOSE(UNIT=2)
      CLOSE(UNIT=3)
      CLOSE(UNIT=4)

```

```

CLOSE(UNIT=5)
CLOSE(UNIT=6)
CLOSE(UNIT=7)
CLOSE(UNIT=8)
CLOSE(UNIT=9)
CLOSE(UNIT=10)

```

```

WRITE(*,*)'FILTERED & SMOOTHED OUTPUT DATA IS LOCATED IN THE '
WRITE(*,*)'DATA FILE OUTDATA.DAT.  FOR GRAPHIC RESULTS COPY'
WRITE(*,*)'  1) ELLIP.DAT'
WRITE(*,*)'  2) ELLIPS.DAT'
WRITE(*,*)'  3) FILDATA.DAT'
WRITE(*,*)'  4) SMDATA.DAT'
WRITE(*,*)'  5) TRUDATA.DAT'
WRITE(*,*)'TO THE MATLAB SUB-DIRECTORY AND RUN ==>SHIP.M.'
WRITE(*,*)'THERE WERE',NP,'  OBSERVATIONS PROCESSED.'
STOP
END

```

```

C*****
C                                SUBROUTINES
C*****

```

```

      SUBROUTINE FINDPHI(PHI,DT)
C *****
C      COMPUTES THE VALUES OF THE PHI MATRIX
C *****
      REAL*4 PHI(4,4),DT

      DO 1501 I=1,4
      DO 1501 J=1,4
      DO 1501 K=1,2
        PHI(I,J)=0.0
1501    CONTINUE

C COMPUTE PHI MATRIX
      DO 1500 I=1,4
        PHI(I,I)=1.0
1500    CONTINUE
      PHI(1,2)=DT
      PHI(3,4)=DT

      RETURN

      END

```

```

      SUBROUTINE INIT(XS1,YS1,XS2,YS2,BRG1,BRG2,XKK,PKK)
C *****
C      THIS ROUTINE INITIALIZES THE STATE
C      AND ERROR COVARIANCE ESTIMATES
C *****
      REAL*4 XKK(4,1),PKK(4,4)
      REAL*4 XS1,YS1,XS2,YS2,BRG1,BRG2

```

REAL\*4 NUMER,DENOM

C INITIAL STATE ESTIMATE

NUMER=(-YS2\*TAN(BRG2))+(YS1\*TAN(BRG1))+XS2-XS1  
DENOM=TAN(BRG1)-TAN(BRG2)

XKK(3,1)=NUMER/DENOM  
XKK(2,1)=0.0  
XKK(1,1)=(XKK(3,1)-YS1)\*TAN(BRG1)+XS1  
XKK(4,1)=0.0

C INITIAL ERROR COVARIANCE ESTIMATE

PKK(1,1)=10000  
PKK(1,2)=0.0  
PKK(1,3)=0.0  
PKK(1,4)=0.0  
PKK(2,1)=0.0  
PKK(2,2)=0.2500  
PKK(2,3)=0.0  
PKK(2,4)=0.0  
PKK(3,1)=0.0  
PKK(3,2)=0.0  
PKK(3,3)=10000  
PKK(3,4)=0.0  
PKK(4,1)=0.0  
PKK(4,2)=0.0  
PKK(4,3)=0.0  
PKK(4,4)=0.2500

RETURN

END

SUBROUTINE GETQ(DT,XKKM1,Q,FLAG)

C\*\*\*\*\*

C ROUTINE TO GET Q MATRIX WHERE

C Q = GAMA(K)\*Q'(K)\*GAMAT(K)

C\*\*\*\*\*

REAL\*4 DT,XKKM1(4,1),Q(4,4)  
REAL\*4 QPR(2,2),GAMA(4,2),GAMAT(2,4)  
REAL\*4 SIGVT2,SIGTH2,VT

INTEGER FLAG

IF ((XKKM1(2,1).EQ.0).OR.(XKKM1(4,1).EQ.0)) THEN

DO 100 I=1,4

DO 100 J=1,4

100 Q(I,J)=0.0

GOTO 200

ENDIF

C CALCULATE Q'MATRIX

SIGVT2=0.0001

SIGTH2=0.01096

VT=SQRT(XKKM1(2,1)\*\*2+XKKM1(4,1)\*\*2)

```

      QPR(1,1)=(((XKKM1(2,1)/VT)**2)*SIGVT2)+((XKKM1(4,1)**2)*SIGTH2)
      QPR(2,2)=(((XKKM1(4,1)/VT)**2)*SIGVT2)+((XKKM1(2,1)**2)*SIGTH2)
      QPR(1,2)=((XKKM1(2,1))*(XKKM1(4,1))/(VT**2))*SIGVT2
*      -(XKKM1(2,1))*(XKKM1(4,1))*SIGTH2
      QPR(2,1)=QPR(1,2)
      IF (FLAG.EQ.0) THEN
        QPR(1,1)=2.50*QPR(1,1)
        QPR(2,2)=2.50*QPR(2,2)
      ENDIF

```

C CALCULATE GAMA MATRIX

```

      GAMA(1,1)=(DT**2)/2.0
      GAMA(2,1)=DT
      GAMA(3,1)=0.0
      GAMA(4,1)=0.0
      GAMA(1,2)=0.0
      GAMA(2,2)=0.0
      GAMA(3,2)=(DT**2)/2.0
      GAMA(4,2)=DT

```

C Q=GAMA(K)\*Q'(K)\*GAMAT(K)

```

      CALL MATRAN(GAMA,GAMAT,4,2)
      CALL MATMUL(GAMA,QPR,4,2,2,TEMP9)
      CALL MATMUL(TEMP9,GAMAT,4,2,4,Q)
      CALL MATSCL(0.01,Q,4,4,Q)

```

200 RETURN

END

SUBROUTINE REINIT(DT,ZX,ZY,ZXM1,ZYM1,LPKKM1,XKKM1,PKKM1)

C \*\*\*\*\*

C THIS ROUTINE RE-INITIALIZES THE STATE AND ERROR

C COVARIANCE ESTIMATES

C \*\*\*\*\*

```

      REAL*4 DT,XKKM1(4,1),PKKM1(4,4)
      REAL*4 ZX,ZY,ZXM1,ZYM1,LPKKM1(4,4)

```

XDIFF=ZX-ZXM1

YDIFF=ZY-ZYM1

IF (DT.EQ.0) THEN

XKKM1(1,1)=ZX

XKKM1(2,1)=XDIFF

XKKM1(3,1)=ZY

XKKM1(4,1)=YDIFF

ELSE

XKKM1(1,1)=ZX

XKKM1(2,1)=XDIFF/DT

XKKM1(3,1)=ZY

XKKM1(4,1)=YDIFF/DT

ENDIF

C WRITE(3,\*)'REINITIALIZED STATES ARE: '

```

DO 100 I=1,4
C      WRITE(3,*)XKKM1(I,1)
100    CONTINUE

PKKM1(1,1)=LPKKM1(1,1)
PKKM1(1,2)=0.0
PKKM1(1,3)=LPKKM1(1,3)
PKKM1(1,4)=0.0
PKKM1(2,1)=0.0
PKKM1(2,2)=0.1111
PKKM1(2,3)=0.0
PKKM1(2,4)=0.0
PKKM1(3,1)=LPKKM1(3,1)
PKKM1(3,2)=0.0
PKKM1(3,3)=LPKKM1(3,3)
PKKM1(3,4)=0.0
PKKM1(4,1)=0.0
PKKM1(4,2)=0.0
PKKM1(4,3)=0.0
PKKM1(4,4)=0.1111

      RETURN

      END

      SUBROUTINE MP(XS1,YS1,XS2,YS2,BRG1,BRG2,ZX,ZY)
C *****
C      THIS ROUTINE COMPUTES THE ESTIMATED
C      X,Y POSITION OBTAINED FROM MEASUREMENTS
C *****
      REAL*4 ZX,ZY
      REAL*4 XS1,YS1,XS2,YS2,BRG1,BRG2
      REAL*4 NUMER,DENOM

C INITIAL STATE ESTIMATE

      NUMER=(-YS2*TAN(BRG2))+(YS1*TAN(BRG1))+XS2-XS1
      DENOM=TAN(BRG1)-TAN(BRG2)

      ZY=NUMER/DENOM
      ZX=(ZY-YS1)*TAN(BRG1)+XS1

      RETURN

      END

      SUBROUTINE ELLIP(XT,YT,P1,P3,P13,XP,YP)
C *****
C      THIS SUBROUTINE COMPUTES ERROR ELLIPSE DATA
C      FROM ERROR COVARIANCE DATA
C *****
C      DIMENSIONS AND DECLARATIONS
      REAL*4 XT,YT,XP(21),YP(21),A,B,THE1,SIG2X,SIG2Y
      REAL*4 SX,SY,PT,CT,ST,P1,P13,P3
      INTEGER*2 NP

```

```

      A=2*P13
      B=P1-P3
      THE1=0.5*ATAN2(A,B)
      A=(P1+P3)/2
      B=0.0
      IF (P13.EQ.0.0) GOTO 10
      B=P13/SIN(2.0*THE1)
10    SIG2X=ABS(A+B)
      SIG2Y=ABS(A-B)
      SX=SIG2X**0.5
      SY=SIG2Y**0.5
      PT=3.141592654/10
      CT=COS(THE1)
      ST=SIN(THE1)

      DO 100 IE=1,21
          XP(IE)=SX*COS(PT*IE)*CT-SY*SIN(PT*IE)*ST+XT
          YP(IE)=SX*COS(PT*IE)*ST+SY*SIN(PT*IE)*CT+YT
100   CONTINUE

      RETURN

      END

```

```

      SUBROUTINE MATMUL(A,B,L,M,N,C)
C *****
C      THIS ROUTINE MULTIPLIES TWO MATRICES TOGETHER
C       $C(L,N) = A(L,M) * B(M,N)$ 
C *****
C      DIMENSIONS AND DECLARATIONS
C      REAL*4 A(L,M),B(M,N),C(L,N)

      DO 10 I=1,L
      DO 10 J=1,N
          C(I,J)=0.0
10    CONTINUE

      DO 100 I= 1,L
      DO 100 J= 1,N
      DO 100 K= 1,M
          C(I,J) = C(I,J) + A(I,K)*B(K,J)
100   CONTINUE

      RETURN

      END

```

```

      SUBROUTINE MATRAN(A,B,N,M)
C *****
C      THIS ROUTINE TRANSPOSES A MATRIX
C       $B(M,N) = A'(N,M)$ 
C *****
C      DIMENSIONS AND DECLARATIONS

```



```

      REAL*4 A(N,M), B(M,N)

      DO 100 I= 1,N
      DO 100 J= 1,M
        B(J,I) = A(I,J)
100    CONTINUE

      RETURN

      END

      SUBROUTINE MATSCL(Q,A,N,M,C)
C *****
C      THIS ROUTINE MULTIPLIES A MATRIX WITH A SCALAR
C      ° C(N,M) = Q * A(N,M)
C *****
C      DIMENSIONS AND DECLARATIONS
        REAL*4 A(N,M), C(N,M), Q

      DO 100 I = 1,N
      DO 100 J = 1,M
        C(I,J) = Q*A(I,J)
100    CONTINUE

      RETURN

      END

      SUBROUTINE MATSUB(A,B,N,M,C)
C *****
C      THIS ROUTINE SUBTRACTS TWO MATRICES
C      ° C(N,M) = A(N,M) - B(N,M)
C *****
C      DIMENSIONS AND DECLARATIONS
        REAL*4 A(N,M), B(N,M), C(N,M)

      DO 100 I = 1,N
      DO 100 J = 1,M
        C(I,J)=A(I,J)-B(I,J)
100    CONTINUE

      RETURN

      END

      SUBROUTINE MATADD(A,B,N,M,L,C)
C*****
C      THIS ROUTINE ADDS TWO MATRICES
C      ° C(N,M) = A(N,M) + B(N,M)
C*****
C      DIMENSIONS AND DECLARATIONS
        REAL*4 A(N,M), B(N,M), C(N,M,L)
      DO 100 I = 1,N
      DO 100 J = 1,M

```



```

      C(I,J,L)=A(I,J)+B(I,J)
100   CONTINUE

      RETURN
      END

```

```

      SUBROUTINE MATINV (A,N,C)
C*****
C      THIS ROUTINE COMPUTES THE INVERSE OF
C      A MATRIX
C      C(N,N)=INV [ A(N,N)]
C*****
C      DIMENSIONS AND DECLARATIONS
      REAL*4 A(N,N),C(N,N),D(20,20)
      DO 100 I = 1,N
        DO 100 J = 1,N
100      D(I,J)=A(I,J)

      DO 115 I=1,N
        DO 115 J=N+1,2*N
115      D(I,J)=0.0

      DO 120 I=1,N
        J=I+N
120      D(I,J)=1.0

      DO 240 K=1,N
        M=K+1
        IF (K.EQ.N) GOTO 180
        L=K
        DO 140 I=M,N
140      IF (ABS(D(I,K)).GT.ABS(D(L,K))) L=I
        IF (L.EQ.K) GOTO 180

        DO 160 J=K,2*N
          TEMP=D(K,J)
          D(K,J)=D(L,J)
160      D(L,J)=TEMP

      DO 185 J=M,2*N
185      D(K,J)=D(K,J)/D(K,K)

      IF (K.EQ.1) GOTO 220
      M1=K-1
      DO 200 I=1,M1
        DO 200 J=M,2*N
200      D(I,J)=D(I,J)-D(I,K)*D(K,J)

      IF (K.EQ.N) GOTO 260

220      DO 240 I=M,N
        DO 240 J=M,2*N
240      D(I,J)=D(I,J)-D(I,K)*D(K,J)

260      DO 265 I=1,N

```

```
      DO 265 J=1,N  
        K=J+N  
265    C(I,J)=D(I,K)  
  
      RETURN  
      END
```

## APPENDIX B. TRACK.FOR

This is the TRACK.FOR program used to generate the TRKDATA.DAT file to be read by SHIPSM.FOR. This program was written by LT Tom Bennett.

```
REAL*4 XT(4,1),XS1(4,1),PHI(4,4),SPDS1,HDGS1,SPDS2,HDGS2
REAL*4 DT,SPDT,HDGT,XS2(4,1),TEMP1(4,1),CASE,XDIFF1,YDIFF1
REAL*4 XDIFF2,YDIFF2,N1,N2,DTOR,RTOD,BRG1,BRG2
INTEGER TIME,TIMEM1
```

```
OPEN(UNIT=2,FILE='NOISE1.DAT',STATUS='OLD')
OPEN(UNIT=3,FILE='NOISE2.DAT',STATUS='OLD')
OPEN(UNIT=4,FILE='TRKDATA.DAT',STATUS='NEW')
```

```
WRITE(*,*)'ENTER A NEGATIVE NUMBER FOR NOISELESS CASE;'
WRITE(*,*)'POSITIVE FOR NOISY CASE'
READ(*,*)CASE
```

```
TIMEM1=0
RTOD=57.29577951
DTOR=0.017453293
```

```
WRITE(*,*)'INPUT DESIRED INITIAL X POSITION OF TARGET'
READ(*,*)XT(1,1)
WRITE(*,*)'INPUT DESIRED INITIAL Y POSITION OF TARGET'
READ(*,*)XT(3,1)
WRITE(*,*)'INPUT DESIRED TARGET SPEED IN KNOTS'
READ(*,*)SPDT
WRITE(*,*)'INPUT DESIRED TARGET COURSE IN DEGREES'
READ(*,*)HDGT
```

```
XT(2,1)=(SPDT/60)*SIN(HDGT*DTOR)
XT(4,1)=(SPDT/60)*COS(HDGT*DTOR)
```

```
WRITE(*,*)'FOR SENSOR 1:'
WRITE(*,*)'INPUT DESIRED INITIAL X POSITION'
READ(*,*)XS1(1,1)
WRITE(*,*)'INPUT DESIRED INITIAL Y POSITION'
READ(*,*)XS1(3,1)
WRITE(*,*)'INPUT DESIRED SPEED IN KNOTS'
READ(*,*)SPDS1
WRITE(*,*)'INPUT DESIRED COURSE IN DEGREES'
READ(*,*)HDGS1
```

```
XS1(2,1)=(SPDS1/60)*SIN(HDGS1*DTOR)
XS1(4,1)=(SPDS1/60)*COS(HDGS1*DTOR)
```

```
WRITE(*,*)'FOR SENSOR 2:'
WRITE(*,*)'INPUT DESIRED INITIAL X POSITION'
READ(*,*)XS2(1,1)
WRITE(*,*)'INPUT DESIRED INITIAL Y POSITION'
```

```

    READ(*,*)XS2(3,1)
    WRITE(*,*)'INPUT DESIRED SPEED IN KNOTS'
    READ(*,*)SPDS2
    WRITE(*,*)'INPUT DESIRED COURSE IN DEGREES'
    READ(*,*)HDGS2

    XS2(2,1)=(SPDS2/60)*SIN(HDGS2*DTOR)
    XS2(4,1)=(SPDS2/60)*COS(HDGS2*DTOR)

300  DO 310 J=1,1000
      WRITE(*,*)'INPUT TIME OF UPDATE (NEG. FOR END OF PROBLEM)'
      WRITE(*,*)'ENTER "9999" FOR SPEED AND COURSE UPDATE'
      READ(*,*)TIME
      IF (TIME.LT.0) GOTO 900
      IF (TIME.EQ.9999) THEN
        WRITE(*,*)'INPUT NEW DESIRED TARGET SPEED IN KNOTS'
        READ(*,*)SPDT
        WRITE(*,*)'INPUT NEW DESIRED TARGET COURSE IN DEGREES'
        READ(*,*)HDGT

        XT(2,1)=(SPDT/60)*SIN(HDGT*DTOR)
        XT(4,1)=(SPDT/60)*COS(HDGT*DTOR)

        GOTO 300
      ENDIF

C  UPDATE TARGET AND SENSOR STATES TO MEASUREMENT TIME
      DT=TIME-TIMEM1

C  COMPUTE PHI MATRIX
      PHI(1,1)=1.0
      PHI(1,2)=DT
      PHI(1,3)=0.0
      PHI(1,4)=0.0
      PHI(2,1)=0.0
      PHI(2,2)=1.0
      PHI(2,3)=0.0
      PHI(2,4)=0.0
      PHI(3,1)=0.0
      PHI(3,2)=0.0
      PHI(3,3)=1.0
      PHI(3,4)=DT
      PHI(4,1)=0.0
      PHI(4,2)=0.0
      PHI(4,3)=0.0
      PHI(4,4)=1.0

C  UPDATE TARGET STATES
      CALL MATMUL(PHI,XT,4,4,1,TEMP1)
      DO 700 I=1,4
        XT(I,1)=TEMP1(I,1)
700    CONTINUE

C  UPDATE SENSOR STATES

```

```

      CALL MATMUL(PHI,XS1,4,4,1,TEMP1)
      DO 710 I=1,4
        XS1(I,1)=TEMP1(I,1)
710    CONTINUE

      CALL MATMUL(PHI,XS2,4,4,1,TEMP1)
      DO 720 I=1,4
        XS2(I,1)=TEMP1(I,1)
720    CONTINUE

      XDIFF1=XT(1,1)-XS1(1,1)
      YDIFF1=XT(3,1)-XS1(3,1)

      XDIFF2=XT(1,1)-XS2(1,1)
      YDIFF2=XT(3,1)-XS2(3,1)

      READ(2,*)N1
      READ(3,*)N2

      IF (CASE.GE.0.0) GOTO 450
        N1=0.0
        N2=0.0

450    BRG1=RTOD*ATAN2(XDIFF1,YDIFF1)+N1
        IF (BRG1.LT.0.0) BRG1=BRG1+360
      BRG2=RTOD*ATAN2(XDIFF2,YDIFF2)+N2
        IF (BRG2.LT.0.0) BRG2=BRG2+360

      WRITE(4,500)TIME,XT(1,1),XT(3,1),XS1(1,1),XS1(3,1),
*      BRG1,XS2(1,1),XS2(3,1),BRG2
500    FORMAT(I4,8F9.4)

      TIMEM1=TIME

310    CONTINUE
900    STOP
      END

```

```

      SUBROUTINE MATMUL(A,B,L,M,N,C)
C *****
C      THIS ROUTINE MULTIPLIES TWO MATRICES TOGETHER
C      C(L,N) = A(L,M) * B(M,N)
C *****
C      DIMENSIONS AND DECLARATIONS
      REAL*4 A(L,M),B(M,N),C(L,N)

      DO 10 I=1,L
        DO 10 J=1,N
          C(I,J)=0.0
10    CONTINUE

      DO 100 I= 1,L
        DO 100 J= 1,N
          DO 100 K= 1,M

```

```
      C(I,J) = C(I,J) + A(I,K)*B(K,J)
100  CONTINUE

      RETURN

      END
```





## LIST OF REFERENCES

Truver, Scott C., "The Navy's 'Revolution at Sea': Surface Warfare in the 21st Century", *Armed Forces Journal International*, November 1987.

International Radio Consultative Committee (C.C.I.R.) Report 322, *World Distribution and Characteristics of Atmospheric Radio Noise*, International Telecommunication Union, Geneva, 1964.

Hall, H.M., Stanford Electronics Laboratories Technical Report No. 7050-7II, *A New Model for Impulsive Phenomena: Application to Atmospheric-Noise Communication Channels*, August 1966.

Spaulding, A.D., National Telecommunications and Information Administration Report No. 84-142, *Locally Optimum and Suboptimum Detector Performance in a Non-Gaussian Interference Environment*, January 1984.

Gelb, Arthur, *Applied Optimal Estimation*, M.I.T. Press, Cambridge, Massachusetts, 1974.

Mitschang, George William, *An Application of Nonlinear Filtering Theory to Passive Target Location and Tracking*, Ph. D. Dissertation, Naval Postgraduate School, Monterey, California, June 1974.

Bennett, Thomas Kevin, *Development of an Adaptive Extended Kalman Filter Ship-Tracking Algorithm Using Bearings-Only Measurements*, M.S.E.E. Thesis, Naval Postgraduate School, Monterey, California, June 1988.

Jazwinski, Andrew H, *Stochastic Processes and Filtering Theory*, Academic Press, New York, New York, 1970.



Meditch, J.S., *Stochastic Optimal Linear Estimation and Control*, McGraw-Hill Book Co., New York, New York, 1969.

Joint Typhoon Warning Center, Guam, Mariana Islands, *1985 Annual Tropical Cyclone Report*, Naval Oceanography Command Center/Joint Typhoon Warning Center, 1985.



## INITIAL DISTRIBUTION LIST

No. Copies

- | 1. | Defense Technical Information Center<br>Cameron Station<br>Alexandria, VA 22304-6145  | 2 |
|----|---|---|
| 2. | Library, Code 0142<br>Naval Postgraduate School<br>Monterey, CA 93943-5002  | 2 |
| 3. | Chairman, Code 62<br>Department of Electrical and Computer Engineering<br>Naval Postgraduate School<br>Monterey, CA 93943-5002    | 1 |
| 4. | Professor Hal A. Titus, Code 62Ts<br>Department of Electrical Engineering<br>Naval Postgraduate School<br>Monterey, CA 93943-5002 | 5 |
| 5. | Professor Jauregui, Code 62Ja<br>Department of Electrical Engineering<br>Naval Postgraduate School<br>Monterey, CA 93943-5002     | 2 |
| 6. | Commander<br>Naval Ocean Systems Center<br>San Diego, CA 92152-5000   | 1 |
| 7. | Ron Miller<br>Naval Environmental Prediction Research Facility<br>Monterey, CA 93943-5006   | 1 |
| 8. | LT William J. Galinis<br>3425 Sherwood Blvd.<br>Delray Beach, FL 33445  | 2 |













Thesis

G135 Galinis

c.1 Fixed interval smoothing algorithm for an extended Kalman filter for over-the-horizon ship tracking.

0 AUG 91

55970

Thesis

G135 Galinis

c.1 Fixed interval smoothing algorithm for an extended Kalman filter for over-the-horizon ship tracking.





thesG135  
Fixed interval smoothing algorithm for a



3 2768 000 81766 2  
DUDLEY KNOX LIBRARY